SOUTHWEST RESEARCH INSTITUTE®

Internal Research and Development 2015

The SwRI IR&D Program exists to broaden the Institute's technology base and to encourage staff professional growth. Internal funding of research enables the Institute to advance knowledge, increase its technical capabilities, and expand its reputation as a leader in science and technology. The program also allows Institute engineers and scientists to continually grow in their technical fields by providing freedom to explore innovative and unproven concepts without contractual restrictions and expectations.

- Space Science
- Materials Research & Structural Mechanics
- Intelligent Systems, Advanced Computer & Electronic Technology, & Automation
- Measurement & Nondestructive Evaluation of Materials & Structures
- Engines, Fuels, Lubricants, & Vehicle Systems
- Geology & Nuclear Waste Management
- Fluid & Machinery Dynamics
- Electronic Systems & Instrumentation
- Chemistry & Chemical Engineering

SOUTHWEST RESEARCH INSTITUTE®

SwRI IR&D 2015 – Space Science

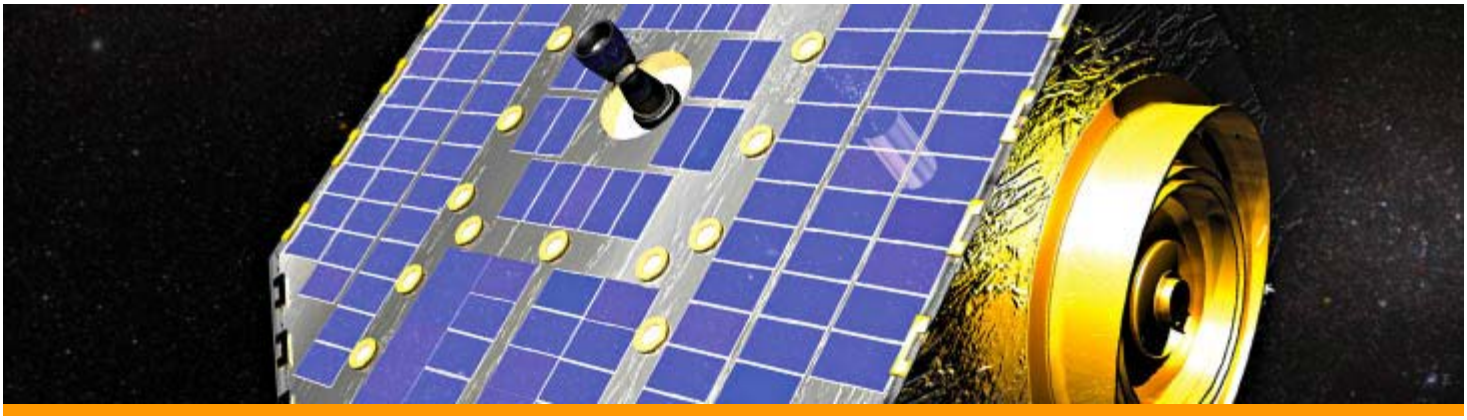

- Capability Development and Demonstration for Next-Generation Suborbital Research, 15-R8115
- Design and Development of an Optimized Far-field Acoustic Imager for Lightning Studies, 15-R8444
- Design and Analysis of Device to Capture Stratospheric Air Samples, 15-R8446
- Testing of Prototype Mass Spectrometer for Earth Atmospheric Studies, 15-R8475
- Technology Development for the High Energy Polarimeter (HEP) Instrument Detector, 15-R8483
- Capability Development of Supernova Models, 15-R8498
- Acoustic Measurements of a High Mass-Flow Cold Jet, 15-R8510
- Viability of a Blended Redundancy Concept for Constrained Spacecraft Applications, 15-R8535
- Augmenting a Novel Magnetohydrodynamics Code for Studying Astrophysical Plasmas and Space Weather, 15-R8568
- Stratospheric Compressor for Lighter-than-Air Vehicles, 15-R8575
- Investigation and Measurement of Balloon Dynamics at the Apex and Base of a Scientific Balloon, 15-R8577

SOUTHWEST RESEARCH INSTITUTE®

SwRI IR&D 2015 – Materials Research & Structural Mechanics

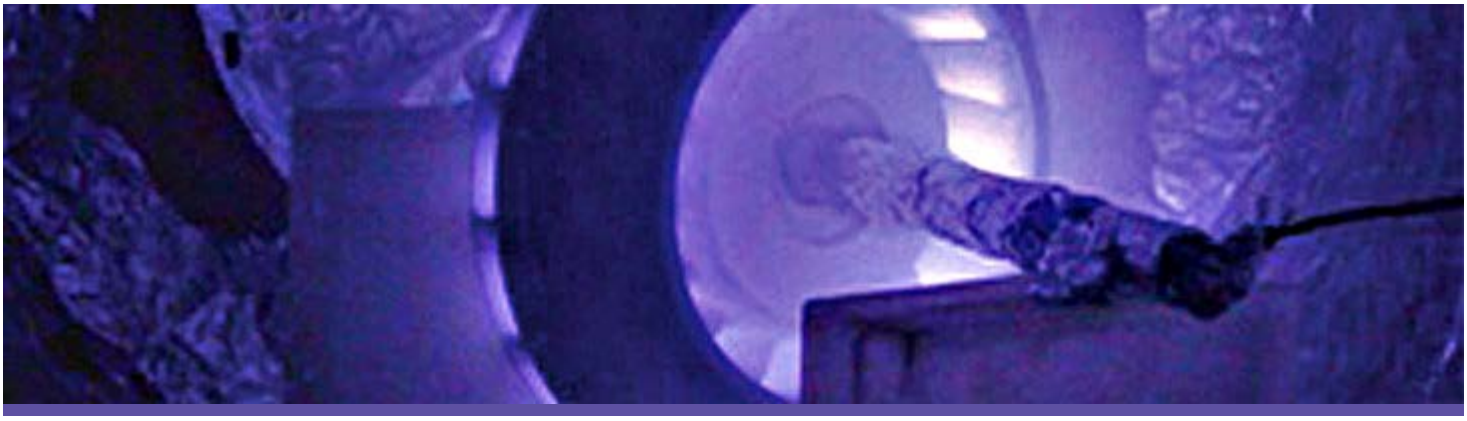

- Online Monitoring System to Detect Microbial Induced Corrosion, 18-R8445
- Dynamic Characterization of Soft Biological Tissues, 18-R8549
- Development and Evaluation of Low-Friction and Low-Wear Coatings for Automotive Valvetrain, 18-R8550
- Effect of Cyclic Relative Humidity on Environmentally Assisted Cracking, 18-R8554
- Evaluating Properties of Chemically-Aged High-Density Polyethylene Piping Material Used in Nuclear Power Plants, 20-R8432

SOUTHWEST RESEARCH INSTITUTE®

SwRI IR&D 2015 – Intelligent Systems, Advanced Computer & Electronic Technology, & Automation

- ROS-Industrial® Strategic Technology Development, 10-R8335
- Low Cost Accurate 6 DOF Industrial Robot Localization System Software Modeling and Testing, 10-R8443
- Cooperative Control of a Deployable Aerial Sensor Platform, 10-R8462
- Low-Cost Safe Gears for Robots and Prosthetics, 10-R8476
- ROS-Industrial® Robotic Product Singulation, 10-R8486
- Automated Perception and Robotic Targeting of Fluorescent Markers, 10-R8489
- Detecting Distracted Drivers Using Vehicle Data, 10-R8496
- Cooperative Framework for Negotiated System Integration Among Heterogeneous Vehicle Systems, 10-R8500
- LTE System Security Research, 10-R8505
- Telemetry System Manager Automatic Program Synthesis, 10-R8532
- Platform-Independent Evolutionary-Agile Optimization, 10-R8536
- Computational Performance Enhancements via Parallel Execution of Competing Implementations, 10-R8537
- Automatic Camera Calibration Algorithm Development, 10-R8546
- Traffic Profile Prediction, 10-R8548

- Automated Detection of Small Hazardous Liquid Pipeline Leaks, 10-R8552
- Radio Frequency (RF) Detection of Fire Source, 10-R8556
- Select Superoptimization of Finite Element Analysis Tools, 10-R8563
- Subtle Anomaly Detection in the Global Dynamics of Connected Vehicle Systems, 10-R8571
- Intelligent Propulsion System for Water-Borne Sensors, 20-R8431

SOUTHWEST RESEARCH INSTITUTE®

SwRI IR&D 2015 – Measurement & Nondestructive Evaluation of Materials & Structures

- Defect Characterization Using Guided Wave Technology, 18-R8436

SOUTHWEST RESEARCH INSTITUTE®

SwRI IR&D 2015 – Engines, Fuels, Lubricants, & Vehicle Systems

- FOCAS HGTR Design Evolution to a High Pressure Fully Transient System — Creation of the Full-Scale Gas Reactor, 03-R8427
- Identifying and Elucidating Low-Temperature Limiters to Catalyst Activity, 03-R8435
- Sampling System Investigation for the Determination of Semi-Volatile Organic Compounds (SVOC) Emissions from Engine Exhaust, 03-R8442
- Battery Duty-Cycle Decomposition for Cycle Life Analysis, 03-R8480
- Development of New Ruthenium Catalysts for the Low-Temperature Reduction of NO_X Emissions from Vehicle Exhaust, 03-R8488
- Methodology Development for I.C. Engine Tumble Port Evaluation, 03-R8494
- Effect of Jet Fuel Properties on Soot Mass and Solid Particle Number Emissions from Aircraft Engines: Development of a Fuel Particulate Matter (PM) Index Concept, 03-R8497
- Lubricant Impact on Fuel Economy — Correlation between Measured Engine Component Friction and Vehicle Fuel Economy, 03-R8502
- Experimental Investigation of Co-direct Injection of Natural Gas and Diesel in a Heavy-duty Engine, 03-R8522
- Detailed Characterization of Emissions from D-EGR Vehicle, and Evaluation of Synergistic Control Technologies, 03-R8547
- Combustion Chamber Design Optimization for Advanced SI Engines, 03-R8551
- Octane Index Effects on Fuel Economy, 03-R8555
- Determination of PAHs in Tires by GC/MS and NMR — A Method Comparison in Regards to

Meeting the EU's PAH Standards for the Tires, 08-R8402

- Determining the Sensitivity of Fuel Lubricity Additive Concentration on Test Parameters and Contact Geometry, 08-R8513
- Validating Using Laser Scan Micrometry to Measure Surface Changes on Non-Concave Surfaces, 08-R8562
- Microwave Methods for Enhanced Combustion in Natural Gas Engine Applications, 10-R8408

SOUTHWEST RESEARCH INSTITUTE®

SwRI IR&D 2015 – Geology & Nuclear Waste Management

- Hypothesis Testing for Subfreezing Mass Movements, 20–R8407
- Investigation Using Satellite-Acquired Multispectral and Synthetic Aperture Radar Data to Detect and Monitor Road Degradation for Heavy Truck Traffic, 20-R8413
- Developing Methodologies for Gravity-Assisted Solution Mining, 20-R8423
- Dynamic Response of Steel-Plate and Concrete Composite Small Modular Reactor Structures Under Explosive and Seismic Loads, 20-R8433
- Assessment of Thermal Fatigue in Light Water Reactor Feedwater Systems by Fluid-Structure Interaction Analyses, 20-R8434
- Developing Methods for the Rapid Evaluation of Pore Fluid Effects on Induced Seismicity, 20-R8456
- Mechanical Stratigraphy and Natural Deformation in the Permian Strata of West and Central Texas and New Mexico, 20-R8511

SOUTHWEST RESEARCH INSTITUTE®

SwRI IR&D 2015 – Fluid & Machinery Dynamics

- Testing and Analysis of Acoustically-Induced Vibration Stresses in Piping Systems, 18-R8478
- Desired Computational Enhancement for Our In-House Lattice-Boltzmann Method-Based Numerical Model for Applications in Oil and Gas Exploration and Biomedical Fields, 18-R8515
- Methodology for Qualifying Flow Regime of Two-Phase Flow within a Pressurized Compressor, 18-R8521
- Algorithms to Improve the Speed of the Numerical Model Based on the Lattice-Boltzmann Method, 18-R8541

SOUTHWEST RESEARCH INSTITUTE®

SwRI IR&D 2015 – Electronic Systems & Instrumentation

- Space-Based Communications Processing, 15-R8469
- Susceptibility of Processor Memory to Radiation Induced Faults, 15-R8531
- Low Cost Lighter-than-Air Flight Control System, 15-R8574

SOUTHWEST RESEARCH INSTITUTE®

SwRI IR&D 2015 – Chemistry & Chemical Engineering

- High Octane Number Gasoline Production from Lignin, 01-R8384
- Development of a Novel Drug-Loaded Composite Scaffold as Bone Graft Substitute Using Advanced Materials Technology, 01-R8415
- Evaluation of Anti-Bacterial Effects of Novel Formulations that Target an Essential Metabolic Pathway of the Agent of Lyme Disease, 01-R8487

SOUTHWEST RESEARCH INSTITUTE®

2015 IR&D Annual Report

Capability Development and Demonstration for Next-Generation Suborbital Research, 15-R8115

Principal Investigator
S. Alan Stern

Inclusive Dates: 01/01/10 – Current

Background — Research applications for new-generation suborbital vehicles include, but are not limited to, microgravity sciences, space life sciences, Earth and space sciences, land use, education and public outreach (EPO), technology development and demonstration, and space systems development and demonstrations (including TRL raising). The primary research advantages of these vehicles include more frequent access to the space environment, lower launch cost compared to conventional sounding rockets, capability for human operator presence, better experiment affordability, gentler ascent and entry compared to sounding rockets, extended periods of turbulence-free microgravity, and increased time in the 250,000 to 400,000 ft (80 to 120 km) region of the atmosphere (the “Ignorosphere”).

Approach — Our long-term business interests in these vehicles are:

- To exploit them for planetary, astronomical, microgravity, aeronomical, and auroral research.
- To provide research-related common systems (flight computers, data recording racks, etc.) and payload integration services to NASA and/or vehicle providers.
- And to provide instrumentation, payload specialists, and flight project expertise to research groups, both domestic and overseas, working in this area.

Therefore, the overarching objective for this project is to put SwRI in the lead of the burgeoning suborbital research field using next-generation, manned vehicles by becoming one of the first, and quite possibly the first, organization to fly payloads with research payload specialists on these vehicles. This will open up to SwRI a series of new business opportunities including funded research and hardware development projects, ground and flight system task-order contracts associated with next-generation suborbital work, and providing payload specialists for next-generation suborbital work.

Accomplishments — Flight experiments were selected (SWUIS-A for remote sensing; JSC biomed harnesses for life science work; BORE [Box of Rocks Experiment] for microgravity research). We secured personnel for SWUIS-A refurbishment, checkout, and calibration, and began refurbishment of the instrument. We completed the design and initiated construction of the BORE microgravity experiment. We received and test fitted a JSC biomed hardness that forms the basis of one of our three suborbital flight investigations. We initiated discussions with XCOR, Virgin Galactic, and Space Adventures regarding flight assignments, terms, and conditions on their suborbital vehicles. We constructed a flight requirements matrix to determine which flight providers are suitable for which of our experiments.

We completed a second set of F-104 training flights, with focused, in-flight investigations to (1) evaluate the wearability and function of the AccuTracker II biomedical harness with standard crew flight suits and life support equipment during typical g-loads, and (2) test the design concept for our BORE microgravity experiment during zero-g parabolas. We completed a zero-g

training flight that included initial zero-g training and team exercises to refamiliarize/practice personal mobility and experiment handling operations in zero-g conditions.

We completed construction of the BORE microgravity experiment. The Blue Origin configuration of the BORE microgravity experiment successfully passed vibration testing. FAA Class II and Class I medicals for each SwRI payload specialist were completed in order to maintain expected suborbital flight medical qualification standards.

We designed the SwRI Payload Specialist Team mission patch, and initiated discussions with two companies on a collaborative effort to test/evaluate a pressure suit under launch g-loads. We completed pressure suit familiarization training and undertook centrifuge training to test/evaluate the pressure suit under launch g-loads.

Figure 1: PI Stern and Co-I Durda completed pressure suit testing and centrifuge evaluation in Nov 2011.

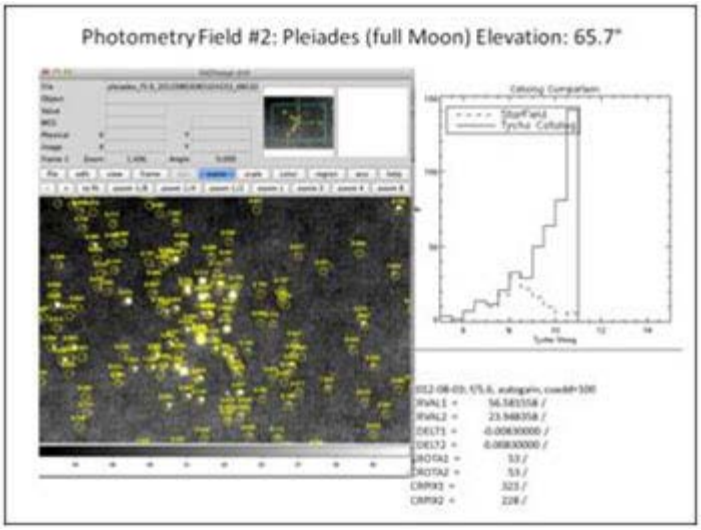

Figure 2: The SWUIS experiment was upgraded and re-calibrated during laboratory and field ops in Aug/Sep 2012.

We completed an upgrade and re-calibration of the SWUIS experiment for flight, and initiated planning for high altitude (75,000 ft) flight training in F-104 and F-18 aircraft. Additionally, we negotiated early flight test phase spaceflights with XCOR, and continued aerobatic jet aircraft training. We completed flight data requirements and collection plans for each suborbital experiment.

We requested and received flight integration requirements documents and initiated work to complete these documents, and clarified crew training requirements with both XCOR and VG.

We checked out all three of our flight experiments after over a year in storage. We built BORE and SWUIS experiment flight boxes and developed flight checklists, conducted a successful test of both experiments, and validated checklists in zero-gravity parabolic aircraft flights.

A two-year, no-cost extension was approved for this project in December 2014, extending the project to January 1, 2017. We conducted annual battery change for the biomonitor flight experiment (required annual maintenance to prevent loss of programmed settings).

We are preparing the BORE payload for flight aboard the Blue Origin suborbital vehicle in early spring 2016 (including cleaning and reconfiguring internal parts after the November 2013 zero-g test flight, reconfiguring for new data cameras provided by Blue Origin, reprogramming and testing the new flight software after delivery from Blue Origin of a new Benchtop Payload Controller, etc.).

The project is presently in a dormant state to conserve funds while waiting for the Virgin Galactic and XCOR vehicles to enter operational service in 2016/2017, at which time payload integration will commence and flight training will be completed.

SOUTHWEST RESEARCH INSTITUTE®

2015 IR&D Annual Report

Design and Development of an Optimized Far-field Acoustic Imager for Lightning Studies, 15-R8444

Principal Investigators
Maher Dayeh
Neal Evans
Stephen Fuselier

Inclusive Dates: 01/01/14 – 07/01/15

Background — Lightning and thunder are among the most fascinating visual and auditory displays on Earth. Surprisingly, these phenomena are still poorly understood, primarily due to the unpredictable and extreme circumstances associated with the lightning environment. Even though significant advances have been made toward understanding lightning over the last decade, a number of outstanding questions remain involving: (1) lightning initiation, propagation, and attachment and (2) thunder generation mechanisms and sources of acoustic emissions associated with lighting. Acoustic waves (thunder) measured at large distances from the lightning channel are strongly affected by atmospheric propagation, making it impossible to infer the original properties of the source. Studies close to the lightning channel negate much of the atmospheric attenuation and propagation path effects and should reveal acoustic properties of the initial shock and its early evolution. The goal of this project is to design, develop, and test an acoustic imager that investigates sound sources close to and along the length of the lightning channel. The acoustic imager is also a proof-of-concept for the feasibility of imaging the sound sources that comprise the thunder that we hear.

Approach — To achieve our goal, we use a microphone array and beamforming signal processing to create a uni-directional reception pattern that accepts signals (sound) from specific directions. The pattern can then be steered vertically along the lightning channel. The imager is tested using rocket-triggered lightning at the International Center for Lightning Research and Testing (ICLRT) at Camp Blanding, Fla. The imager consists of an array of 16 free-field microphones (PCB 130E20) that are phase-matched, have sufficiently wide frequency response (20 to 20,000 Hz), and are useable from 30 to 122 dB. Once deployed, the microphones are covered with rubber caps, which provide attenuation, protection from rain, and wind noise reduction. The array is 15 meters long and is made of 8020 structural aluminum beams, raised over several tripods and anchored to the ground.

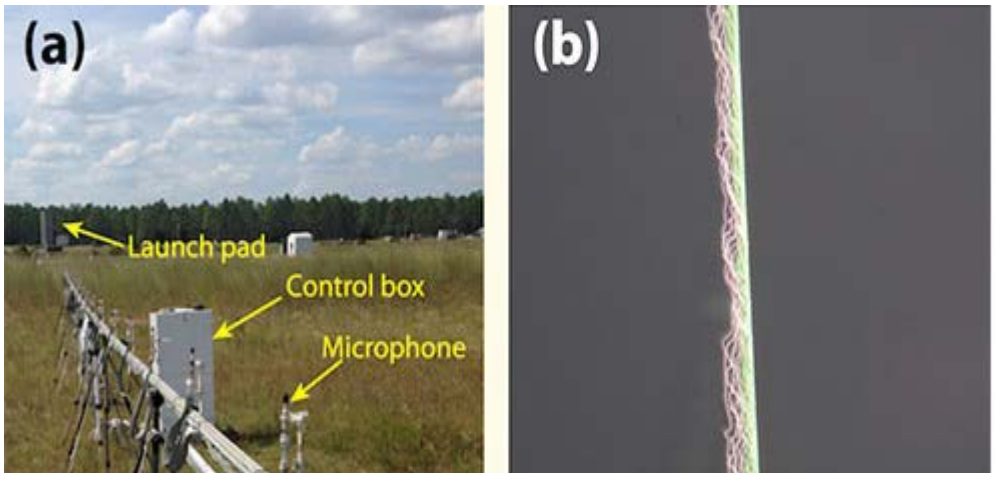

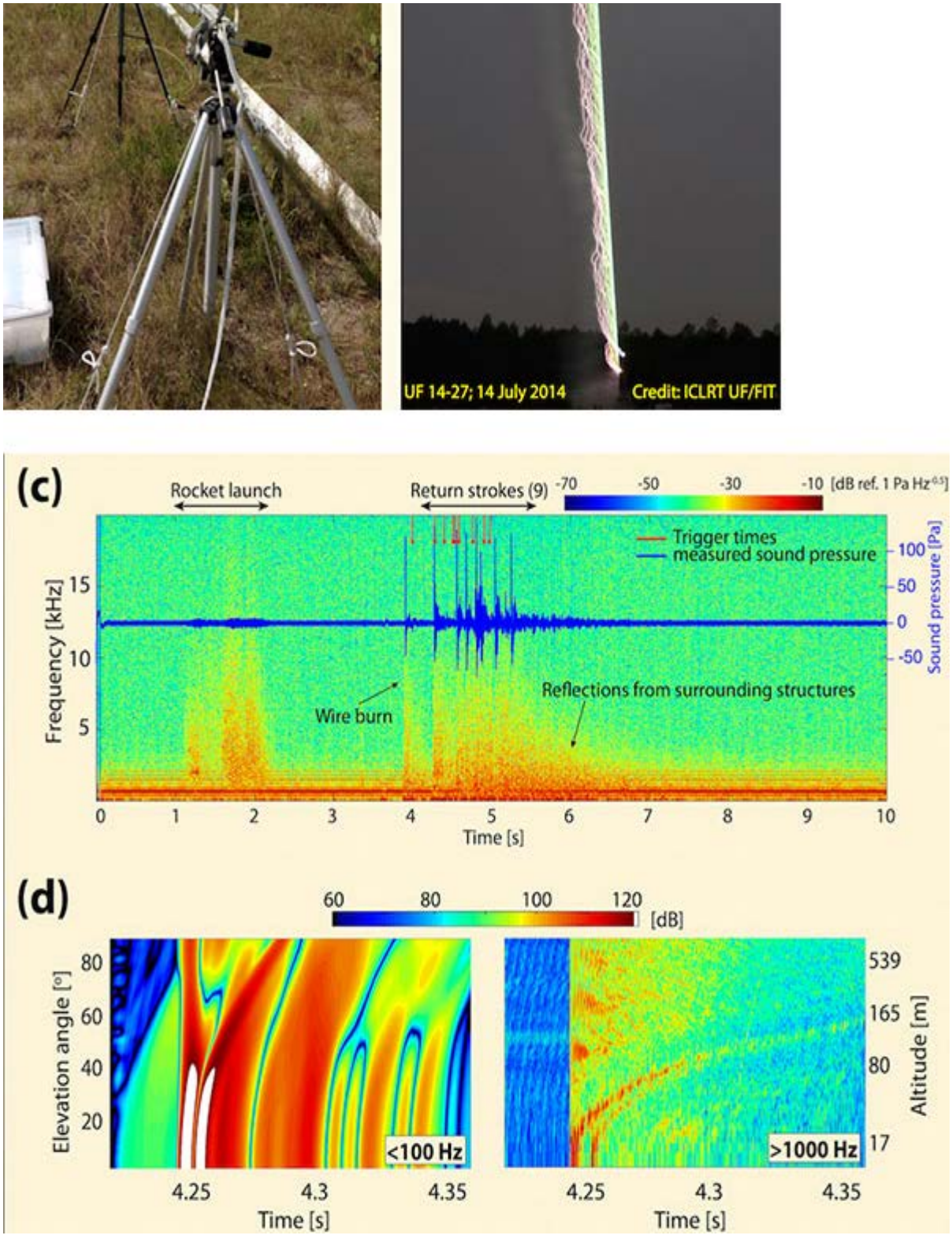

Figure 1: (a) Photograph of the acoustic imager facing the rocket-triggered lightning launch pad. (b) A six-second exposure photograph of the triggered lightning event. (c) Spectrogram and time series of the acoustic record as measured by the first microphone. (d) Constructed beam-steered images of the first return stroke at two different frequency ranges.

Accomplishments — During summer 2014, the imager was deployed at the ICLRT and oriented in an end-fire position facing the triggered lightning rocket launch pad (Figure 1a). A total of 11 successful triggered lightning events were measured, comprising 41 total return strokes (RS). Detailed analysis of a triggered event with 9 RS showed a successful proof-of-concept, and provided the first-ever image of thunder [Dayeh et al. 2015]. The results made scientific headlines and were reported in numerous news

portals worldwide. Figure 1b shows a six second-exposure photograph of the triggered lightning event. The initial copper wire burn glows green, while nine subsequent return strokes are more purplish. Figure 1c shows the spectrogram of the acoustic record with clear signatures of the rocket launch and the associated RS. Figure 1d shows the reconstructed beam-steered acoustic images of the first RS at low and high frequencies. The "curved" appearance of the RS signature at high frequencies is associated with sound speed propagation effects. Figure 2 shows a close up of the lightning event along with the acoustic image of the first RS (inset), corrected for sound speed propagation and atmospheric absorption effects, thus visualizing the sound coming out from the lightning channel. The journal *Nature* has selected this illustration to be featured in its “Images of the Year” special edition.

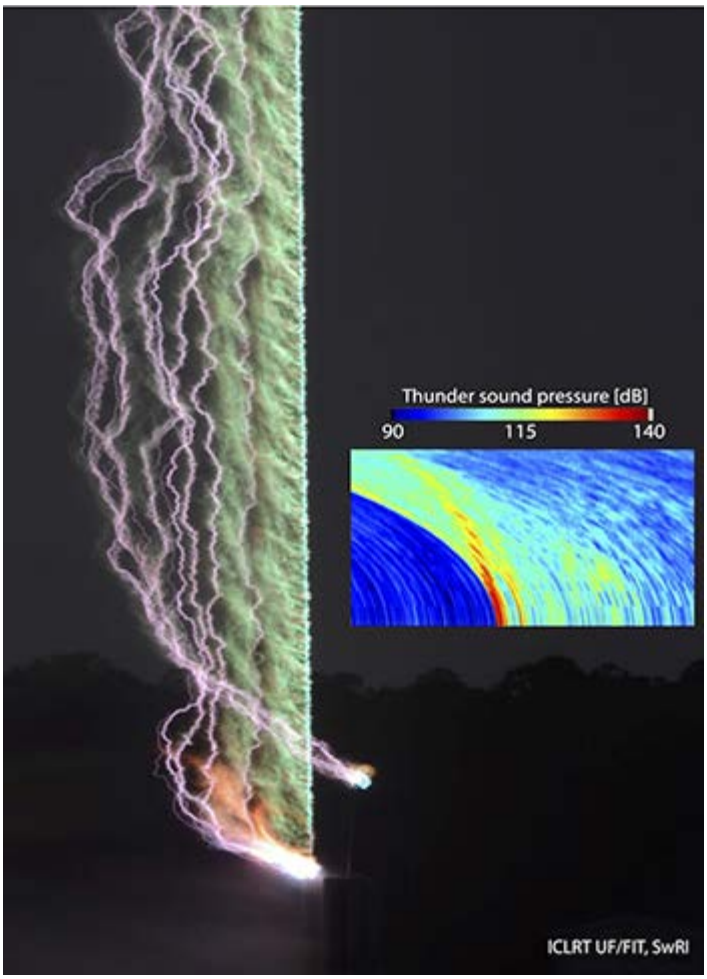

Figure 2: Photograph of a triggered lightning event and the first-ever acoustic image of thunder (inset), constructed from the first return stroke.

SOUTHWEST RESEARCH INSTITUTE®

2015 IR&D Annual Report

Design and Analysis of Device to Capture Stratospheric Air Samples, 15-R8446

Principal Investigators
Kathleen Mandt
Edward Patrick
Ryan Blase
Wendy Tseng
Kristin Favela
William Williamson

Inclusive Dates: 01/01/14 – Current

Background — This work is a collaborative effort between two SwRI research divisions to design and analyze a device to collect atmospheric samples in the Earth's upper atmosphere. The purpose of this device is to address a serious gap in Earth atmospheric measurements needed to understand the energy balance, transport, and chemistry in the upper atmosphere. The device will include two components. The first is AirCore®, which collects columns of air during descent from high altitudes in a manner that preserves an altitude profile of constituents such as carbon dioxide, methane, and nitric oxide. This device has been proven up to altitudes as high as ~30 km. The second component is a discrete sampling device that will collect air samples of 1L in volume for laboratory analysis of isotopic composition.

Approach — The project had four objectives:

- What is the upper altitude (or lower pressure) limit of AirCore?
- What is the amount of fractionation that takes place as air enters and within the AirCore tube as a function of pressure?
- What is the upper altitude limit for collecting a discrete sample as a function of flight vehicle descent velocity?
- What other greenhouse gases can be measured using the device?

Accomplishments — We completed the initial setup of the system for evaluating the AirCore and conducted tests to characterize the system. In the process of characterizing the system, we found preliminary evidence for mass fractionation in the column and have determined the fill time for the column under static conditions. Further tests showed signs of significant diffusion suggesting that there is a lower pressure limit for use of AirCore.

2015 IR&D Annual Report

Testing of Prototype Mass Spectrometer for Earth Atmospheric Studies, 15-R8475

Principal Investigators
Kathleen Mandt
Greg Miller
Myrtha Haessig
Jorg-Mich Jahn

Inclusive Dates: 06/18/14 – 10/18/14

Background — The NASA sounding rocket program provides the ideal opportunity to prove the flight-readiness and scientific capabilities of instruments that currently lack the flight heritage required for major NASA missions. The goal of this project was to propose a simplified configuration of an SwRI-built mass spectrometer for *in situ* measurements in support of a NASA sounding rocket project. The NASA project requires measurements of the total neutral density and the composition of neutrals in the region above 250 km. Neutral composition is poorly understood in this region of the atmosphere due to a serious gap in measurements. At the present time, atmospheric models are the only method for estimating composition at these altitudes, and these models are subject to large uncertainties because no composition measurements have been made since the 1980s. Currently, the predictions for atmospheric density and temperature can only be validated with satellite drag data, which determine the total mass density (in kg/m^3) of the exosphere based on the drag induced by atmospheric particles on a satellite. They do not provide the composition of the atmosphere as a function of altitude. Recent estimates of the composition of the winter polar exosphere have found differences between densities estimated by satellite drag measurements and atmospheric models that ranged between 25 and 70 percent.

Approach — The primary objective of this project was to characterize the operation of a linear time-of-flight mass spectrometer (TOF-MS) for the simultaneous detection of hydrogen, oxygen, nitrogen and carbon dioxide at the range of pressure regimes expected during a sounding rocket ascent and descent stage. This effort was used to establish the required data integration times and leak rates into the analyzer for the measurement of the compounds of interest above 250 km. Completion of this project required four primary tasks:

- Preparing the Multi-Bounce Time of Flight (MBTOF) to be calibrated in linear mode
- Calibrating of MBTOF in linear mode for relevant gas mixtures
- Testing of the pulser under vacuum
- Testing of the power supply under vacuum

Accomplishments — Each of the proposed tasks was completed successfully. We were able to demonstrate that the mass resolution of the linear TOF-MS was clearly sufficient to resolve H, H_2, and He, as well as N_2, O_2 and CO_2. The sensitivities were determined for each of the constituents relevant to the science measurements proposed and were found to be sufficient for the LCAS proposal. Both the pulser and power supply operated successfully under vacuum.

2015 IR&D Annual Report

Technology Development for the High Energy Polarimeter (HEP) Instrument Detector, 15-R8483

Principal Investigator
Steven Myers

Inclusive Dates: 07/28/14 – 11/28/14

Background — SwRI, University of New Hampshire (UNH), and Goddard Space Flight Center (GSFC) teamed to submit an astrophysics proposal under the NASA Astrophysics Small Explorer (SMEX) Announcement of Opportunity, NNH14ZDA013O. The title of the proposal was POlarimetry of Energetic Transients (POET). The proposal was submitted on December 18, 2014. The proposed mission included two instruments: High Energy Polarimeter (HEP) and Low Energy Polarimeter (LEP). The HEP instrument is a collaboration between SwRI and UNH, of which the HEP Detector Module (HDM) was at a lower than TRL-6 level. The purpose of this project was to design, build, and test a prototype of the HDM, subjecting it to relevant spaceflight environments to increase the Test Readiness Level (TRL) level to TRL-6.

Approach — SwRI designed both the scintillator-PMT package and the detector module housing to serve as the mechanical prototype. SwRI oversaw the detector module fabrication of a full, 49-cell housing using the UNH machine shop. SwRI procured a total of eight PMTs, four plastic scintillators, and four CsI(Tl) scintillators. SwRI successfully packaged the eight scintillators and PMTs and partially populated the detector module housing. The remaining 41 slots in the detector module housing were populated with mass simulators from UNH. UNH successfully provided the electronics to functionally test the units. SwRI took the detector housing to BAE Systems, located in Merrimac, N.H., and subjected the unit to three-axis vibration testing to Orbital Pegasus acceptance levels. UNH then subjected the detector assembly to three cycles of thermal vacuum testing using the UNH thermal vacuum facility. UNH provided the pre- and post-functional testing as well as functional testing during the thermal vacuum testing.

Accomplishments — The prototype HDM passed environmental testing. The full functional test (FFT) data showed no degradation in functional performance of the active elements. One element (G1) did not show the expected behavior; however, this element had abnormally low gain and would have been rejected for this reason during a flight build. The light output of CsI(Tl) depends slightly on the temperature, and this is seen in the shifts of the G element photopeaks. The shifts were as expected. The unit successfully passed the TRL-6 qualification. On September 1, 2015, the POET team received a written and verbal debrief from NASA Headquarters on the reason why the POET proposal was not selected for funding. The work under this project was cited as major strength to the proposal: "A prototype representing the form, fit, and function of the High Energy Polarimeter Detector Module (HDM) has been successfully tested for vibration, vacuum, thermal, and performance. This establishes TRL 6 for the HDM."

SOUTHWEST RESEARCH INSTITUTE®

2015 IR&D Annual Report

Capability Development of Supernova Models, 15-R8498

Principal Investigators
Amanda J. Bayless
Peter W. A. Roming
Robert Thorpe

Inclusive Dates: 10/01/13 – Current

Background — One of the most crucial processes for shaping the composition of the universe is the death of massive stars (> 8 M_{Sun}) manifested as supernovae (SNe). Understanding this process is important as it has significant impacts on our understanding of cosmology, chemical enrichment, galaxy evolution, star formation rate, stellar evolution, compact object remnants, circumstellar medium, and dust formation. The computing speed and resources are now such that more complicated and more realistic models of SNe are being produced. Additionally, in the coming years >100,000 core-collapse SNe per year are expected to be discovered. The SuperNovae Analysis aPplication (SNAP) is a new tool for the analysis of SNe observations and validation of SNe models. A system of databases, SNAP will house all archived observations for all SNe events and will also house verified models of SNe spanning a wide range of parameter space. This system will allow for new SNe observations to be uploaded and immediately compared to the available models to constrain parameter space. This system also allows new models to uploaded and compared to all archived observations to test for validity all within a few hours, saving months of work.

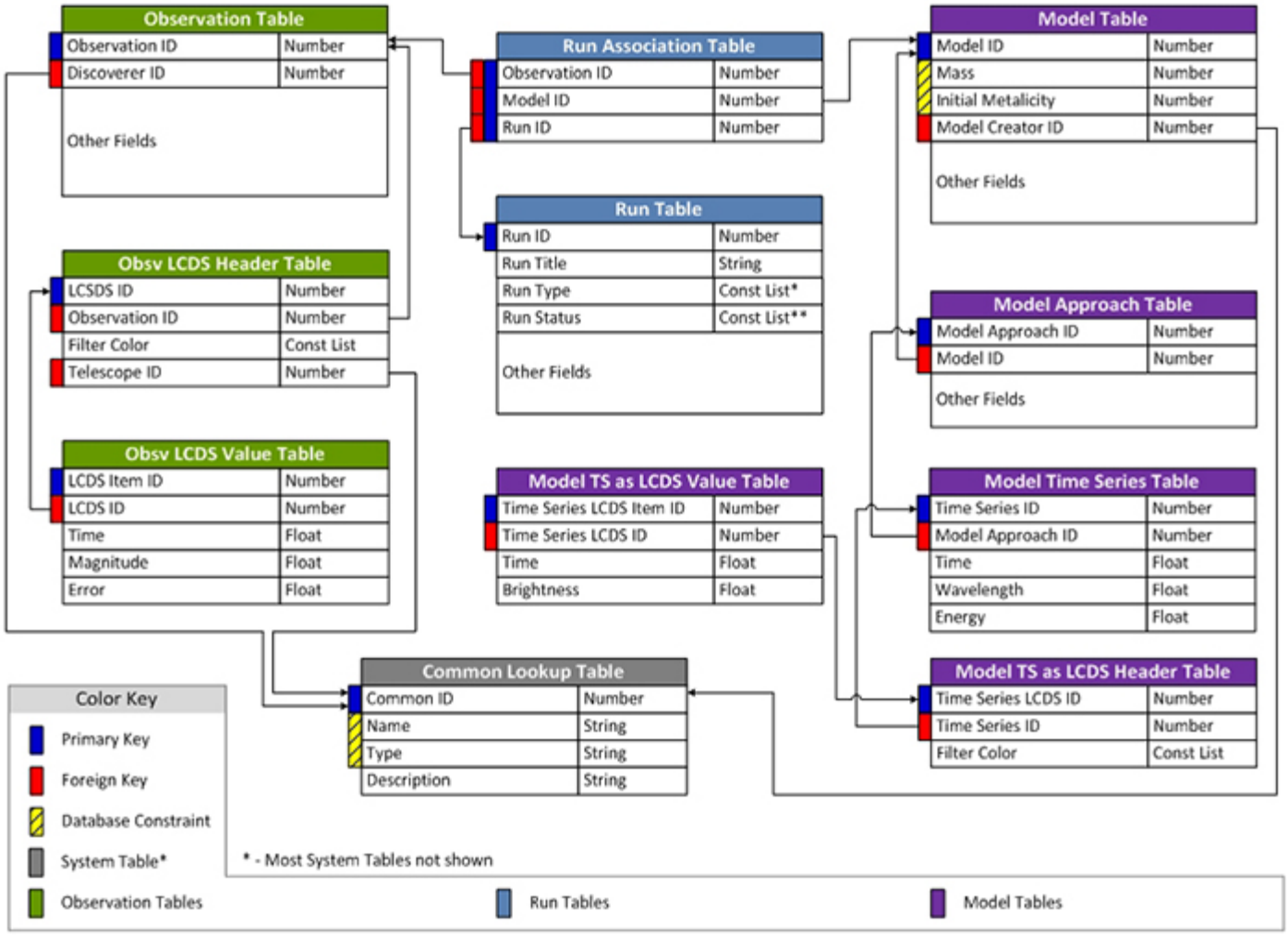

Figure 1: High-level SNAP database structure used to perform the SN analysis.

Approach — The SNAP software consists of three main components: a) database, b) web application and c) software functions to export observations and models and import runs and run associations (Figure 1) and is hosted on SwRI computers. The mock-up of the web application is available at http://snap.space.swri.edu/index.html and will be the host for the full application, which is under construction.

Accomplishments — The current state of the SNAP database is a skeleton system that uses the archived observations from the Swift Observatory and models from Los Alamos National Laboratory. Simulated results from the data analysis of SNAP are given in Figure 2. Each model fit is run though a χ^2 statistical test. The best fitting model light curve in the database is given as a potential solution (or an initial constraint on parameter space) and plotted against a given event. This project has resulted in a three-year, $330,000 contract from NASA to further develop this SNAP system.

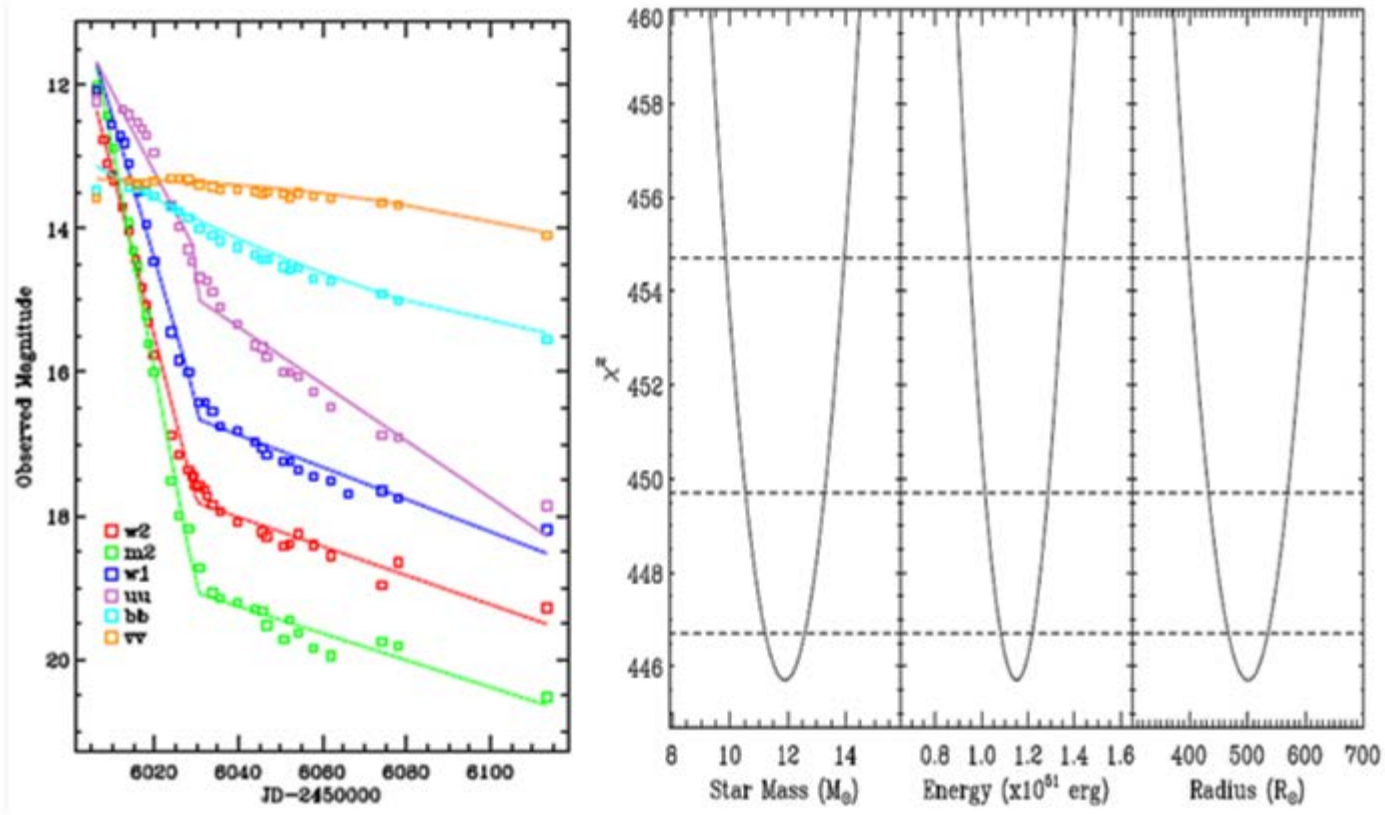

Figure 2: (left) Swift light curves of SN2012aw (squares; Bayless et al. 2013) with a simulated model (line). The error in the Swift light curves are approximately the size of the data points. (right) Simulated χ^2 curves from the model for three of the available parameters. The minimum value is the best solution. The intersections of the dotted lines with the curve give the 1σ, 2σ, 3σ error in the fit.

2015 IR&D Annual Report

Acoustic Measurements of a High Mass-Flow Cold Jet, 15-R8510

Principal Investigators
Maher Dayeh
Neal Evans

Inclusive Dates: 12/04/14 – 04/04/15

Background — Aerodynamic noise is an un-avoidable byproduct of high velocity gas flow in numerous technical applications, including commercial and military aircraft, rockets, and subsonic jet flows in several industrial piping systems. This noise poses direct health issues to working crews and creates unnecessary noise to nearby communities. Characterization of the acoustic field created by fast jets in duct systems enables us to better understand sound propagation modes and eventually model, predict, and reduce the loud noises at nearby distances.

During 2014-2015, work was underway to investigate the feasibility of acoustic imaging of lightning using microphone arrays (project 15-R8444). At the same time, another project aimed at investigating acoustically induced vibrations (AIV) in high-flow piping systems was being performed by researchers at the SwRI gas blowdown facility (project 18-R8478). The researchers realized that setups from both projects would enable the acquisition of a unique acoustic dataset in which the cold jet acoustic field could be characterized.

The goal of this collaborative project was to deploy the acoustic imager used in R8444 to characterize the internal and external acoustic signatures associated with the vibrational tests proposed in R8478, hence creating a complementary dataset and maximizing both projects.

Approach — To achieve the goal of this project, we proposed to carry multiple acoustic measurements in front of a cold flow jet using different acoustic array configurations. The results would enable us to:

1. Characterize the tradeoffs between dissipation effects and nonlinear effects in a multi-jet source.
2. Characterize the noise field at different radial distances and exhaust normal angles.
3. Provide external acoustic measurements for the jet relief valve noise.

To achieve (1) and (2), we planned on carrying a series of measurements using endfire, broadside, and radial alignments of the microphone array. To achieve (3), we planned a broadside configuration at a distance of one meter from the relief valve location.

Accomplishments — During the period between November 2014 and December 2014, 15 blowdown tests were performed and their acoustic signatures had been recorded. The experimental part of the work was a success. However, post-processing analysis revealed an electronic issue that appeared to affect some of the measurements due to an unexplored DAQ problem (during continuous recordings for long times at fast sampling rates). This has partially affected our plans of performing all of the anticipated analysis. Nonetheless, we were able to successfully finish the valve noise measurement. Results showed a significant reduction in high-frequency energy when comparing internal to external valve-generated noise, with peak transmission occurring in the frequency range of the most strongly excited pipe modes (approximately 100 to 1,000Hz). The average transmission loss was approximately 90 dB.

Analysis on other intended objectives was partially performed and the results are non-conclusive. Further testing and thorough analysis are required to understand and quantify the electronic response that appeared to affect the acoustic measurements during long continuous recordings. A proposal to an

external agency is currently being prepared to expand on the work.

2015 IR&D Annual Report

Viability of a Blended Redundancy Concept for Constrained Spacecraft Applications, 15-R8535

Principal Investigators
Jennifer L. Alvarez
Buddy Walls

Inclusive Dates: 03/02/15 – 07/02/15

Background — Prior to execution of this research, we formulated concepts for what we consider to be a unique approach to redundancy in spacecraft electronics. This unique redundancy concept is directly applicable to avionics for many spacecraft manufacturers and to the growing business area of SwRI space-based solid-state recorder technology currently in development for NASA and Department of Defense clients. The purpose of the research was to address key risk items in the technical approach of this blended redundancy concept and to advance the technology so that it encompasses applications beyond specific avionics configurations. The goal of this research was to develop, document and protect SwRI-owned intellectual property that can be applied to multiple application areas and that can be claimed as background intellectual property on upcoming proposals.

Approach — The technical approach analyzed the trades of warm- and cold-sparing redundancy concepts in terms of reliability, the complexity of emergency controller software, and the physical implementation of the solution. Further, approaches for cross-strapping redundant inputs to the avionics that allow for selective cross-strapping and redundancy based on mission requirements were assessed. The research abstracted the problem to a use case that represents a notional set of elements common to many spacecraft architectures for the purposes of the investigation.

Accomplishments — The successful execution of this project positions SwRI to offer a unique and flexible approach to redundancy in spacecraft avionics and solid-state recorders. We have shown that this approach is more efficient and flexible in terms of the power, mass, and cost of the electronics, plus in spacecraft harnessing, which is widely recognized as a major contributor to mass in spacecraft and cost in integration and testing activities. The SwRI blended-redundancy approach provides similar system reliability for candidate five-year Geostationary Earth Orbit or Deep Space missions as traditional, less cost-efficient avionics redundancy architectures. We believe that these benefits will be attractive to SwRI clients and will establish a strong position for SwRI in future competitive proposals. Significant benefits of the SwRI approach over traditional approaches include:

- Reduced number of unique board designs compared to a traditional fully redundant approach.
- Internal cross-strapping for reduced spacecraft and test cable harness complexity and mass.
- Ability to repurpose internal cross strapping at build-time to provide additional independent circuits to maximize interface density.
- Reduced non-recurring engineering costs.
- Reduced test equipment costs.
- Reduced recurring engineering costs.
- Reduced testing complexity.

SOUTHWEST RESEARCH INSTITUTE®

2015 IR&D Annual Report

Augmenting a Novel Magnetohydrodynamics Code for Studying Astrophysical Plasmas and Space Weather, 15-R8568

Principal Investigators
Derek A. Lamb
Craig E. DeForest
Timothy A. Howard

Inclusive Dates: 07/01/15 – Current

Background — Magnetohydrodynamics (MHD) is the study of electrically conductive, magnetized fluids. Much of the Universe, including the solar atmosphere our group seeks to understand, exists in a state in which the equations of MHD apply. Real MHD systems are too complex for analytic solution, and so researchers turn to simulations of these systems. Conventional finite-difference plasma simulations are hundreds to thousands of times more dissipative (electrically resistive) than the real solar plasma, so conventional simulations use far finer grids than are necessary to represent the system under study. This makes simulations computationally expensive, and severely limits the fidelity with which conventional simulations can represent electric-current-bearing systems on the Sun, such as solar flares and the magnetically stressed regions that release coronal mass ejections (CMEs). With prior internal and external funding, we have developed Field Line Universal relaXer (FLUX) code, which reformulates the equations of MHD to take advantage of the analogy between magnetic field lines and the magnetic fields they represent. Our approach discretizes the magnetic field, automatically preserves the magnetic field topology, and results in a thousandfold increase in efficiency compared to conventional codes.

Approach — The objective of this project is to augment FLUX to enable it to solve two new classes of problem: CME eruption and solar wind evolution. All of the previous results obtained with FLUX have been under the approximation that the plasma gas pressure is negligible compared to the magnetic pressure. Enabling these new classes of problem requires three specific augmentations to FLUX: 1) verify and demonstrate the correct treatment of mass by the code in the case of quasi-stationary, quasi-one-dimensional flows; 2) change the modeling engine to allow for non-quasi-stationary flows by adding an inertial term to the force balance equation that FLUX solves; 3) verifying and refining the existing module that implements magnetic reconnection.

Accomplishments — Prior to the start of this project, the FLUX code had been dormant for several years. Our initial efforts have centered around implementing and testing the code on modern hardware, software, and development platforms, updating and improving the documentation, and bringing the existing code in line with modern coding standards. We have performed several relaxations of simple test systems while working to complete the first augmentation. The Figure shows one of these tests, a relaxation of a simple twisted magnetic flux rope.

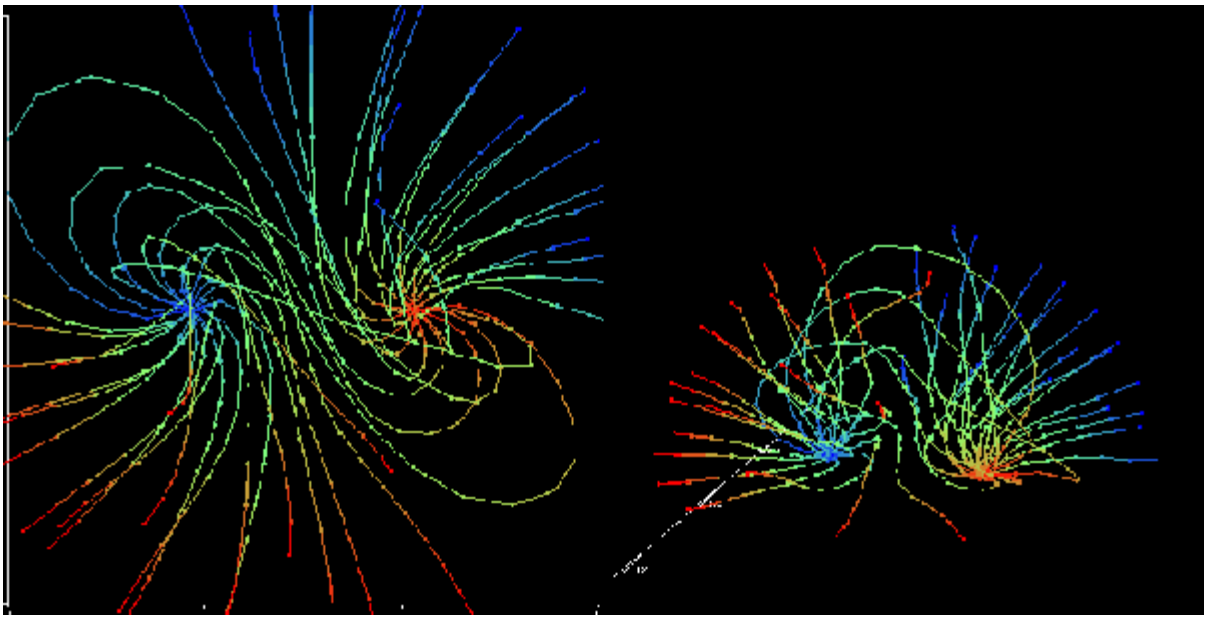

Figure 1: Two views of a relaxed state of a simple FLUX system consisting of a single twisted magnetic flux rope. The colored lines are the sole elements of the simulation, and each represents a finite quantity of magnetic flux. Closed magnetic field lines start and end in the red and blue footprints. As the system relaxes and loops cross the simulation's upper hemispherical boundary (not shown), the loops are held open on that boundary.

2015 IR&D Annual Report

Stratospheric Compressor for Lighter-than-Air Vehicles, 15-R8575

Principal Investigators
James Noll
Grant Musgrove

Inclusive Dates: 07/13/15 – Current

Background — A vehicle with trajectory control and persistent operation capabilities up to 120,000 feet altitude does not currently exist and is a game-changing technology sought for military and scientific applications. The extremely low air density and steady winds at these altitudes make station-keeping with a single aircraft or lighter-than-air (LTA) vehicle impractical. However, a network of LTA vehicles with limited trajectory control can transit through an area of interest and achieve persistence over an area as a collective group. Low power directional control of the LTA vehicle can be achieved by exploiting wind differences at different altitudes. Technology that enables efficient movement of air into and out of an LTA vehicle's ballonet allows repeatable altitude changes for long duration flights.

Approach — The objective of this research is to determine and characterize the best method to add air mass to an LTA vehicle for altitude and trajectory control applications in the stratosphere. A matrix of performance parameters for compressors that facilitate altitude control of LTA vehicles was generated. Preliminary design concepts for the compressor aerodynamic flow path were developed using a one-dimensional analysis. The results of this preliminary design were used to formulate initial requirements and size the supporting systems for the stratospheric compressor. A review of the overall system feasibility concluded that further study was warranted in a second phase of study.

In Phase II, the preliminary aerodynamic flow path developed will be simulated in three-dimensional space using computational fluid dynamics (CFD). The performance capabilities will be revised and the derived requirements for the supporting systems will be updated. An integrated modeling tool for sizing the compressor and its subsystems will be created, with particular emphasis on overall compressor system mass and power requirements as a function of altitude and desired air flow rate. In parallel, a preliminary design for test equipment and procedures to assess compressor performance characteristics will be generated.

Accomplishments — In Phase I of this project, preliminary compressor designs for buoyancy control at high altitudes were created. Feasibility of the designs was assessed based on mass and power of compressor systems. Findings in Phase I indicate there are viable compressor designs for achieving trajectory control of an LTA platform suited for small commercial and military payloads intending to fly over specific targets, as well as large scientific payloads with capability to steer away from population centers. Phase II is in progress and will validate assumptions made in the initial aerodynamic modeling, perform more rigorous study of heat management, and develop test methodology for performance evaluation of stratospheric compressor systems.

SOUTHWEST RESEARCH INSTITUTE®

2015 IR&D Annual Report

Investigation and Measurement of Balloon Dynamics at the Apex and Base of a Scientific Balloon, 15-R8577

Principal Investigators
I. Steve Smith, Jr.
James Noll
Brock Martin
Ethan Chaffee

Inclusive Dates: 07/10/15 – Current

Background — The large balloon reflector (LBR) (Figure 1) is a 10-meter aperture (20m diameter), inflated, spherical THz antenna designed to fly on a large scientific balloon at 120,000 to 130,000 feet. The realization of a large, near-space, 10-meter class reflector for THz astronomy and microwave/millimeter-wave remote sensing and telecommunications has long been a goal of NASA and the DoD. The LBR is one of 12 concepts selected in 2013 out of ~550 submissions by the NASA Innovative Advanced Concept (NIAC) program to conduct a fast-paced design study. The LBR team consists of SwRI, University of Arizona (UA), Applied Physics Laboratory (APL), and Jet Propulsion Laboratory (JPL). The concept was originally conceived between UA and SwRI.

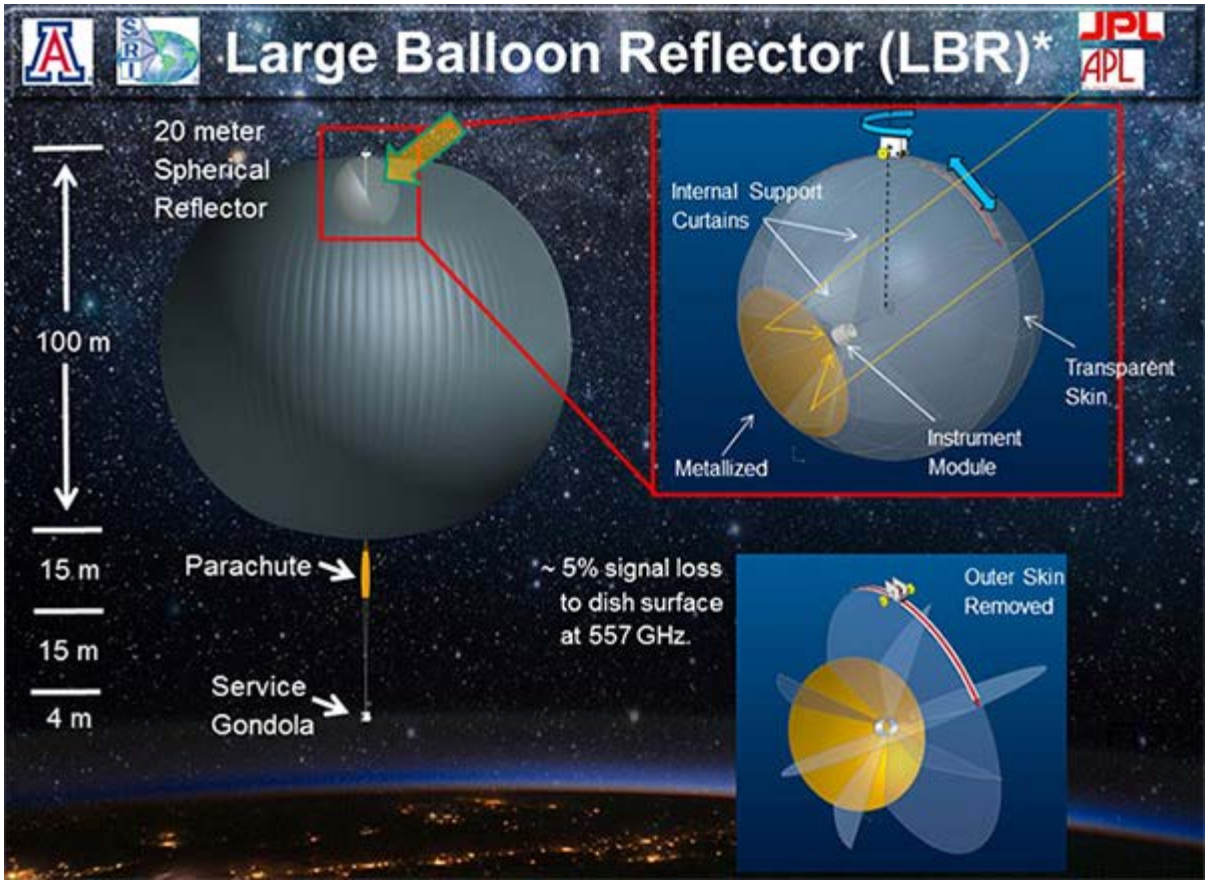

Figure 1: Large balloon reflector concept

LBR has won both Phase I and II funding under the NIAC program. During our Phase II mid-term review on April 27, 2015, the review panel wanted to see quantitative evidence that locating LBR within the carrier balloon instead of tethering it below the payload gondola provided a sufficient pointing stability advantage to warrant the additional operational complexity. Since there is little or no data for the balloon apex dynamics or simultaneous data between the apex and a suspended payload, additional data was needed. In late May, NASA's Science Mission Directorate authorized a free piggyback balloon test flight so we could obtain the required data. This was contingent on us getting flight instrument packages flight ready in time for the flight in late August; the next opportunity would not occur until a year later. They indicated that once we have this data in-hand, we would be in a strong position to propose and obtain funding to fly a LBR engineering model.

Approach — The objective of this project was to develop two flight packages to obtain simultaneous dynamics data from both the apex of a balloon and its suspended payload under the same flight conditions. This data would then be used to quantitatively answer the question of whether it was better to place the LBR at the balloon apex or from the payload. To accomplish this task, we needed to:

1. Construct small, efficient instrument packages using COTS hardware to be flown at the apex of a scientific carrier balloon and on the payload gondola suspended below it. The packages will leverage the experience and hardware gained in recent SwRI efforts and will contain accelerometers, inclinometers, temperature sensors, and cameras. The instrument packages will be used to measure the flight dynamics data (three-axis accelerations, rotations, magnitudes, rates, frequency, modes, etc.).
2. The measured dynamics data will be used to constrain and validate numerical models. We will perform a differential analysis of the relative merits of locating LBR in the top of the stratospheric balloon or tethered below the payload gondola. These results will be used to position us for the next phase of development and funding.

Accomplishments — We were able to successfully design, fabricate, test, and integrate two LBR sensor packages (LBRSP): an up-looking balloon apex and a down-looking gondola sensor. As part of the package, we were also able to integrate a UA star camera (Figure 2). Both packages, apex and gondola, were able to link and transmit data to each other via an onboard Wi-Fi for data redundancy in the event one was damaged or lost.

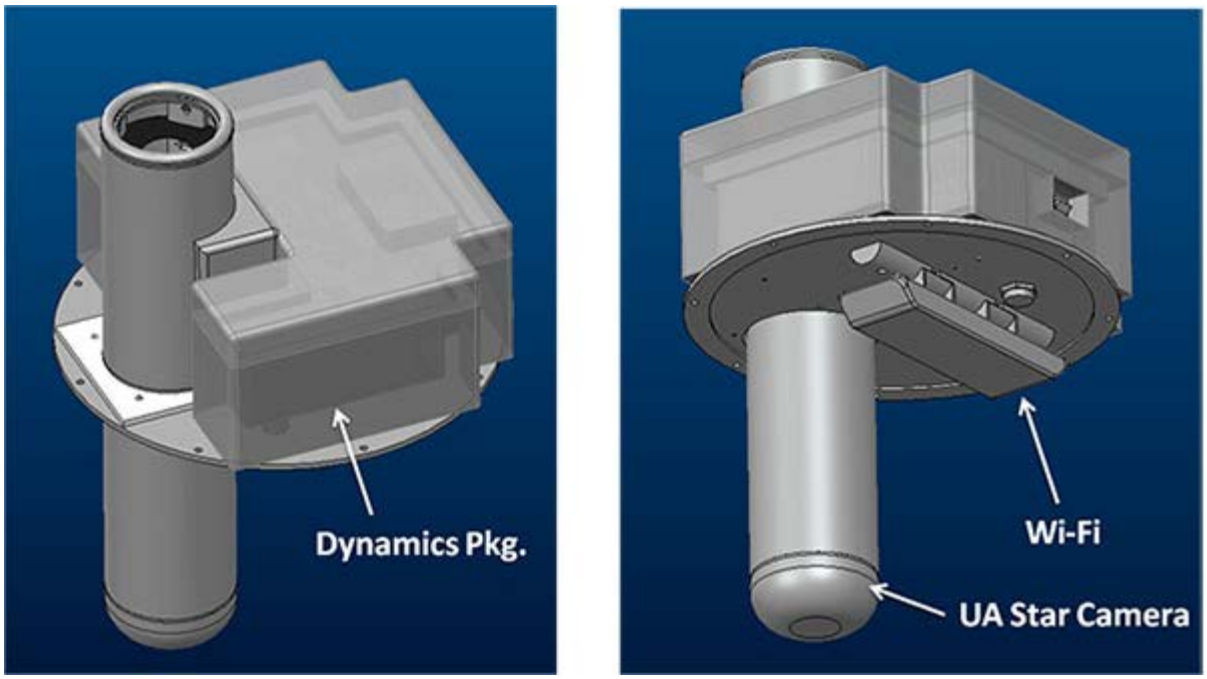

Figure 2: LBRSP mechanical layout

The NASA piggyback flight was conducted from Fort Sumner, N.M., on September 4, 2015. An image of the balloon and gondola can be seen in Figure 3. The LBRSPs were able to acquire, record, transmit, and receive data for the entire flight lasting a total of 7.5 hours, including the ascent, float, and descent. All instrumentation was successfully recovered.

Figure 3: Balloon and gondola just before launch

Initial data analysis has been completed adequately to successfully fulfill the objectives of this effort. The apex data shows that there are several oscillation modes at the apex of the balloon, but all of these modes have periods longer than 5 seconds. The strongest modes are at 8.2 sec., 22.5 sec., and ~300 sec. These are relatively low frequencies that are easier to compensate in a pointing system. The gondola jitter is much more pronounced than the apex. The gondola shows several short period oscillations between 2.0 and 0.8 seconds that are much more difficult to compensate with a pointing system. In summary, from a pointing control point of view, it is preferable to have the LBR at the balloon apex than suspended from the gondola.

SOUTHWEST RESEARCH INSTITUTE®

2015 IR&D Annual Report

Online Monitoring System to Detect Microbial Induced Corrosion, 18-R8445

Principal Investigators
Todd Mintz
Amy De Los Santos
Spring Cabiness
Larry Miller

Inclusive Dates: 01/01/14 – 12/31/14

Background — Microbial-induced corrosion (MIC) is a phenomenon whereby microorganisms presence and activities result in the degradation of a material or component. In particular for the oil and gas industry, various bacteria have been linked to accelerated corrosion. Because of the detrimental effect that MIC can have on infrastructure, pipeline inspection methodologies to monitor this type of corrosion are required. However, current inspection methodologies are time consuming and costly. Thus, online detection systems for MIC are of great interest.

Approach — The objectives of the project are to develop a new *in-situ* technique to monitor MIC using surface enhanced Raman spectroscopy (SERS). Raman spectroscopy works via a coupling between incident laser light (visible, near infrared, or ultraviolet) with molecules at the surface of a material. Interactions between the laser light and surface molecules results in a shift in wave number of the incident beam that is characteristic of the surface molecules. By this method, the resulting Raman spectra can be used to discriminate between different bacteria strains. By depositing gold particles on the surface of the sample material, the Raman spectra intensity is enhanced (i.e. SERS). The approach to validating the SERS technique includes biological tests in an artificial growth medium, which are required for ideal growth of the bacteria being tested. The sensitivity of SERS compared to standard laboratory and field techniques was examined in this environment. Furthermore, SERS was also conducted in a

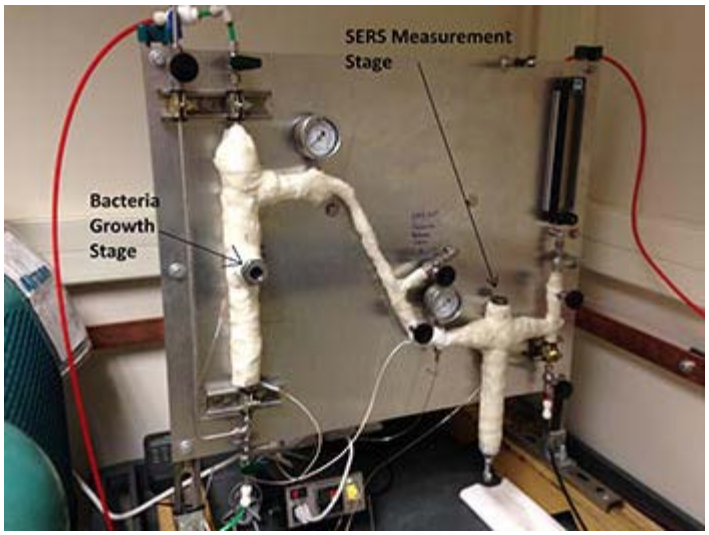

Figure 1: High-pressure flow system

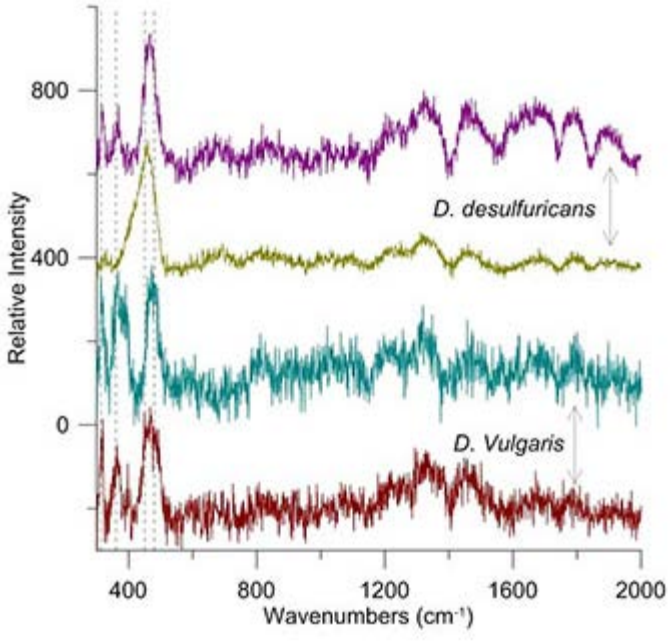

high-pressure gas pipeline environment, as shown in Figure 1. The SERS results in the flow loop will be compared to the results obtained in the artificial growth medium.

Figure 2: Raman spectra for sulfate-reducing bacteria D. Vulgaris and D. Sulfuricans

Accomplishments — Use of SERS to distinguish between bacteria strains can offer an *in-situ* characterization tool to distinguish the types of bacteria that are growing in a media stream or gas pipeline. During this project, two types of sulfate-reducing bacteria in a biological growth media were grown. It was demonstrated that SERS could be used to distinguish a difference between the two strains, as shown in Figure 2. The work conducted showed that the growth of the two strains of bacteria used in this study was not affected by the deposited gold particles. Furthermore, the results also showed that SERS was able to distinguish bacterial growth on the surface of the samples prior to any visual indication of bacteria growth in the media. Finally, bacteria were grown in a flow loop at 1,000 psi and 38°C, and SERS measurements were made on test samples in this flow loop.

SOUTHWEST RESEARCH INSTITUTE®

2015 IR&D Annual Report

Dynamic Characterization of Soft Biological Tissues, 18-R8549

Principal Investigators
Daniel P. Nicolella
Sydney Chocron
Art Nicholls

Inclusive Dates: 04/01/15 – 11/01/15

Background — Human injury occurs as a result of relatively high-loading-rate events such as falls, automobile accidents, sporting injuries, and blunt and ballistic impact to warfighters. However, the vast majority of human tissue material property data is collected at low-loading rates. Since almost all biological materials are strain-rate dependent, there is a significant gap in our ability to accurately predict injury and therefore design injury mitigation strategies and equipment. Furthermore, very little is actually known about human tissue injury mechanisms and the effect of aging and disease on human injury risk. High-rate dynamic testing of soft biological materials presents significant challenges. SwRI is uniquely positioned to directly address these challenges with the application of a combination of a unique set of technologies and capabilities.

Approach — The objectives of the project are to: 1) develop a methodology to characterize soft biological tissues in tension at moderately high strain rates using a combination of SHPB tension experiments, 3D optical strain measurement, direct force measurement, and numerical modeling, 2) characterize the behavior of select soft biological materials as a function of age and disease over a range of strain rates, and 3) validate the new technique by comparing data collected using an independent test method (traditional materials test machine) at overlapping strain rates and finite element simulations.

Accomplishments — A momentum trap has been designed, manufactured, and implemented on the SwRI tensile SHPB, and a series of preliminary experiments was performed. The momentum trap will enable the intensity of the incident wave on the test specimen to be decreased such that stress equilibrium is achieved prior to specimen failure. The use of a momentum trap will also eliminate the interference of the reflected wave with the incident wave when using the long incident pulses required for use on biological materials that can stretch up to 100-percent strain.

An environmentally controlled test chamber was designed and constructed to provide test environment similar to *in vivo* conditions. The system includes a rectangular plexiglass chamber, heating element, humidity element, and a temperature and humidity controller. The chamber was designed such that it can be installed on the Bose® ElectroForce test machine as well as the Split Hopkinson Pressure Bar (SPBH) test system. All future soft tissue testing using the Bose and SHPB will be conducted at 370C and >90% humidity.

A total of 29 SSL tests have been performed to date using the quasi-static test machine (Bose ElectroForce 3400). The ligament testing was split into two rounds: the initial round used full thickness lumbar supraspinous ligament (SSL) segments. The ligaments were tested at room temperature at strain rates ranging from 0.01/sec to more than 100/sec. The second round of testing used only the dorsal portion of the SSL and the ligaments were either tested at room temperature and humidity or simulated body conditions within the environmental chamber (370C and >90% humidity) at strain rates ranging from 0.01/sec to more than 100/sec.

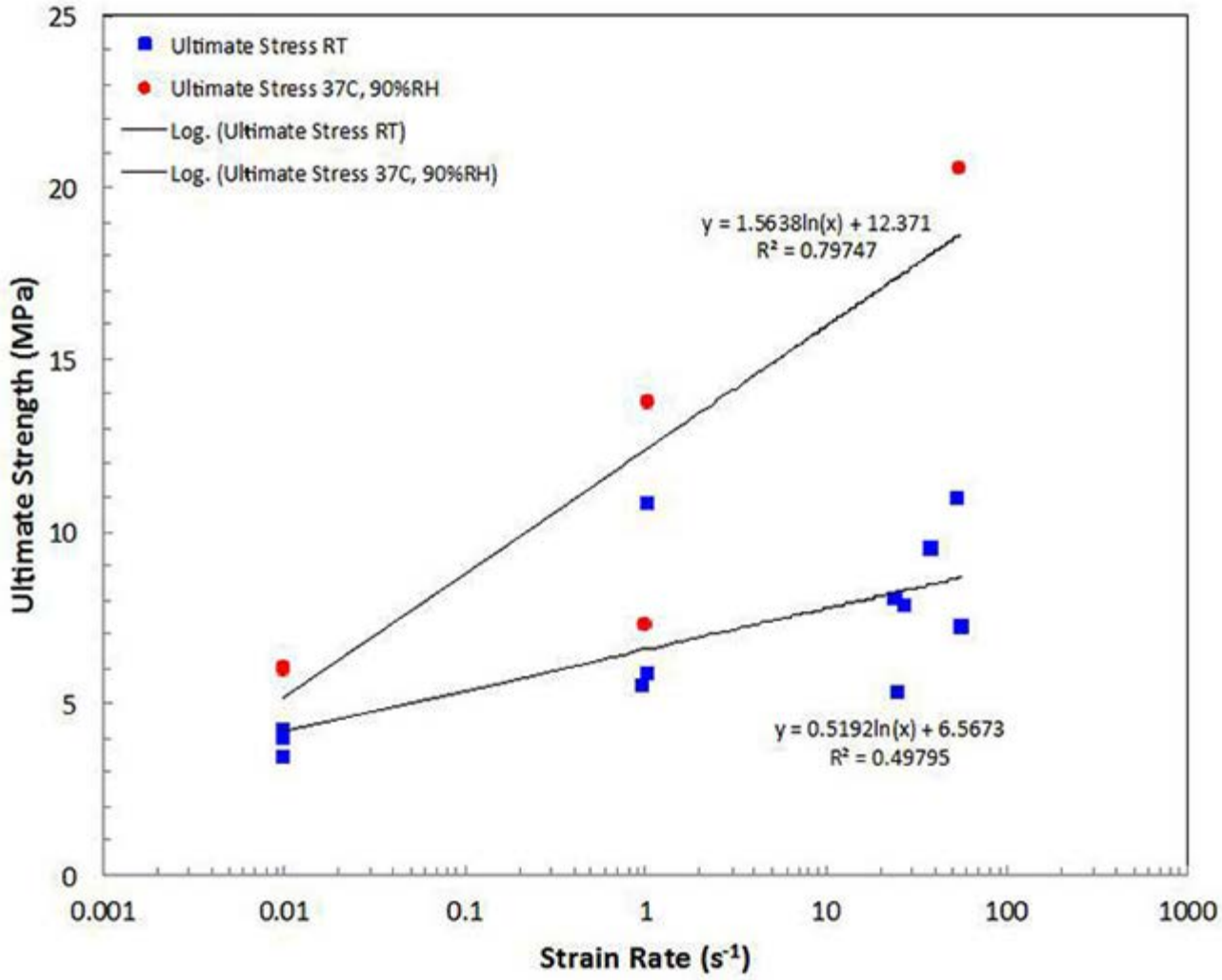

Figure 1: Strain rate and temperature effects on the strength of the supraspinous ligament.

2015 IR&D Annual Report

Development and Evaluation of Low-Friction and Low-Wear Coatings for Automotive Valvetrain, 18-R8550

Principal Investigators
Jianliang Lin
Peter Lee
Christopher Bitsis
Ronghua Wei

Inclusive Dates: 04/01/15 – Current

Background — Efficient engines contribute to reduced exhaust gas emissions and improved fuel economy. The valvetrain accounts for 10 to 20 percent of the total mechanical friction in gasoline engines, especially at low engine speeds and loads. Furthermore, camshaft frictional losses can often be higher in diesel engines. Therefore, reducing coefficient of friction (COF) of valvetrain is critical in reducing fuel consumption and emission, and improving engine efficiency.

The primary objective of the project is to develop low-friction and low-wear coatings for automotive valvetrain components, and evaluate the coating performance using actual engine friction tests. The goal of the project is to provide the automotive industry with a new coating system and cost-effective technology that assist the industry in achieving the 2025 CAFE (corporate average fuel economy) fuel emission targets, particularly on mid-level and low-end automobiles.

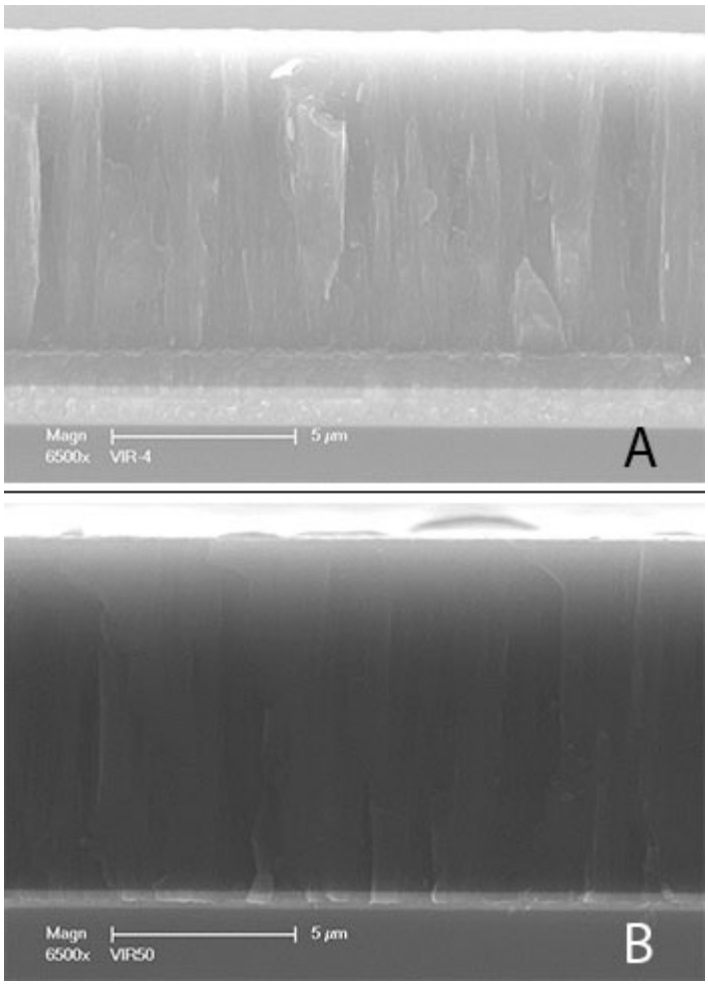

Figure 1: Cross-sectional SEM micrographs of (a) the low friction TiSiCN nanocomposite coating and (b) HiPIMS-DLC coating.

Approach — Low-friction titanium silicon carbon nitride (TiSiCN) nanocomposite coatings and diamond-like carbon (DLC) based coatings have been developed using different techniques, including plasma-enhanced magnetron sputtering (PEMS) for TiSiCN coatings, and high-power impulse magnetron sputtering (HiPIMS) and plasma immersion ion deposition (PIID) for DLC coatings. The processing parameters and structure of the coatings were optimized to achieve a combination of low COF and low wear of the coatings based on the evaluation from the ball-on-disk and the block-on-ring wear tests. The best performing TiSiCN nanocomposite and DLC-

based coatings will be applied on camshaft and camshaft bearings, which will be evaluated in SwRI's single cylinder TriboEngine and a production light-duty gasoline engine. Engine test results will be compared to those obtained from a baseline (uncoated) setup under the same test conditions.

Accomplishments — To date, different groups of TiSiCN nanocomposite and DLC coatings have been developed using the PEMS, HiPIMS, and PIID processes. The structure and properties of the coatings have been optimized systematically by varying key processing parameters and the coating elemental composition. The optimized low-friction TiSiCN and DLC coatings exhibited super dense structure, excellent adhesion, and good toughness. Figure 1 presents the typical microstructure of a low friction TiSiCN coating and a HiPIMS-DLC coating (10 μm).

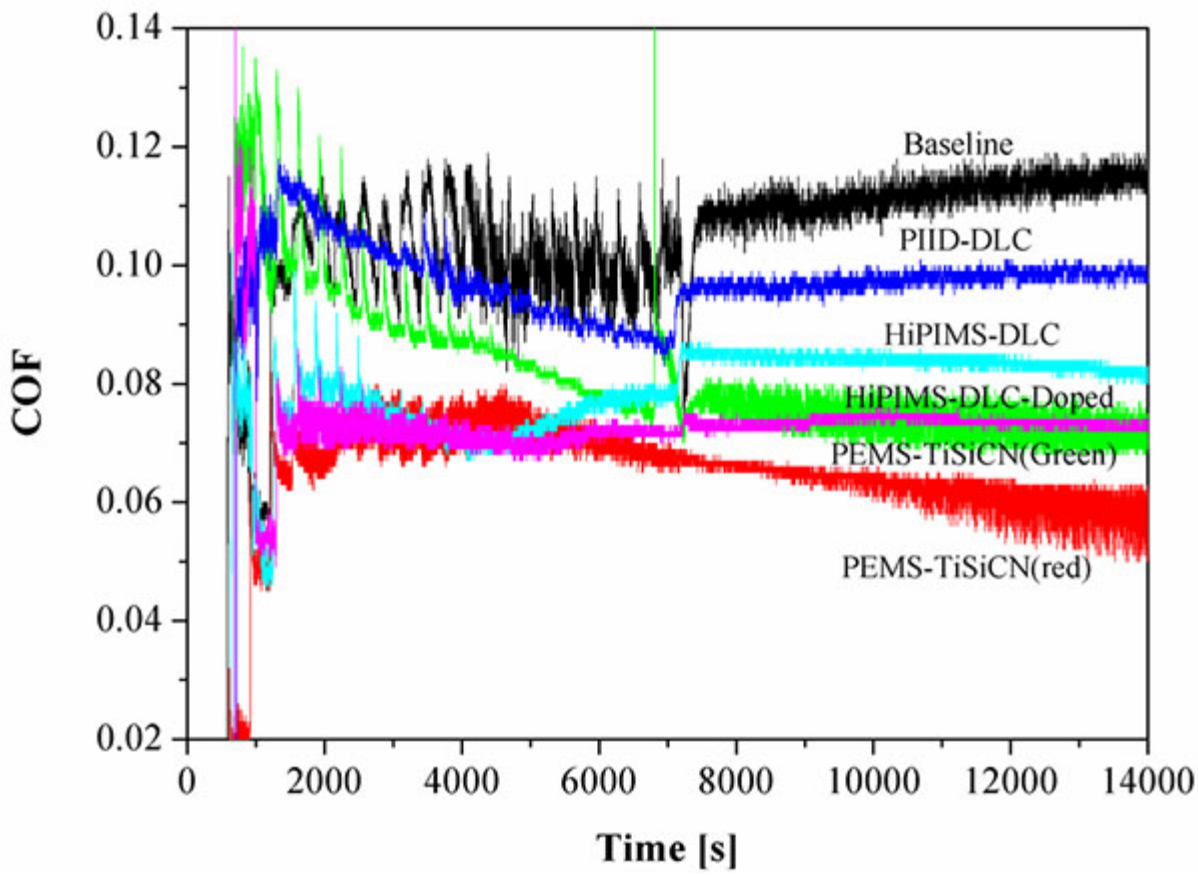

Figure 2: A comparison of the COF of the low friction TiSiCN and DLC coatings measured using a block-on-ring tribometer. The optimized PEMS-TiSiCN coating exhibited a more than 50-percent reduction of the friction (COF=0.055) as compared to the baseline (COF=0.12) in the steady state.

The tribological properties for the TiSiCN and DLC coatings were evaluated using ball-on-disk (dry) and block-on-ring (lubricated) wear tests. The TiSiCN coatings exhibited COFs of 0.2 and 0.055 in dry and lubricated conditions, respectively. In contrast, the DLC coatings showed lower friction in dry sliding (0.05-0.06) but relatively higher friction in engine lubricant (0.07-0.08). Figure 2 shows a comparison of the COF of a baseline, the TiSiCN, and DLC coatings measured using a block-on-ring tribometer. All coated samples showed reduced COF as compared to the baseline. The best performing TiSiCN and DLC coatings exhibited a more than 50-percent (COF=0.055) and 37.5-percent (COF=0.075) reduction of the friction as compared to the baseline (COF=0.12) in the steady state, respectively. The optimized coatings are going to be applied on camshaft and camshaft bearings, which will be evaluated in engine tests in early 2016.

SOUTHWEST RESEARCH INSTITUTE®

2015 IR&D Annual Report

Effect of Cyclic Relative Humidity on Environmentally Assisted Cracking, 18-R8554

Principal Investigators
James Dante
Todd Mintz
Erica Macha
James Feiger

Inclusive Dates: 04/01/15 – Current

Background — The annual cost of corrosion for the U.S. Department of Defense aircraft systems is estimated to be over $10 billion. It is estimated that more than 80 percent of structural cracks that have been detected initiate at corrosion sites, raising concerns that corrosion has a potentially high impact on structural integrity. In an attempt to compensate for these environmental effects, a margin of safety during design considerations is employed. These margins of safety are based on crack growth rate (CGR) data that has been collected under immersion conditions. Recent work, however, has shown that CGR can be as much as 10 times higher than values acquired in lab air under certain environmental conditions. Measurements of CGR under aggressive atmospheric conditions are required not only to understand the specific effects of environmental spectra on CGR, but also to define how environmentally assisted cracking should be addressed in engineering design approaches for components and structures.

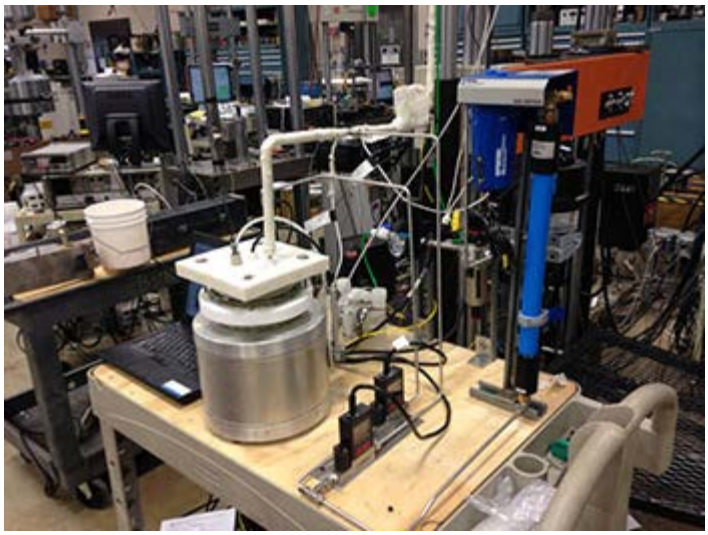

Figure 1: Environmental control system designed to control relative humidity and temperature around a fatigue sample.

Approach — The overarching goal of this work is to develop an initial framework to address atmospheric environmentally assisted cracking. The approach includes the development of an atmospheric testing cell with controlled relative humidity (RH) and temperature constructed around a standard fatigue test system. Testing under controlled environmental conditions and dynamic loading conditions will be used to demonstrate how atmospheric parameters directly affect CGR. Using well-established multi-electrode array techniques developed at Southwest Research Institute, correlations between corrosion modes and changes in crack growth rate will be established. This will serve as the basis for understanding fundamental mechanisms of atmospheric cracking processes. Finally, existing environmental sensor data will be analyzed in a manner analogous with structural usage spectra. Environmental spectra developed from this analysis will be used to define conditions for measuring CGR under controlled mechanical loads.

Accomplishments — An environmental control system (Figure 1) was integrated around a CT fatigue sample. Within the test cell, RH values can be controlled between 15 percent and 95 percent (+/- 2 percent) while temperature is controllable from room temperature to 45°C (+/- 2 degrees). Initial fatigue

testing has been performed using alloy Al 7075-T651 compact tension (C(T)) samples, which had 1 g/m2 of sodium chloride (NaCl) deposited on the surface. Fatigue crack growth rate (CGR) tests were run at a constant frequency of 1Hz with a load ratio (R) of 0.5. CGR and RH as a function of time (Figure 2a) reveal a factor of three increase in CGR at high RH. Further analysis reveals that CGR is always highest during intervals of decreasing RH (Figure 2b). A tool has been partially developed to compare environmental data acquired by corrosivity sensors. Data from the tool can also be used to identify the duration of conditions critical for accounting for environmental effects on fatigue. Eventually, it is believed that the approach developed within this project will be used for predicting crack growth rate for aircraft structural integrity.

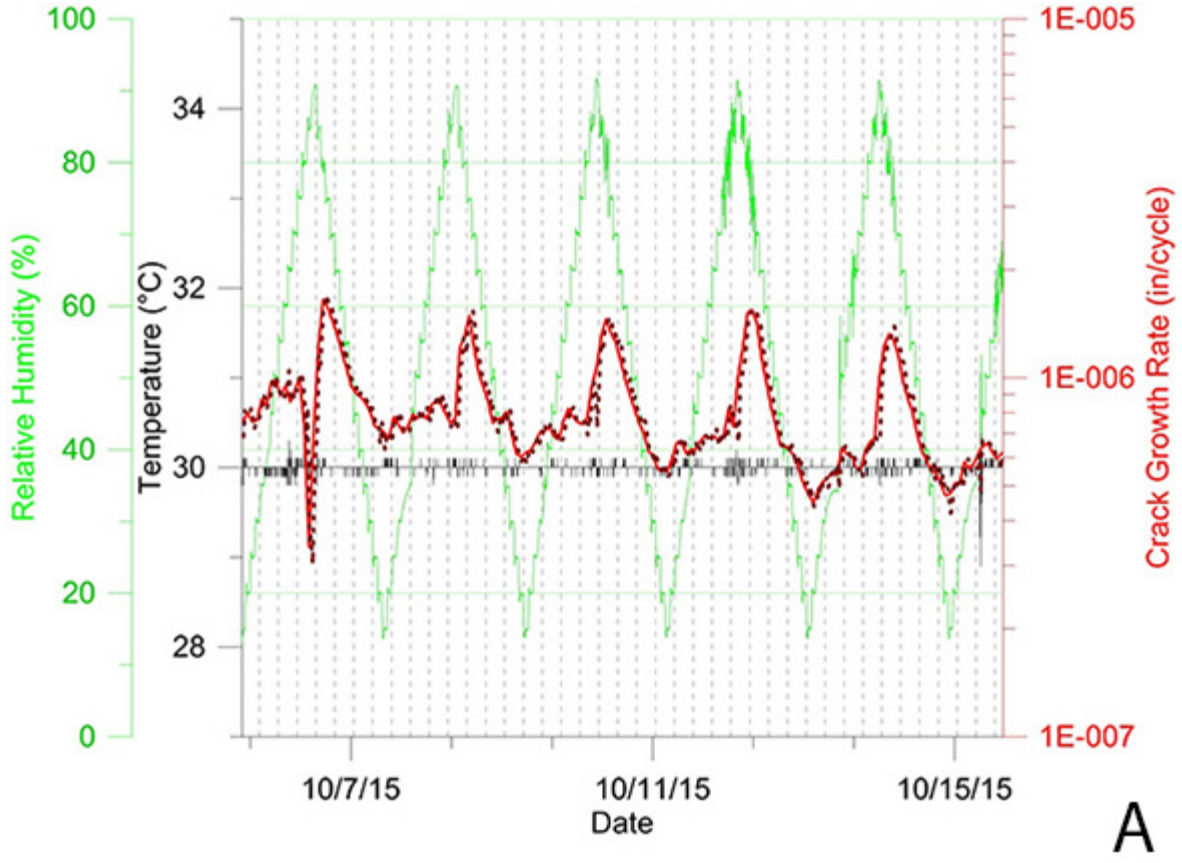

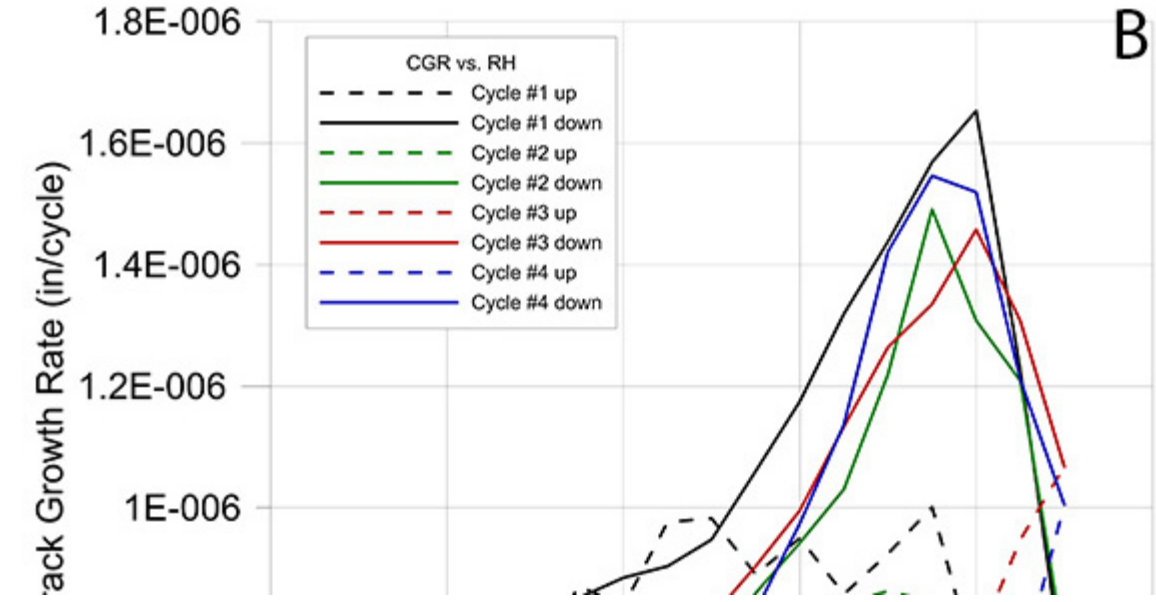

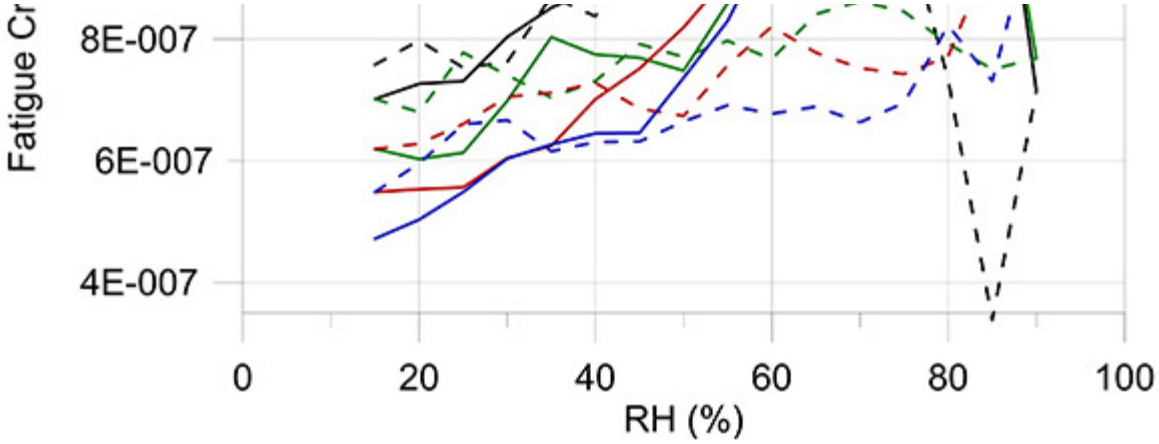

Figure 2: (a) Crack growth rate of Al7075-T651 compact tension specimen, loaded with 1 g/m^2 of sodium chloride, and relative humidity as a function of exposure time. (b) Crack growth rate as a function of relative humidity.

SOUTHWEST RESEARCH INSTITUTE®

2015 IR&D Annual Report

Evaluating Properties of Chemically-Aged High-Density Polyethylene Piping Material Used in Nuclear Power Plants, 20-R8432

Principal Investigators
Pavan Shukla
Mike Rubal

Inclusive Dates: 12/13/13 – 08/12/15

Background — The principal objective of this project is to evaluate material properties of chemically aged high-density polyethylene (HDPE) piping used in nuclear power plants (NPPs). In the United States NPPs, HDPE pipes are increasingly being used in safety-related components, such as essential service water (ESW) systems, including buried and aboveground sections. Because carbon steel piping in the ESW system corrodes with age, it requires costly maintenance and has become a safety concern. To mitigate corrosion risks, NPP operators have begun to replace carbon steel ESW piping with HDPE. There are concerns, however, regarding the use of HDPE pipes in safety-related components. Even though there is a generalized belief that HDPE pipes have service lives of 50 years or more with minimal degradation, and thus are safer compared to carbon steel pipes, there is limited evidence supporting this assumed service lifetime and associated performance. Therefore, this project was aimed at evaluating properties of the material as it ages, and estimating its remaining service life.

The available methods for testing HDPE pipe failures and service lifetime have limitations, because they do not account for both chemical and mechanical degradation. The available testing methods are solely based on the mechanical strength of HDPE materials. These methods show two types of pipe failures: ductile pipe rupture occurring with ballooning of the pipe specimen and yielding of the HDPE material in the failure area, and nonductile, slit, and pinhole failures. In the available test methods, the allowable service life (i.e., for 50 years or more) is dependent on the stress applied at the pipe wall. HDPE materials undergo chemical degradation in the form of oxidative degradation due to the chemical environment in contact with the external and internal surfaces of the HDPE pipe. For the HDPE pipes in NPPs, the internal environment is service water, which contains oxygen and radical generating disinfectants, such as chlorine or chlorine dioxide (ClO_2). The external environments are generally soil

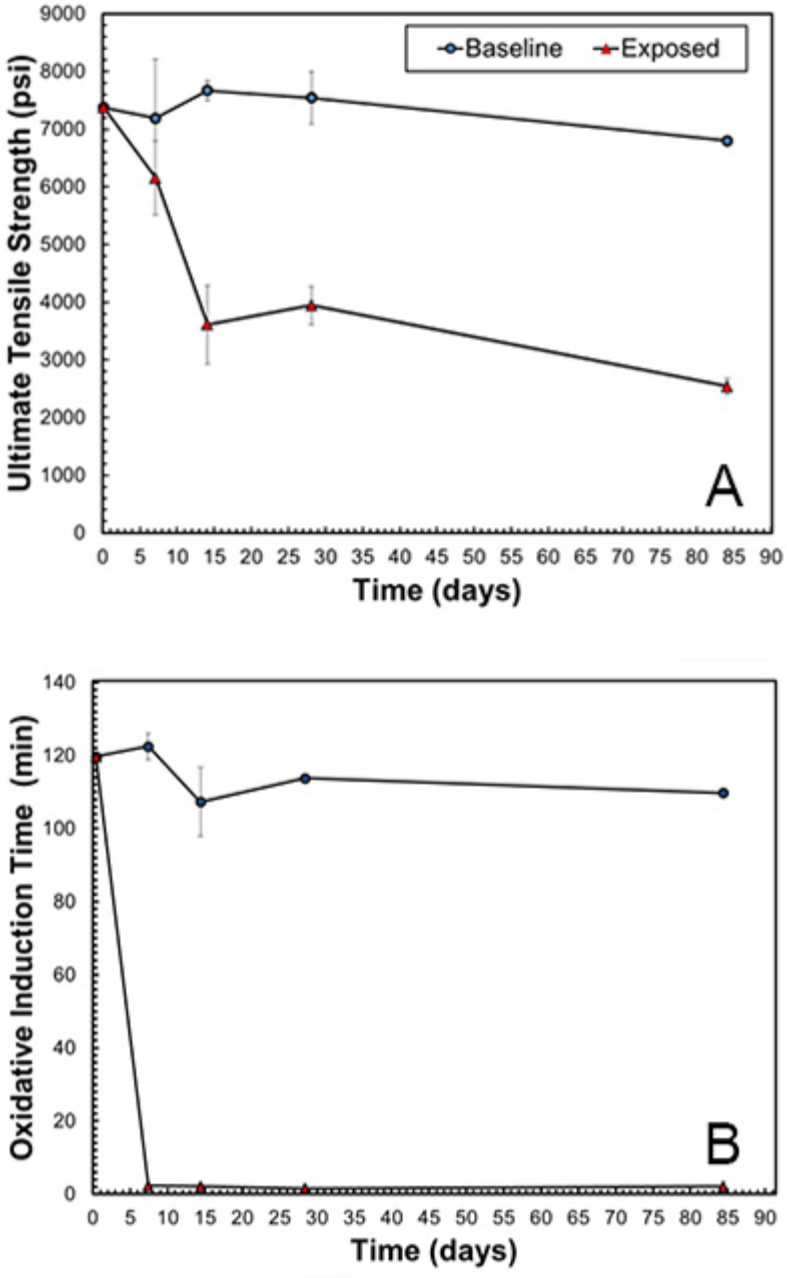

Figure 1: (a) Average ultimate strength for high density of polyethylene (HDPE) dog bone samples exposed to the baseline solution and the chlorine dioxide (ClO_2) solution versus exposure time, and (b) oxidative induction time measurements of HDPE dog bone samples exposed to either the baseline solution and the ClO_2 solution versus exposure time

or air. The presence of oxidizing species in the service water leads to oxidative degradation. The oxidative-degradation resistance of HDPE is increased by adding antioxidants, such as stabilizers and carbon black. When these antioxidants are significantly depleted from HDPE, the dissolved oxygen and other chemical species degrade the polymer at the pipe inner surface. This degradation leads to reduced molecular weight and diminished mechanical strength of HDPE. When degradation of the inner surface material is severe enough, an embrittled surface layer develops cracks, which tend to propagate through the pipe wall, driven by internal pressure.

Approach — The overall technical approach consisted of four elements: (i) mechanical testing, (ii) chemical treatment under oxidative conditions, and (iii) developing a model for estimating antioxidant concentration and depletion rate with time. In the overall approach, the mechanical testing was used to correlate the antioxidant level and oxidative degradation to mechanical properties. The mechanical testing data was used as a master curve for predicting the service lifetime of HDPE pipes. In Element iii, involving predicting the evolution of the antioxidant concentration in the HDPE pipes, a model was developed based on diffusion theory. The sample data from Element ii was used to estimate model parameters. It was important to develop a model because antioxidant concentration in a field HDPE pipe varies with the radial thickness due to gradual depletion of the antioxidant. Further, in the laboratory scale experiments with limited time exposure, this variation is difficult to replicate due to very low depletion rates of the

antioxidant. The model was used as an extrapolation tool to estimate long-term depletion of antioxidant for a given thickness of the pipe. The model results were used to estimate service lifetime of the HDPE with a given wall thickness.

Accomplishments — The project accomplishments included characterizing the mechanical and chemical properties of the HDPE piping materials as they age in oxidizing solution. Two types of samples were prepared for the aging tests. The first consisted of "dog bones" of a HDPE (TUB121) prepared by injection molding and aged at 40°C in either a baseline solution (pH = 2) or a solution containing an oxidant, ClO_2 (average concentration of 82 ppm for duration of exposure experiment) at a pH of 2. The second type consisted of 4-in. thick blocks of HDPE exposed at 40°C from one side with a solution 90 to 140 ppm of ClO_2 at pH of 2. For the HDPE blocks, samples were later machined into dog bones or discs over a series of depths from the surface to develop a correlation between the depth and material properties. After exposure tests, samples were analyzed by tensile, oxidative induction time (OIT), Fourier Transform Infrared spectroscopy, creep, and dynamic mechanical analysis for molecular weight.

Figure 1 compares the tensile results and OIT data for the first type samples (dog bones made of TUB121). It was found that mechanical and chemical properties of the exposed samples decreased rapidly with exposure to the ClO_2 solution. For example, the ultimate tensile strength decreases by 50 percent after two weeks of exposure to ClO_2 solution. This correlated with the loss of antioxidant in the HDPE as exhibited by the dramatic reduction of the oxidative induction time after a week of exposure. These data indicate that both mechanical and chemical properties of HDPE significantly change after exposure to the ClO_2 solution.

Analysis of the second type samples (4-in thick blocks) also shows a rapid decrease in OIT values. As shown in Figure 2, for the relatively short exposure times used in the tests, these phenomena are limited to a short distance from the exposed surface. As seen in Figure 2, the OIT values for samples prepared from the bulk of the HDPE remained more or less unaffected by the exposure. This surface limiting aspect is also noticed in the mechanical properties. For example, the ultimate tensile strength of the samples directly from the exposed surface shows significant reduction in the mechanical properties compared to the bulk and unexposed material. However, ultimate tensile strength of the samples at a small distance from the exposed surface is the same as the bulk and unexposed material, and remains unchanged over the experimental exposure times.

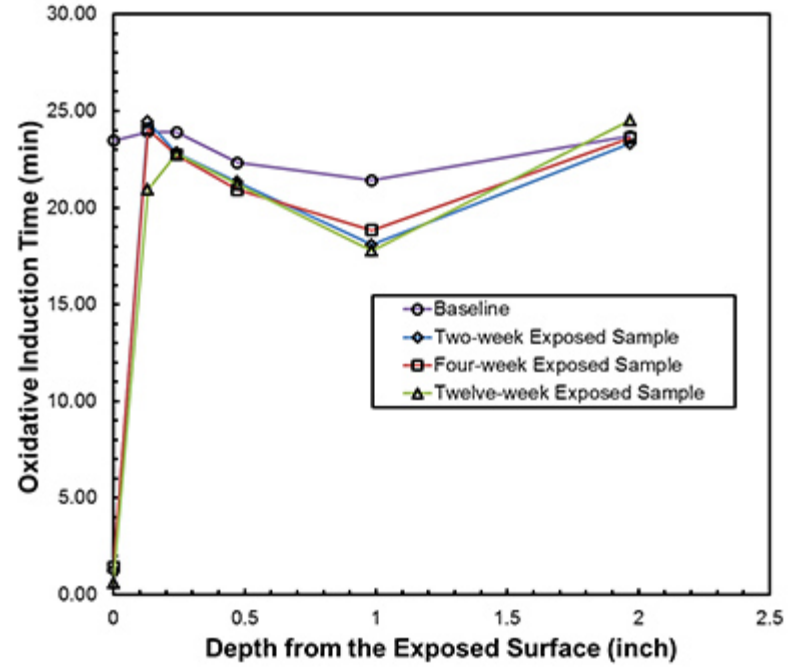

Figure 2: Oxidative induction time comparison between high density of polyethylene block samples exposed for various times and the effect of exposure as a function of the depth from the exposed surface

The OIT values in Figure 2 were used to estimate the antioxidant concentration with depth in the 4-in block sample. The concentration values with time were used to estimate the depletion rate of antioxidant from the HDPE matrix. This was input in the diffusion-based model, and antioxidant levels were predicted in

a 4-in thick wall HDPE pipe. The model computed values of the normalized antioxidant levels are presented in Figure 3.

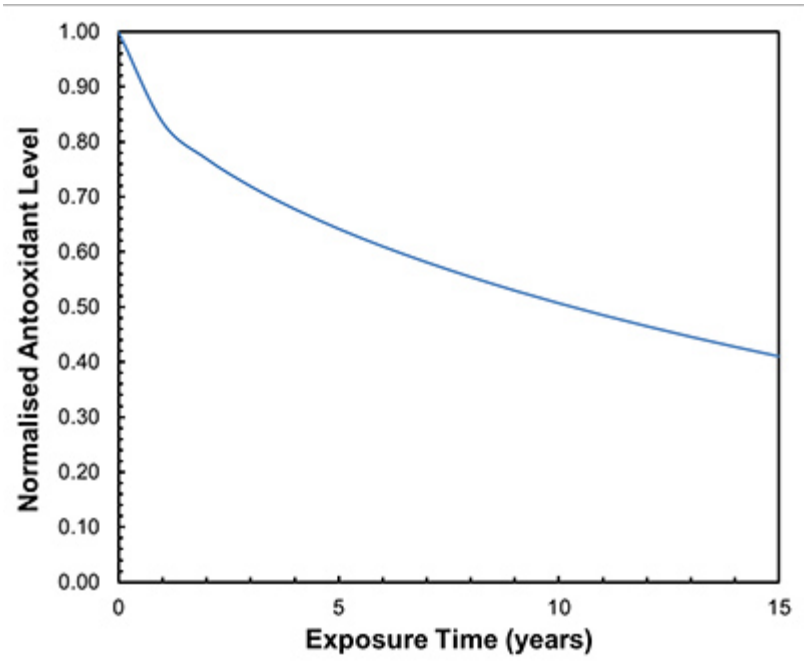

Figure 3: Computed normalized antioxidant levels with exposure time in a 4 in thick HDPE pipe

The following conclusions are drawn from this work:

- Oxidative induction time is a good indicator of loss of antioxidants from HDPE. It was further observed that the strength of the material decreases by 50 percent or more when the antioxidants are depleted from the bulk of HDPE. Considering this, loss of antioxidants at 50 percent with respect to initial concentration of HDPE is a reasonable reference or threshold to estimate the service life of HDPE components in NPPs.
- When the material is exposed to an oxidizing environment, the loss of antioxidants from HDPE is controlled by the diffusion of the antioxidants from the material. The diffusion of the antioxidants through the bulk material is a slow process, as observed in the block experiments. Therefore, long-term exposure experiments are needed to accurately determine the depletion rate of the antioxidants from the material.
- There are no readily available methods to measure *in-situ* antioxidant levels of an in–service HDPE component, such as pipes at nuclear power plants. The most feasible method is to use coupons to measure the depletion rate of the antioxidants from HDPE.
- Depletion rate data from coupons or laboratory experiments can be used to obtain key model parameters. These parameters can be input in the diffusion-based dynamic mass–balance model to extrapolate the cumulative levels of the antioxidants in the in–service HDPE component. A threshold value of 50 percent can be used to estimate the service life of HDPE components.

SOUTHWEST RESEARCH INSTITUTE®

2015 IR&D Annual Report

ROS-Industrial® Strategic Technology Development, 10-R8335

Principal Investigator
Shaun Edwards

Inclusive Dates: 09/17/12 – 12/11/14

Background — In a previous IR&D effort, the principal investigator worked closely with Robot Operating System (ROS) developers at Willow Garage to develop an open-source ROS-Industrial software stack (software suite) to support the use of ROS for industrial applications. The technology developed under this previous effort brought the use of powerful ROS capabilities, such as advanced perception and path/grasp planning, to industrial robotics applications.

Since the completion of the previous project, the ROS-Industrial open-source program has attracted significant interest in the industrial robotics community. Two examples of this interest are the growth of the open-source development community and the ROS-Industrial Consortium. The open-source community has grown to include a worldwide network of commercial, independent, and government labs working towards a common goal of enabling advanced industrial robotics and automation through open-source development. The ROS-Industrial Consortium, in its third year, now includes 32 members worldwide. The consortium provides commercial investment and input into the ROS-Industrial program. Specifically the consortium provides funding for technology development through focused technical projects (FTPs).

The objective of the ROS-Industrial Strategic Technology Development effort is to continue technology development and expand the capabilities of ROS-Industrial while supporting the consortium and open-source community.

Approach — The approach of the ROS-Industrial technical effort is to expand the capabilities through continued software development both at SwRI and through external development teams, as well as demonstrate real-world applications. Specifically this effort will:

- Provide guidance to the ROS-Industrial open-source community, outlining development efforts for external teams.
- Expand the ROS-Industrial driver set, providing compatibility and interoperability with major industrial robot vendors.
- Integrate advanced path planning and perception algorithms with a focus on those that are useful in industrial applications, such as machining and painting.
- Demonstrate ROS-Industrial in multiple real-world applications through cooperation with commercial companies.

The software developed under this effort will be released open source under the ROS-Industrial program.

Accomplishments — The project has completed the following milestones:

- The ROS-Industrial software has grown, with many contributions coming from external development teams in the open-source community.
- The ROS-Industrial software now supports most major industrial robot vendor platforms. This capability was demonstrated at the Automate tradeshow in early 2013.
- Integration of ROS-Industrial with the MoveIt Library, which provides advanced path planning capabilities with close integration of 2D/3D perception.
- Real-world problems solved with ROS-Industrial under consortium FTPs.

- Library development for optimizing industrial pick-and-place cycle times
- Application development for automated deburring, polishing, and finishing of machined aerospace parts is in progress (see Figure 1).
- Application development of a robotic cutting system utilizing a portable measurement device to define cutting paths is in progress.

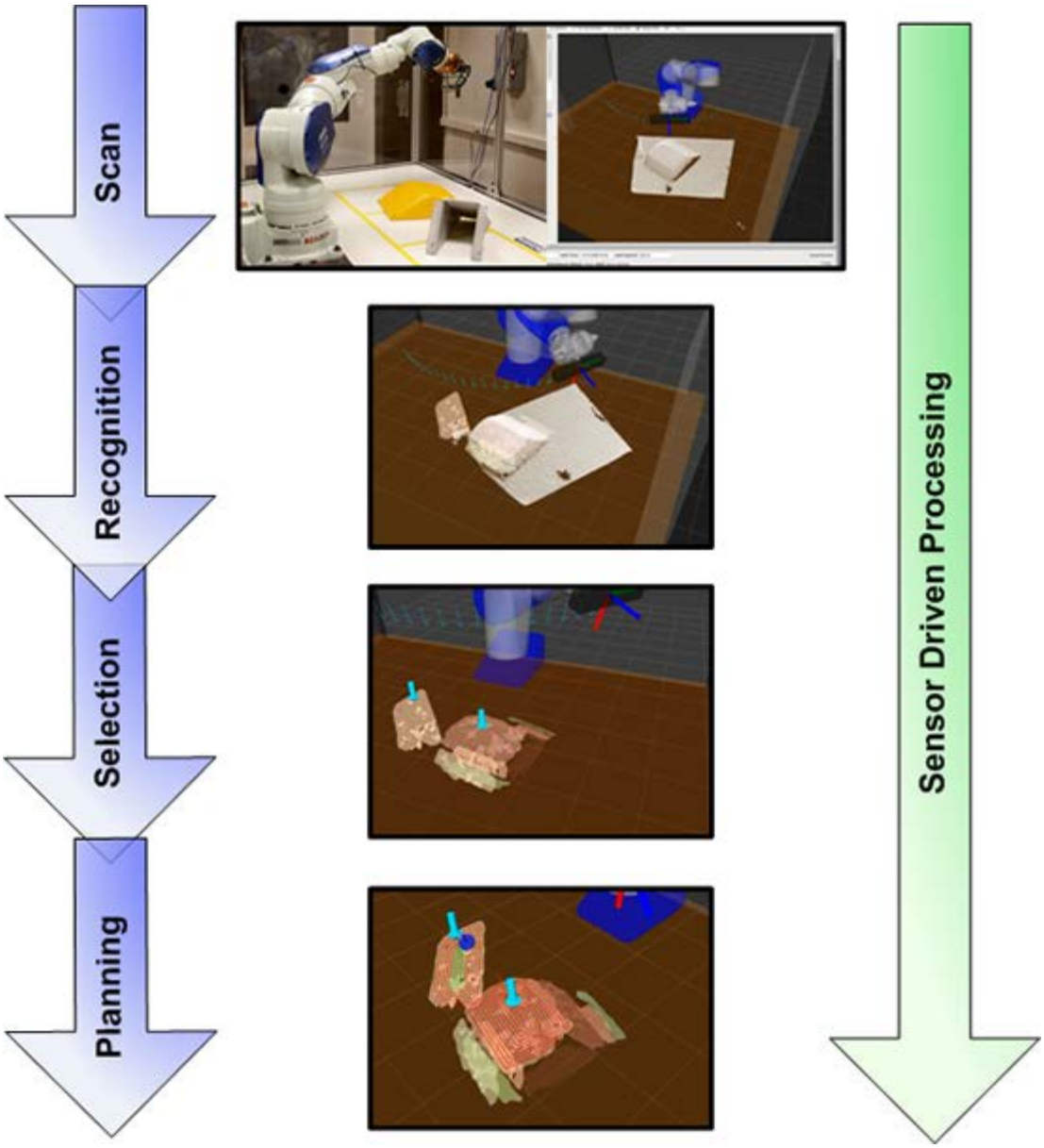

Figure 1: Automated deburring, polishing, and finishing application enabled by ROS-Industrial. Using ROS-Industrial perception and planning capabilities, sensor driven processing is a reality.

SOUTHWEST RESEARCH INSTITUTE®

2015 IR&D Annual Report

Low Cost Accurate 6 DOF Industrial Robot Localization System Software Modeling and Testing, 10-R8443

Principal Investigators
Christopher Lewis
Paul Hvass

Inclusive Dates: 01/01/14 – Current

Background — Close range photogrammetry uses multiple cameras to track or measure objects. Due to rapid hardware improvements, digital cameras are being considered to provide real-time feedback to robotic manipulators and autonomous vehicles. Vision-based tracking systems have the potential to eliminate positioning errors caused by mechanical inaccuracies, loading, wheel slippage, etc. Low-cost highly accurate positioning opens a wide range of applications to robotic automation. They may also replace coordinate measurement machines for metrology. Many factors affect the accuracy of close range photogrammetric systems. One goal is to understand the roles that geometry, lens quality, pixel resolution, calibration procedures, target geometry, and other factors play in overall system accuracy. Another goal is to predict the accuracy of the overall system from component characteristics.

Approach — The accuracy of locating objects in images is fundamental to photogrammetric techniques. Therefore, we characterized the accuracy of locating objects using fiducials of various sizes mounted on an optical bench and using motion stages. From this investigation, we verified theoretical predictions relating size and viewing perspective for planar circular fiducials. We also developed a projection model that accounts for the shift between the center of a circle and the center of the observed ellipse. The fiducial localization noise model is the progenitor to both intrinsic and extrinsic calibration accuracy as well as for overall system accuracy. We developed both Monte-Carlo and covariance techniques for predicting accuracy of each phase and then the accuracy of the final system.

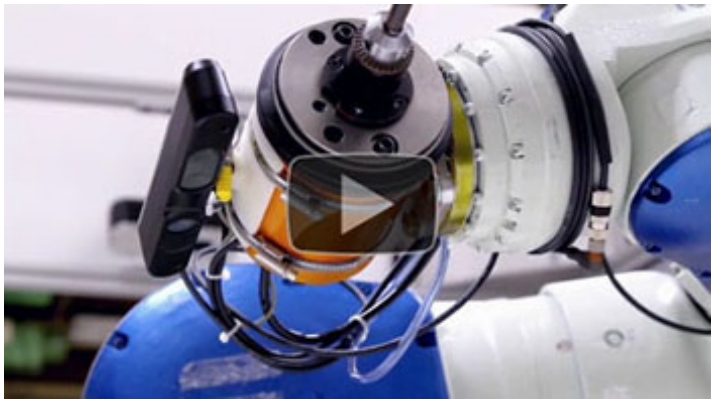

This short video, hosted by ROS-Industrial, describes the calibration framework.

Accomplishments — We developed a general calibration framework to automate a variety of robot-camera calibration tasks. This tool interfaces to robots, imaging sensors, and other hardware to automatically collect observations and submits them for optimization. When deployed with the Robot Operating System, calibration results are immediate and persistent. This tool has been used to:

- Precisely locate 2D and 3D cameras mounted on a robot's wrist.
- Calibrate a network of 3D cameras which scan large parts on a chain conveyor for robotic painting.
- Automatically calibrate a network of nine cameras relative to a robot.
- Predict the localization accuracy of a camera network throughout the working envelope.
- Automate the intrinsic calibration procedure using a novel computational method, which significantly improves the calibration accuracy.

2015 IR&D Annual Report

Cooperative Control of a Deployable Aerial Sensor Platform, 10-R8462

Principal Investigators
Richard D. Garcia
Jason Gassaway
Jerry Towler
Kristopher Kozak

Inclusive Dates: 04/01/14 – 10/01/15

Background — While unmanned aircraft have proven their viability in both the commercial and military market, unmanned aircraft technology continues to suffer from limited payload capacity, limited perception, and dependency on global positioning system (GPS) as a primary localization method. These limitations are significantly compounded on small aircraft (<10kg) as they cannot sacrifice payload or power to employ large sensor suites or high computational equipment. These limitations quickly become operational failures in obstacle-rich environments or where GPS may be unavailable or corrupted.

The primary objective of this research effort is to develop algorithms, equations, and techniques that will enable an autonomous unmanned ground vehicle to safely and effectively deploy, recover, and navigate an aerial platform. The proposed work will enable an unmanned ground vehicle (UGV) to use its own high fidelity sensors to localize and control an aerial platform, off-loading obstacle detection and avoidance to the ground vehicle. By offloading many of the sensing and computational requirements from the aerial platform to the ground vehicle, the aerial platform can be lighter and simpler in construction, with an emphasis on mission payload. This technique will enable safe and effective flight during extremely low-altitude operation (including under foliage), and will enable flight in GPS-denied environments.

Approach — To accomplish the above objectives, we are developing algorithms that allow the UGV to identify and localize the aerial platform using sensors mounted on the UGV. Although extensive experience leads us to believe that a combination of ranging data (provided by a multi-planar laser range finder or radar) and imagery, possibly assisted by lightweight fiducials, will provide accurate localization at close range (~20m), specific sensor configuration design will use metrics collected from several manual flights representative of the operational area of the aircraft. Once the appropriate configuration of sensors has been selected, manual flight data can be used to tune basic localization calculations, which will be verified for accuracy using a VICON motion capture system.

Accomplishments — During the course of the project, the team successfully implemented an active tether that allows for extremely long-duration flight times and provides a 100 Mb/s connection between vehicles. Flight duration and positional control of the UAS was successfully tested in the VICON motion capture system, allowing for waypoint-based control of the UAS using the Robot Operating System (ROS). Outdoor autonomous flights were performed using the tether to provide sustained duration flight over a ground vehicle. During these flights, the UAS relayed overhead imagery to the ground vehicle, which calculated relative position of the UAS using opportunistic feature detection and tracking.

SOUTHWEST RESEARCH INSTITUTE®

2015 IR&D Annual Report

Low-Cost Safe Gears for Robots and Prosthetics, 10-R8476

Principal Investigators
Paul Hvass
Glynn Bartlett

Inclusive Dates: 08/20/14 – 04/01/15

Background — Robotics and prosthetics/assistive devices use high-reduction ratio gear trains to convert high motor speeds (low torques) to much lower speeds (higher torques). This is typically accomplished using heavy/expensive steel gears including harmonic, cycloidal, planetary, or worm types. While each of the gear types can be constructed so as to provide the desired high-reduction ratio, they are also heavy and/or expensive. The objective of this project was to design and build a prototype of a novel, low-cost, fiber-reinforced plastic, safe hypocycloidal gear train suitable for robotic and prosthetic applications.

Approach — Milestone 1 of this project was a feasibility study to evaluate a conceptual low-cost safe 50 Nm hypocycloidal gear train (HGT) for the robotics and prosthetics market. The results of that study included power density analysis, economic analysis, and a 3D-printed mockup of the HGT (Figure 1). Success of the first milestone led to Milestone 2, which included the design and fabrication of a first-article plastic prototype, and physical demonstration of its safety clutch mechanism. It should be noted that the investigators elected to scale the design to 100 Nm for Milestone 2 to better serve interested clients.

Accomplishments — The gear train has been successfully demonstrated to exhibit the desired properties of high-reduction ratio power transmission, low weight, and of safety clutch action, though further testing and design optimization is needed before the design will be commercially viable. The HGT is a strong candidate for continued development for material handling robots where small backlash is acceptable, and for prosthetic devices where low

Figure 1: The 3D-printed HGT mockup from Milestone 1

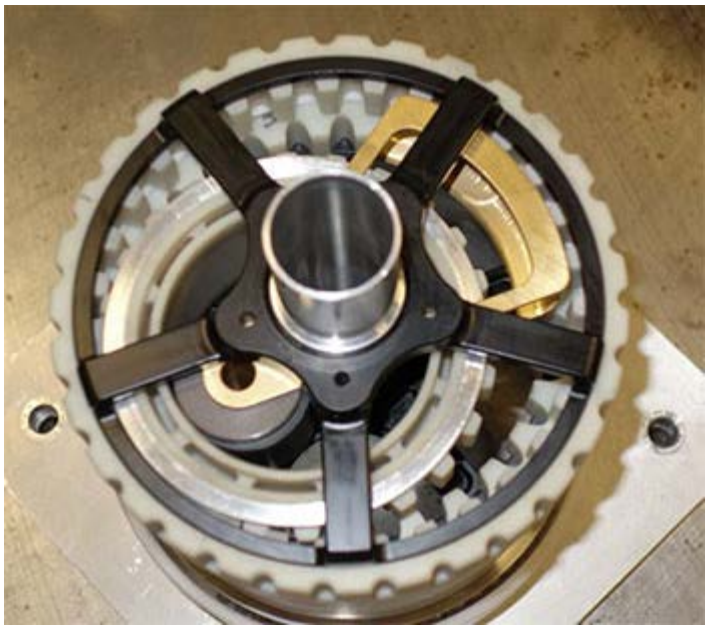

Figure 2: First-article plastic prototype resulting from

Milestone 2 efforts

weight is desirable. A provisional patent for this invention has been filed and a final patent application is underway. SwRI is approaching interested parties in the robotics and biomedical market who may be interested in a commercialization effort that will necessarily entail further design refinements and life testing.

SOUTHWEST RESEARCH INSTITUTE®

2015 IR&D Annual Report

ROS-Industrial® Robotic Product Singulation, 10-R8486

Principal Investigator
Shaun Edwards

Inclusive Dates: 07/30/14 – 11/30/14

Background — There are many examples within manufacturing production and product distribution where products are piled on conveyors, buffer areas, or in bins. Typically humans are assigned the task of pulling product from these piles and singulating them onto a conveyor or part carrier. Humans are extremely efficient at recognizing which part is on the top of the pile and then quickly picking and placing the part. Industry and automation experts have studied this problem and implemented highly custom machines that are typically designed specifically for a particular part, or range of parts. While this works for many high-volume, low-mix production operations, it fails when there are a wide range of part types and volumes within the same facility that require singulation.

Approach — The project focused on identifying robust methods for rapid robotic singulation for piles of small packages (Figure 1). The application domain of particular interest is order fulfillment in large distribution centers. The methods for investigation focused on solving the problem of picking small packages from unstructured piles for creating a singulated product stream.

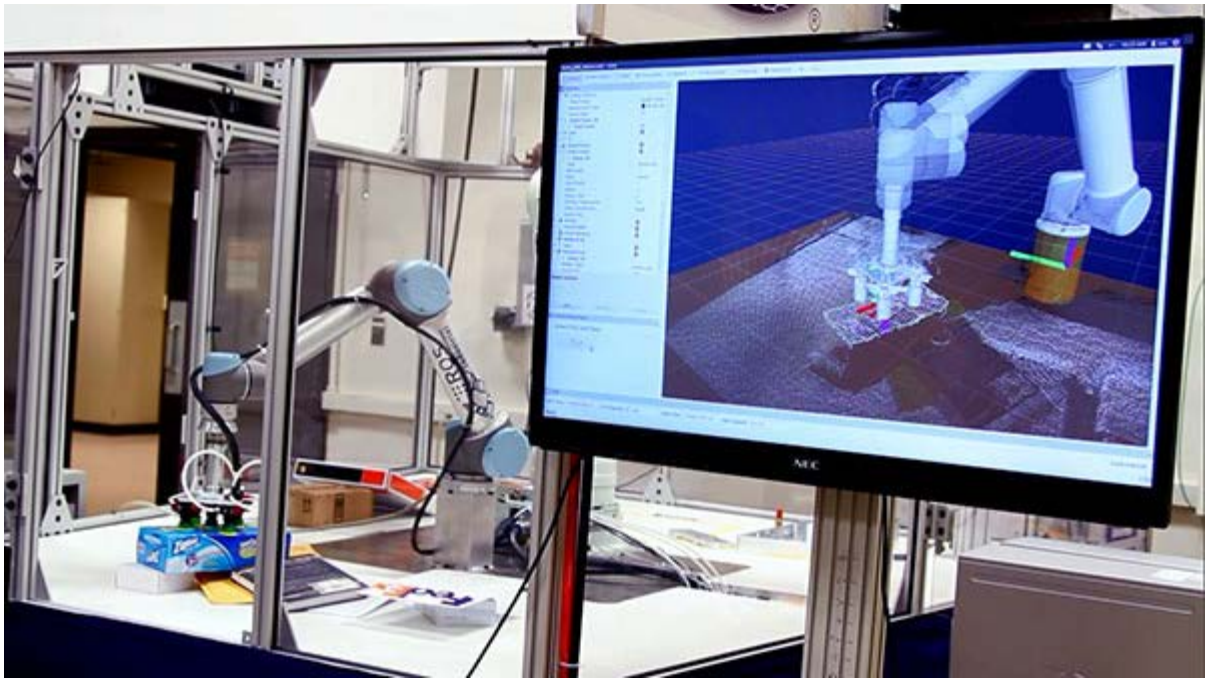

Figure 1: Demonstration cell with robot and live perception system results for singulating a package from a random pile.

Accomplishments — The project achieved its goal of robustly and reliably detecting and singulating a random assortment of packages (see video below). The cycle was optimized such that the perception step was performed in parallel with robot motion, eliminating the vision system as a bottleneck. The perception

performance of on average 250ms per pick allows for theoretical cycles time of between 30 and 60 picks per minute, depending on the complexity of robot motion.

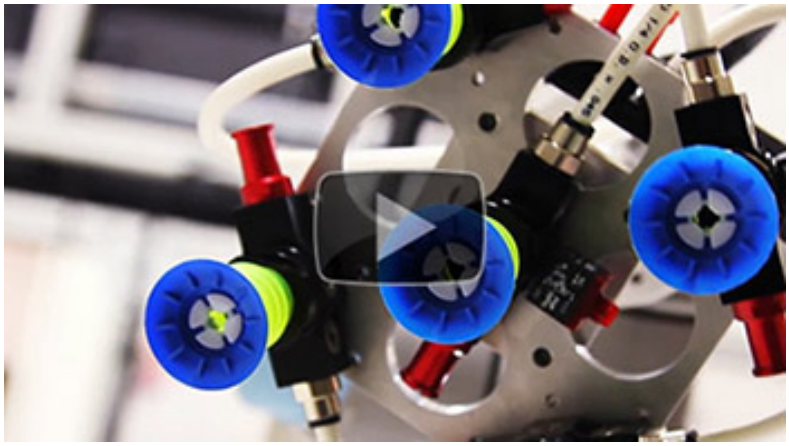

2015 IR&D Annual Report

Automated Perception and Robotic Targeting of Fluorescent Markers, 10-R8489

Principal Investigators
Michael Rigney
Thomas Whitney III
Christopher Lewis

Inclusive Dates: 08/01/14 – 12/31/14

Background — Cell manipulation/engineering techniques include the ability to integrate fluorescent molecules (markers) into T-cells that are genetically engineered to bind with specific cancer cells. This quick-look project demonstrated integrated perception and robotic targeting of fluorescent markers via a surrogate process.

Approach — An existing 3D sensor and low-power laser were mounted to a robotic manipulator and calibrated. Ultraviolet illumination yielded high-contrast images of fluorescent markers. Marker 3D location in the sensor's measurement frame was transformed to the robot coordinate frame. Laser calibration yielded a virtual robot tool point that path planning software targeted onto the marker locations. System integration, calibration, and path planning was facilitated by functionality within the SwRI-developed open-source software framework for industrial robotics called ROS-Industrial that leverages the Robot Operating System (ROS) for advanced robotics research and applications.

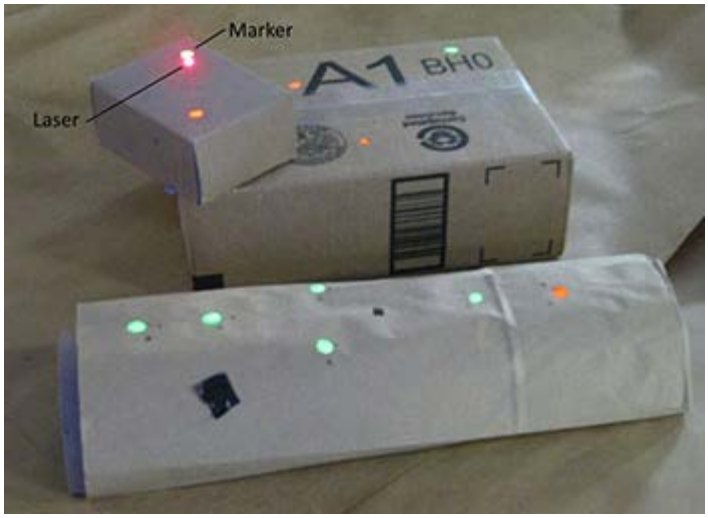

Figure 1: Fluorescent markers and targeting laser

Accomplishments — Detection and targeting of a sequence of marker locations was demonstrated. A targeting error of approximately 6.5 mm was achieved (0.8% of sensor FOV). Accuracy was limited by performance of the low-cost 3D sensor. Use of an alternate sensing technique (stereo endoscope) in future work is expected to provide 3D measurement accuracy sufficient for the envisioned cancer treatment approach. Further development and testing is being discussed with a genetic engineering collaborator. Three-dimensional endoscopic imaging has been previously demonstrated. Future work would explore laser targeting capabilities using endoscopic instruments.

SOUTHWEST RESEARCH INSTITUTE®

2015 IR&D Annual Report

Detecting Distracted Drivers Using Vehicle Data, 10-R8496

Principal Investigators
Adam K. Van Horn
David W. Vickers
Michael A. Brown
Michael A. Dittmer

Inclusive Dates: 10/01/14 – Current

Background — The collection, refinement, manipulation, and analysis of large data sets are at the core of many business models today, with the increasing connectivity of people and devices. The rapid developments in active safety and connected and autonomous vehicles have greatly increased the volume of data produced on modern roadways. There are a number of organizations looking to leverage these new data sources in a myriad of ways, such as developing a deeper understanding of driver behavior. With an ever-increasing rate of data generation, more and more organizations will be looking to employ data mining and machine learning to generate value from their data.

Approach — The objective of this project is to evaluate the application of data-analytic and machine-learning techniques to vehicle behavior data sets to investigate the feasibility of detecting distracted driving. Data-driven methods are being investigated for predicting distracted driving using available data sources. This research will focus on the case of an onboard diagnostic (OBD) and use internally generated data, such as on-board Global Positioning System (GPS), inertial measurement unit (IMU) devices and video cameras. The data will be analyzed in an automated fashion to detect events indicative of distracted driving and then patterns will be found in the data preceding these events using a variety of machine learning techniques. These techniques will first be applied to high-level data sets to determine if there are any overall trends (e.g., standard statistical analysis) that indicate distraction. Samples of data from individual vehicles and drivers will be evaluated to determine more specific time-series based indicators of distracted driving. This analysis will include an evaluation of which sensors provide the most predictive power. The culmination of the previous research is the evaluation of data in streaming fashion. The focus of this stage will be to evaluate whether it is feasible to detect, in real time, whether or not a particular vehicle is being driven by a distracted driver based on whether the vehicle is behaving in a way that usually precedes a distracted driving event.

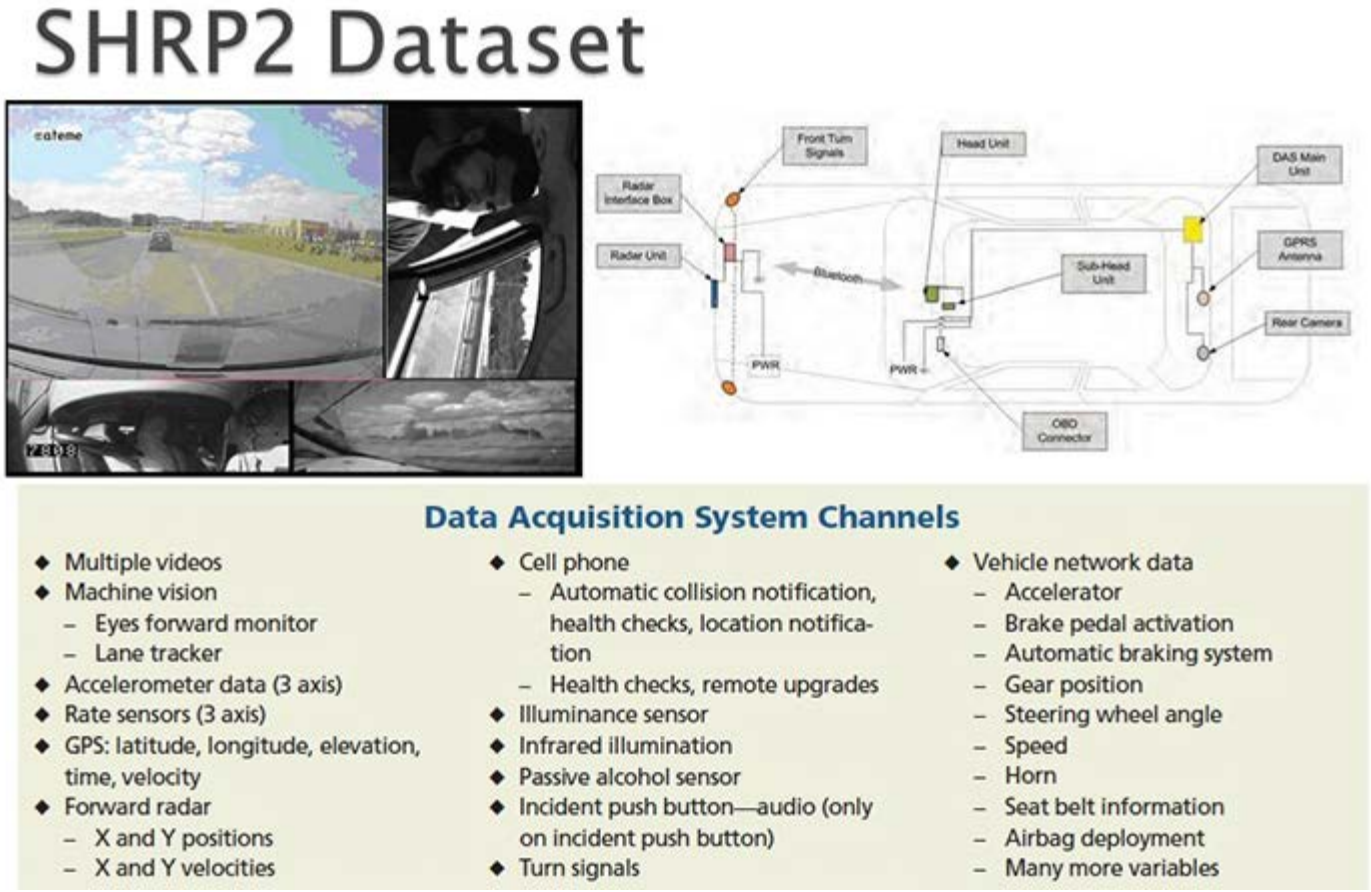

Figure 1: Example data streams of the second Strategic Highway Research Program (SHRP2)

Accomplishments — Time-series data and other pertinent data (i.e. event type, weather conditions, etc.) regarding 8,880 traffic events have been obtained from the Virginia Tech Transportation Institute from their second Strategic Highway Research Program (SHRP2), a naturalistic driving study (Figure 1). This raw data has been cleaned, normalized, and loaded into a NoSQL data store. Initial analysis to determine those factors that are the strongest predictors of events has begun.

2015 IR&D | **IR&D Home**

SOUTHWEST RESEARCH INSTITUTE®

2015 IR&D Annual Report

Cooperative Framework for Negotiated System Integration Among Heterogeneous Vehicle Systems, 10-R8500

Principal Investigators
Cameron Mott
Stephan Lemmer
Paul Avery

Inclusive Dates: 10/01/14 – 09/30/15

Background — Individual vehicle autonomy is advancing rapidly with regard to capabilities in perception, localization, and navigation to the point where a single vehicle is fully capable of autonomous operation. Ongoing research efforts conducted by various corporate entities are integrating multiple autonomous vehicles (also referred to as "agents") to work together towards a specific goal. This is often done through a central, fully connected supervisory controller or by simplifying the vehicles and utilizing rudimentary behavior sets. An extraordinary improvement could be provided by enabling functionally diverse agents to self-negotiate their role (if any) within the system, and to automatically integrate into the global tasks and goals of existing agents. This project focused on the methodology and supporting algorithms necessary to enable agents to integrate and dynamically coordinate towards a system goal in a distributed manner.

Approach — The research focused on the task negotiation and knowledge exchange aspects of this problem, under the assumption that the system has an autonomous capability and its goal is already provided. To better represent the concepts, the project has been referred to as "SyNRG: System Negotiation and Redistribution of Goals."

To accomplish the objectives of the research effort, the team created three major software components:

1. IISS (Inter-agent Information Sharing System): Enables agents to share relevant data between vehicles, such as the system goal, performance metrics, and individual capabilities.
2. KRA (Knowledge Representation Algorithms): Represents the information managed by the IISS, including direct sensor data and interpreted data.
3. CNA (Cooperative Negotiation Algorithm): Manages the system integration and task allocation behavior of the agents.

A few limitations were identified during the initial investigations of the project that would need to be addressed over the course of the project:

- A communication connection between vehicles may not always be available.
- Some *a priori* information may be available, while other information may not be clearly known or defined ahead of time.
- When a large number of vehicles is included, some algorithms and strategies may degrade significantly.

Accomplishments — The technical approach was applied in a simulation programming environment over the course of the project. Agents were created that offered a variety of capabilities and negotiated teams based on the system goal. Once a team of agents was established, the agents would use the SyNRG task distribution methodology to dynamically estimate the cost of performing the task and select an optimal agent to execute it. Team creation, task estimation, and knowledge sharing tasks were successful for every run.

A cost model was developed for each agent that allowed it to estimate the cost of performing specific tasks, and subsequently compare the estimated performance with any other agents that were similarly capable. A heuristic algorithm that provides a real-time solution to the optimization problem was created to address the difficulties associated with large number of agents attempting to compare the performance of a significant number of tasks. This helped to provide a system-optimized solution to accomplish the goal. Figure 1 presents an example representation of distributing tasks dynamically between autonomous agents.

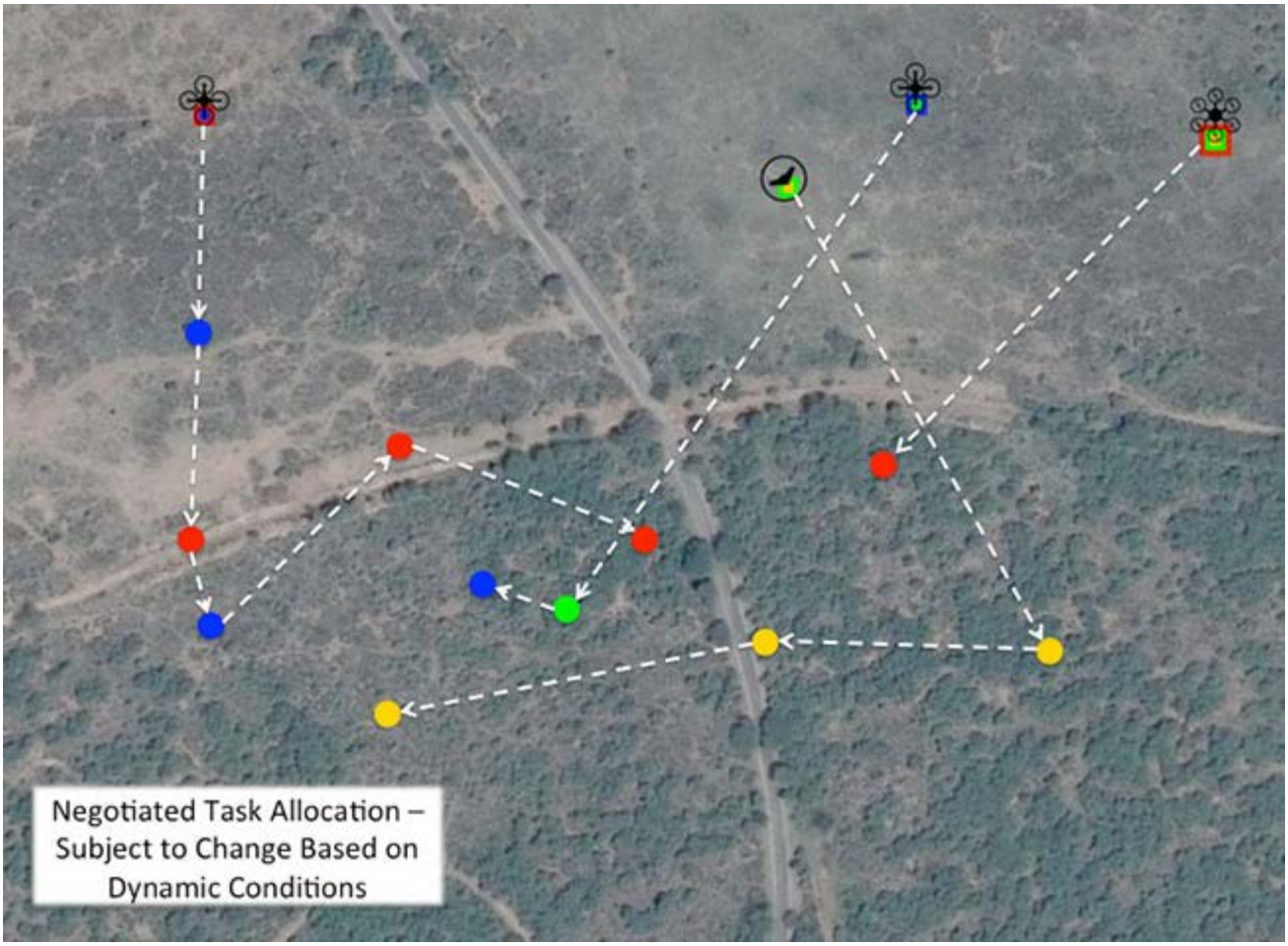

Figure 1: Representation of distributed agents (in this case unmanned aerial vehicles) and color-coded tasks. Each agent has negotiated among the other agents to determine the optimal distribution of tasks and the order, as indicated by the white arrows.

SOUTHWEST RESEARCH INSTITUTE®

2015 IR&D Annual Report

LTE System Security Research, 10-R8505

Principal Investigator
Brian Anderson

Inclusive Dates: 10/20/14 – Current

Background — Cyber physical systems, which are expected to drive our future economy and to be critical to our national security, will need secure and reliable wireless communications. Cellular communications systems have very broad coverage and fourth-generation (4G) long-term evolution (LTE) cellular technology has excellent bandwidth and low latency. Localized or personal cellular access points that may be deployed inside a home, office building, or crowded event venue are expected to be very popular in the future as cellular operators work to extend coverage, allowing more users to take advantage of cellular services in a congested or closed space. Cellular connectivity may replace or co-exist with Wi-Fi access.

However, small cheap base stations probably won't be painstakingly designed with security in mind and they will likely be affordable to hobbyists and "hackers." A hacked base station could be used to intercept communications, track users, or prevent users from connecting to the desired operator network. System designers want to know whether the LTE user equipment they may be embedding in their systems could be vulnerable, so this research investigated one aspect of LTE system security, the "rogue" base station.

Approach — This research project developed and tested a methodology for identifying suspicious or rogue LTE base stations. A couple of commercially available systems for detecting a rogue base station were announced after this research project was initiated, but these were only effective against 3G systems and not LTE systems. This project was broken into two phases: 1) a study phase to investigate LTE signal and protocol parameters for detecting a suspicious system and 2) a development and test phase to demonstrate parameter usage in algorithms designed to identify a suspicious base station.

Accomplishments — A number of LTE signal and protocol parameters were identified and incorporated into algorithms that could be used to identify a suspicious LTE base station. Laboratory-scale cellular systems were created that exhibited some of the suspicious parameters. Algorithms were developed and tested to ensure they could differentiate suspicious base stations from normal cellular base stations, and a cell phone application that incorporated some of the algorithms was developed and demonstrated.

2015 IR&D Annual Report

Telemetry System Manager Automatic Program Synthesis, 10-R8532

Principal Investigators
Patrick Noonan
Austin Whittington
Ben Abbott

Inclusive Dates: 01/14/15 – 05/14/15

Background — The current telemetry component provider landscape is diverse in approach and capability, and this landscape continues to evolve as new test articles require new components, which leads to new system management requirements and complexities, especially in the area of configuration. To combat this evolving landscape, the integrated network enhanced telemetry (iNET) program has defined an extensible markup language (XML) grammar that defines how telemetry devices are to configure themselves, the metadata description language (MDL). This vendor-independent grammar is being increasingly adopted across the board by the telemetry industry. As such, a general method for creating MDL while considering the constraints (or capabilities) of individual devices is needed. The only viable approach to this problem is for the vendors to supply the new or updated constraints along with any new or updated devices. However, there are various classes of users, or layers of users, that require the ability to add further constraints on top of the vendor constraints.

Approach — Standardized XML technologies were used to develop an experimental framework that automatically generated XForms, or user interface elements, directly from an XML schema, while also constraining the relevant fields. The generated user interface was then capable of providing immediate feedback, in the form of error messages describing the failed constraint(s), as the user input configuration data. The supplied constraints were written using XPath expressions, providing interoperability and straightforward conversion to other XML-based languages. Once the XForms were created, templates that contained basic data and partial frameworks for devices were used as initial instance data to feed into the interface. This allowed for defined specialization of the interfaces, as the initializing data combined with the constraints meant that portions of the user-editable data could be intelligently completed without user input. After the XForms were filled out, populated XML fragments containing all the information were stored in a database. Then, using marshalling techniques to combine all necessary devices/elements of the desired output, a final XML output file was produced. This approach resulted in an XML file that described a valid device configuration, which was used to successfully configure the target device.

Accomplishments — The experimental framework demonstrated that the hierarchical automatic program synthesis approach would work for the telemetry domain by combining standardized XML technologies in a specialized way to synthesize system management based on a hierarchy of constraints from multiple sources. However, the generated XForms were not user friendly because the user interface had an XML-centric look-and-feel. To address this, a method was developed for styling the XForms with JavaScript, while also retaining their functionality. In doing so, the user was presented with a rich user interface experience containing a custom layout and exposing only the fields relevant for their task.

SOUTHWEST RESEARCH INSTITUTE®

2015 IR&D Annual Report

Platform-Independent Evolutionary-Agile Optimization, 10-R8536

Principal Investigators
Phil Westhart
Joel Allardyce
Ben Abbott

Inclusive Dates: 03/10/15 – 12/04/15

Background — Graphics processing units (GPUs) have become more readily available as computational processors. Several languages and toolboxes have emerged to allow for the end user to migrate code execution onto a GPU. However, these coding frameworks change frequently to keep pace with the rapidly evolving field of GPU technologies. The more stable OpenCL, an open source version of CUDA that is not bound to NVIDIA GPU execution, has released two major versions and two minor versions since its initial release in 2008. A GPU-based solution has already been implemented in code similar to the challenge problem and seen 30x speedup in execution. This empirically demonstrated performance surge makes a GPU solution attractive as the focus of the optimization effort.

In this solution, a broad range of optimization techniques will be defined and categorized. These techniques will include GPU solutions, compiler solutions, and other optimization techniques as discovered. The techniques will be applied to the target problem in various experimental setups until an ideal execution environment is established.

Approach — The objective of this approach aims to identify a set of optimization techniques with configurable settings that can be adjusted in response to the current execution environment, enabling the software solution to easily be ported to next generation execution platforms. While our approach will cover a range of optimization techniques, the primary focus will be placed on GPU execution. The GPU implementation in this proposal will be implemented in OpenCL, rather than CUDA. OpenCL does not have any restrictions on target platforms, making it ideal for an evolutionary-agile, platform-independent solution. Platform independence allows the code to execute on any brand GPU, as well as any brand CPU, if desired.

The approach will also contemplate compiler optimizations, including potential compilation migration to other code languages. The various FORTRAN and C compilers each have their own strengths and weaknesses. Consideration will be given to compilers that compile to an intermediate language prior to final compilation to machine code. A multi-step compilation process such as this allows the original code to stay in its native form while still receiving the benefits that a different source code language would offer.

Noticeably absent from this approach are algorithmic optimizations. The implementation of the algorithm was performed by the scientists who understand the science behind the math. Gross modifications of the source code in the name of efficiency will hurt the ability of the scientists to expand upon the algorithm if desired. Since the long-term maintenance of the code will likely fall back on these scientists, leaving the source code in its original state allows for easy extension and maintenance where necessary.

Accomplishments — A variety of techniques for computational optimization has been developed. These techniques include compiler optimization flags, compile-time source code optimization, and run-time parallelization using CPU and GPU techniques. These techniques have successfully been applied to the planetary formation simulation challenge problem to yield speedups ranging from 1.2x to 8.8x faster. The speedup obtained shows a wide variety, which corresponds to the degree to which a particular test set

can be parallelized. The development of the techniques was completed with generalization in mind. To this extent, templates for the OpenCL implementation have been generated. These templates are currently being applied to the second challenge problem.

SOUTHWEST RESEARCH INSTITUTE®

2015 IR&D Annual Report

Computational Performance Enhancements via Parallel Execution of Competing Implementations, 10-R8537

Principal Investigators
David Vickers
John Harwell
Robert Klar
Sue Baldor
Ben Abbott

Inclusive Dates: 03/10/15 – Current

Background — The lattice-Boltzmann method (LBM) facilitates the analysis of fluid flows. It represents physical systems in an idealized way where space and time are discrete. It provides less computationally demanding descriptions of macroscopic hydrodynamic problems. Many of our clients have problems that are amenable to solution using the LBM. However, ongoing work on these problems suffers from overly long computational times for the simulation runs. This research takes advantage of the availability of large numbers of processors to evaluate a speculative space of optimization techniques during the execution of simulation runs. A genetic algorithm (GA) approach is being evaluated for the dynamic selection of an optimum implementation that efficiently executes the LBM algorithm to efficiently adapt to temporal phase changes in the simulation.

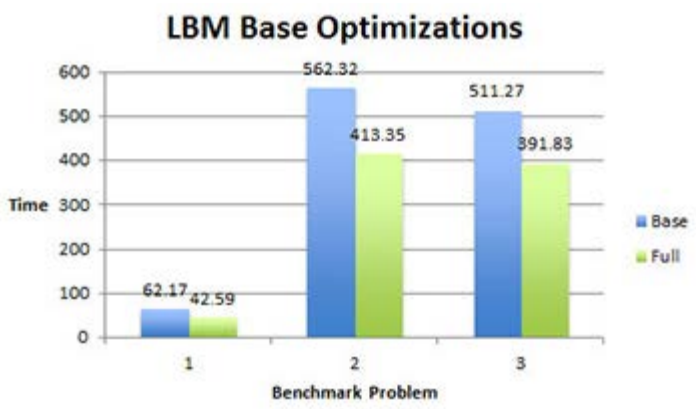

Figure 1: Non-thermal fluctuation base optimization

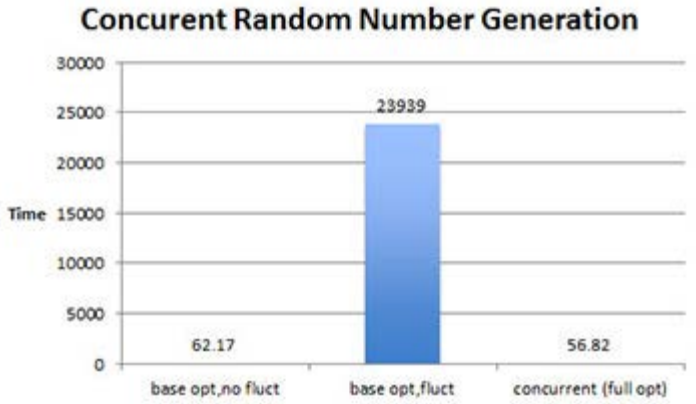

Figure 2: Thermal fluctuations and their optimization

Approach — The objective of the project is to use the lattice-Boltzmann method problem first and then the symplectic N-body algorithms with close approaches (SyMBA) problem to evaluate the applicability of a GA approach to optimizing the performance of computationally intensive simulation code. The original code provided by the problem presenters is first analyzed and optimized using a base set of transformations to produce a baseline suitable for the specialized GA-focused research. The code is then marked up to allow PARADYN to experiment with a variety of possible variations on the construction of the code, the organization of the data, and the flags used to compile the code. A set of genes (ways to vary the code, data, and flags) is defined and the set of alleles to be used (specific variations on the genes) is specified. The framework then executes multiple versions of portions of the simulation in parallel and evaluates the performance of those portions. New variations

are created by the framework based on the best performing versions. The continual evolution of the versions being run allows the simulation to eventually perform better than the baseline solution (Figure 1) and to adapt to changes in the state of the simulation (Figure 2).

Accomplishments — Baseline optimized versions of both the LBM code and the SyMBA code have been created. Figures 1 and 2 show the improvements that were made during the base optimization phase of work on the LBM problem. As Figure 1 shows, up to ~2x speedup was achieved for problems not including thermal fluctuations. Figure 2 shows an example improvement made during the baseline phase for problems including thermal fluctuations. The improvement is more than 800x. Genes and alleles have been defined for the LBM code, and the necessary plugins to the PARADYN framework have been implemented. The LBM code has been marked up for use by PARADYN. An example optimization run of the LBM code with PARADYN is show in Figure 3. This figure demonstrates PARADYN's ability to dynamically adapt to changes in the simulation, as can be seen when the particles are released at t=10,000. Figure 4 illustrates PARADYN's ability to select more and more optimized solutions as the simulation progresses, eventually reaching better performance than the baseline optimizations as evinced by the trend line. A comparison of the original code performance, along with the current PARADYN performance, is shown in Figure 5. A 5-8X speedup has been achieved to date for non-thermal fluctuation problems. The PARADYN framework was designed and implemented in a modular and reusable way that facilitates its use on the SyMBA project as well. Genes and alleles are being defined for the SyMBA code, and the code is being marked up for use within the framework.

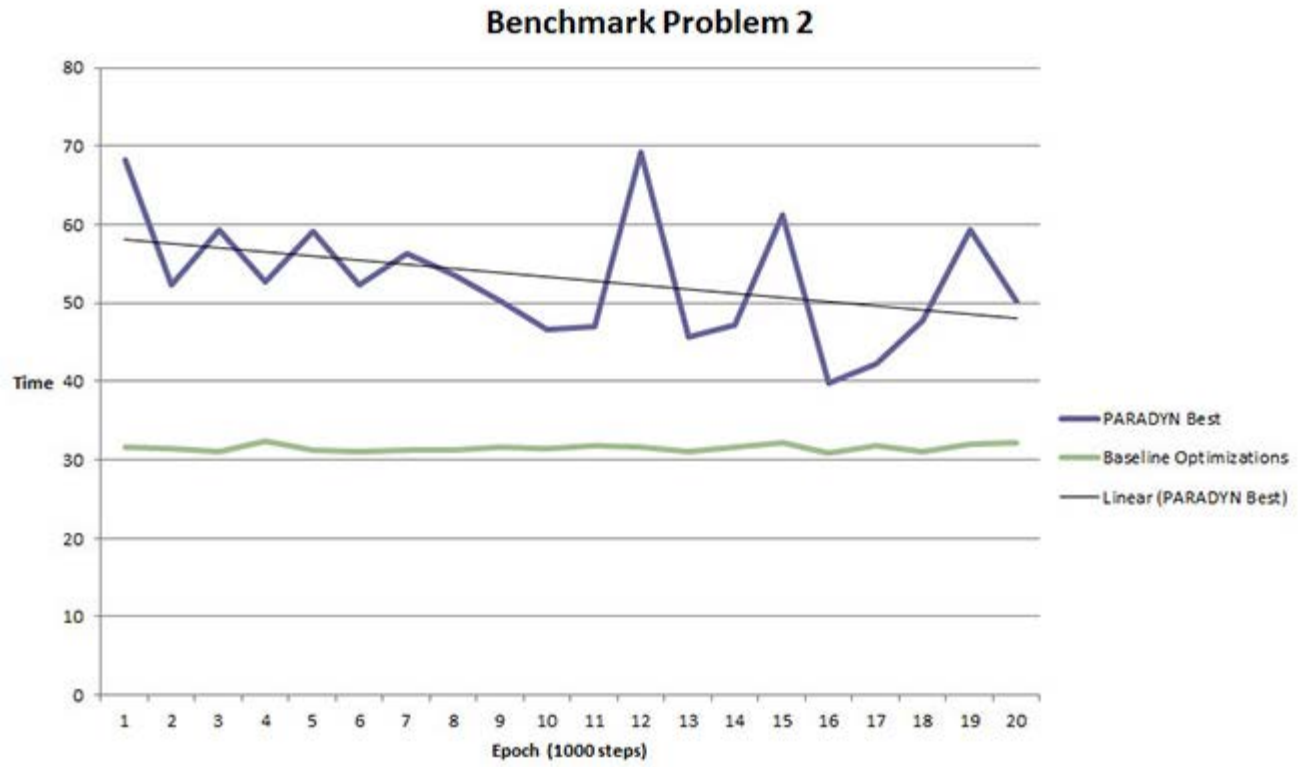

Figure 3: Responding to particle introduced in Epoch 11

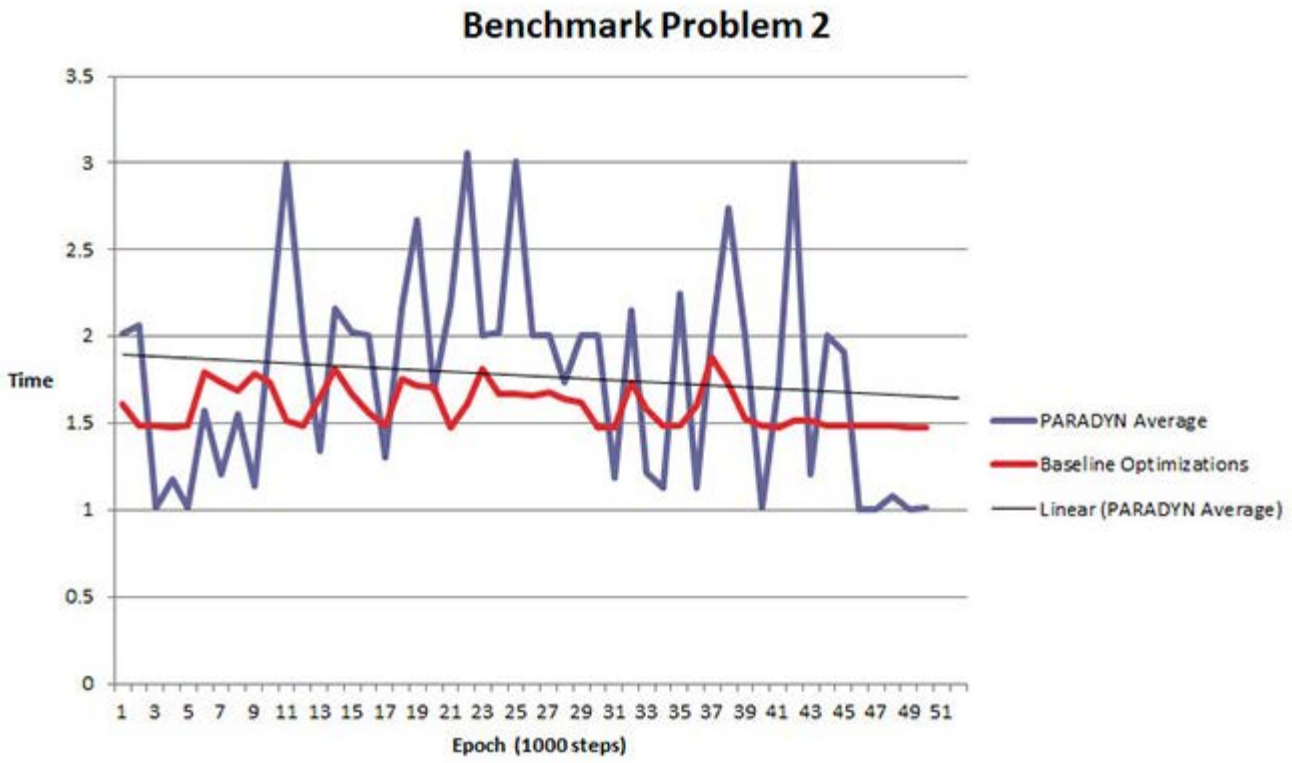

Figure 4: Finding better performance

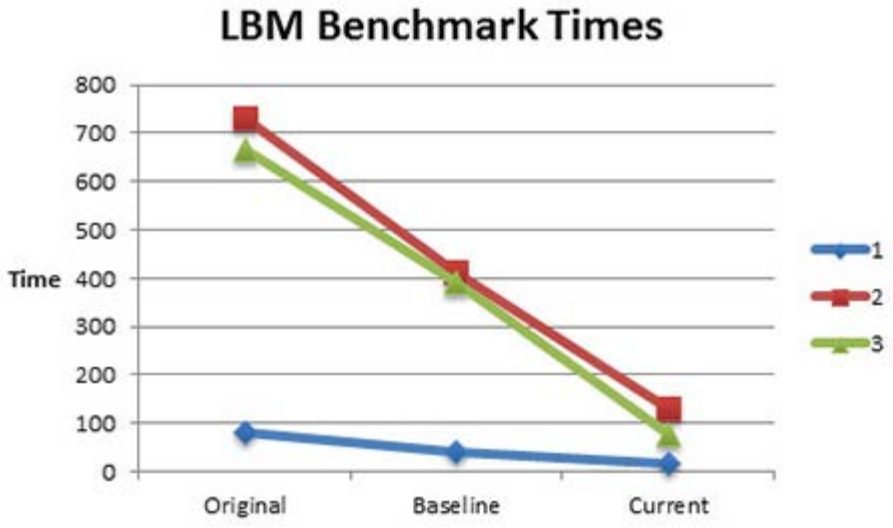

Figure 5: Baseline and GA-based improvement

SOUTHWEST RESEARCH INSTITUTE®

2015 IR&D Annual Report

Automatic Camera Calibration Algorithm Development, 10-R8546

Principal Investigator
Edmond DuPont

Inclusive Dates: 04/01/15 – 08/01/15

Background — Vision-based perception is already very common in production automobiles, supporting active safety and driver assist functions; however, these camera systems are primarily monocular. OEMs and suppliers are currently considering stereo cameras for use in next-generation vehicles. Stereo cameras enable measurement of range/depth to objects, which facilitates improved ability to detect and recognize vehicles and other objects, determines the distance to objects, and extracts drivable surfaces as it navigates through various environments. Such technologies are becoming necessary to enable developing highly automated and autonomous vehicles. Stereo cameras must be precisely aligned relative to each other to produce accurate disparity images. This project applied time-lapsed motion of the stereo cameras to capture multiple views of a natural scene to extract and correlate three-dimensional feature points available within the scene. The stereo cameras provided synchronized frames where opportunistic features were extracted over time and motion within the scene and used to find matching correspondences between the two cameras. The calibration pipeline focused on improving the rectification of the stereo images for better alignment between the intrinsic projective geometry of stereo camera images.

Approach — Traditional camera calibration involves the use of a calibration pattern of known dimensions to be held in front of the cameras by an operator. The challenges with this tedious approach are that it requires one or more trained operators for positioning the board and ensuring suitable coverage of the camera field of view, and there is no specific methodology that generates a reproducible calibration. A calibration architecture was developed to automatically detect "opportunistic" three-dimensional features from the environment to match between stereo cameras and track the features over multiple frames. At each set of synchronized frames, we matched features in the left camera's image against those in the right camera's image to find the inlier feature point correspondences. The matched features are computed as the vehicle traverses the scene to generate the projective rectification homographies to transform the left and right images such that their epipolar lines are aligned. The results provide an improved transformed right image to improve the block matching for generating the disparity image.

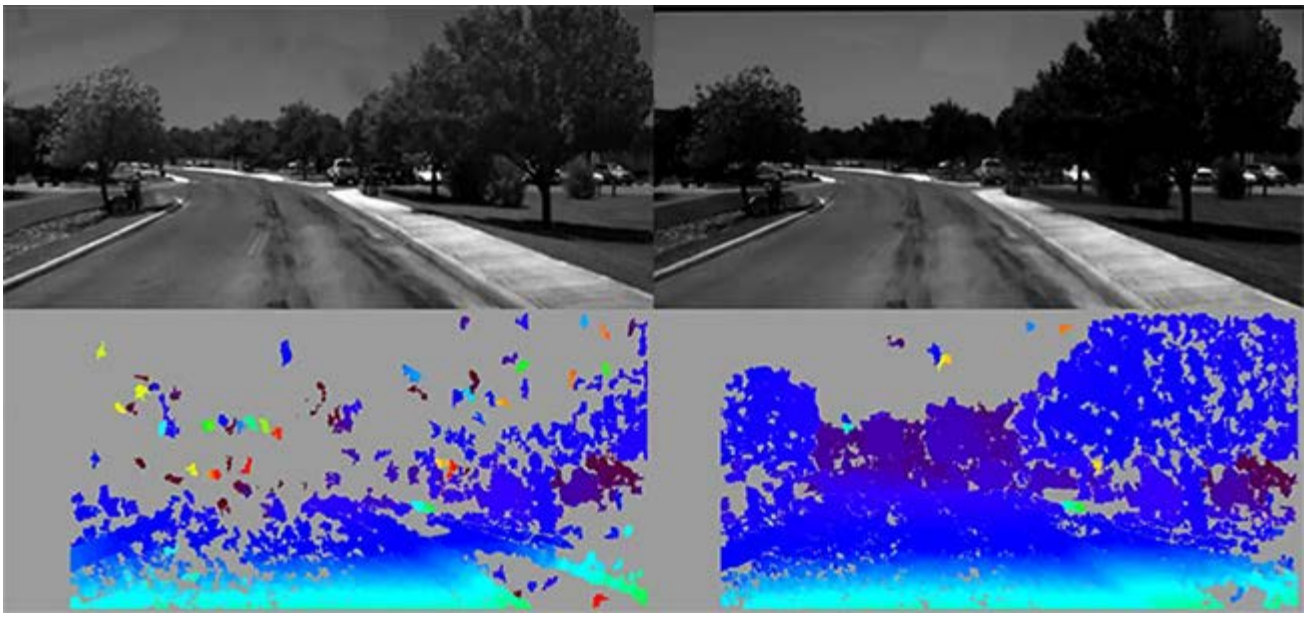

Figure 1: Compare block matching between open-source calibration (left) and automation calibration (right).

Accomplishments — The resulting camera calibration architecture provides an improved capability to develop robust automatic calibration systems of interest to military, agricultural, and automotive clients to reduce costs due to complete recalibration.

SOUTHWEST RESEARCH INSTITUTE®

2015 IR&D Annual Report

Traffic Profile Prediction, 10-R8548

Principal Investigators
David W. Vickers
Adam K. Van Horn
Matt D. Weatherston
Kenneth L. Holladay

Inclusive Dates: 04/01/15 – Current

Background — Advanced Traffic Management System (ATMS) software receives a continual stream of data from roadway sensors, police computer-aided dispatch systems, courtesy patrols, emergency vehicles, and its operators. As ATMSs have increased in complexity, they have generated and stored a large amount of traffic and event data. The daily operations of a traffic management center (TMC) focus on reacting to changing traffic patterns and incidents as they occur. There is a need to be able to predict more quickly traffic responses to planned events, quickly detect traffic anomalies, and alert the public faster and with more accuracy to the possibilities of travel delays. The goal of this project is to investigate the techniques necessary to change the TMC approach from the current "detect, respond, mitigate" to a proactive "predict, act, prevent." To do so, the ATMS must be able to predict traffic profiles from historical and current data. Predicted traffic profiles are made up of forecasts for the near future values (e.g. within the next 30 minutes) of traffic attributes such as speed, volume, and occupancy.

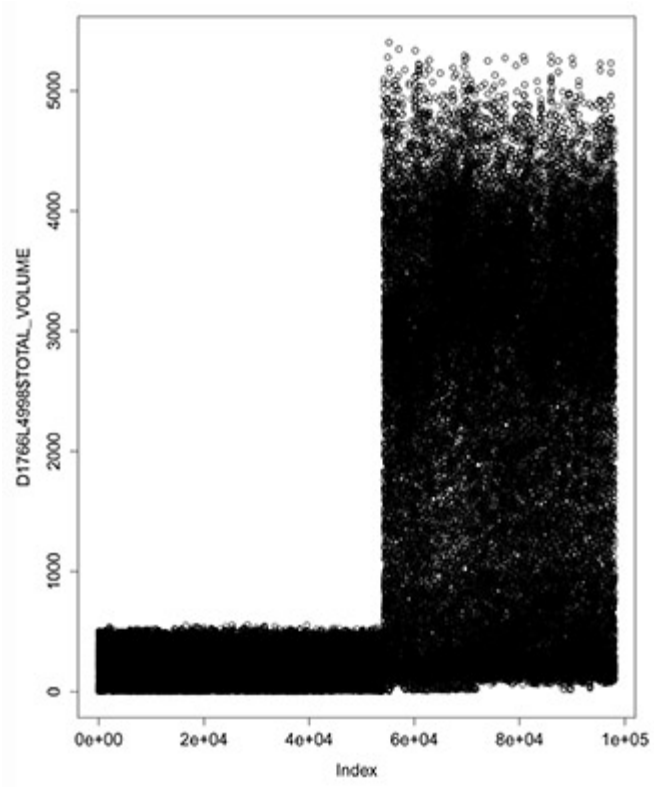

Figure 1: Volume configuration change

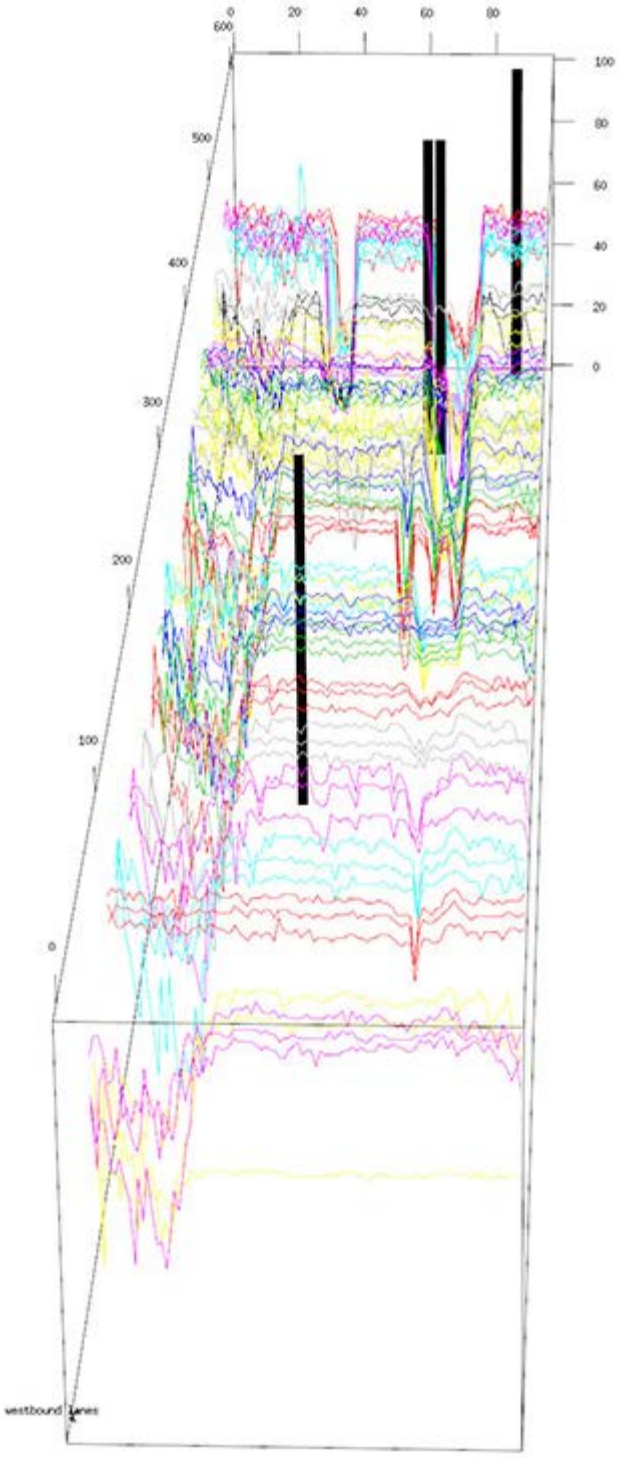

Figure 2: Twenty-four hours of traffic speed along a segment of I-4 with event locations and times marked

Approach — This project is experimenting with combining current data with historical data and inputs describing planned and unexpected circumstances (such as sports events, construction, weather, or accidents) to evaluate the ability to predict traffic profiles. Frequently careful analysis of the data is necessary to correct for abnormalities and artifacts introduced into the data. Figure 1 illustrates a sudden change in the values of the volume data when a configuration was changed. The data after the sudden change in the values must all be divided by 10 to be correct. Figure 2 illustrates an interactive visualization of traffic data (in this case vehicle speed during a 24-hour period along a segment of I-4) along with events (the vertical bars) that impact the data. The objective of the research is to evaluate the feasibility of adding

traffic profile prediction capabilities to SwRI supported ATMS software. Among the goals of the project are:

- Testing baseline traffic profile prediction algorithms using recent data.
- Evaluating algorithms for adding offsets to the recent data baselines using periodic functions of traffic.
- Testing mechanisms for detecting abnormal conditions.
- Characterizing the impact of the attributes of detected conditions.
- Evaluating the effectiveness of algorithms for integrating the impact of abnormal conditions into traffic profile predictions.
- Measuring the improvements in traffic profile predictions from combining current data, periodic historical data, and abnormal traffic condition data as a basis for prediction.
- Validating the utility of the combined algorithm.

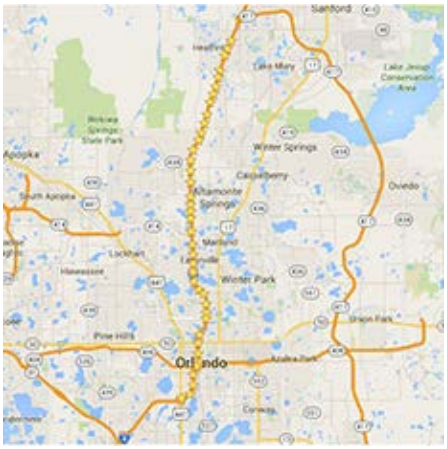

Figure 3: Detectors on I-4 in Orlando

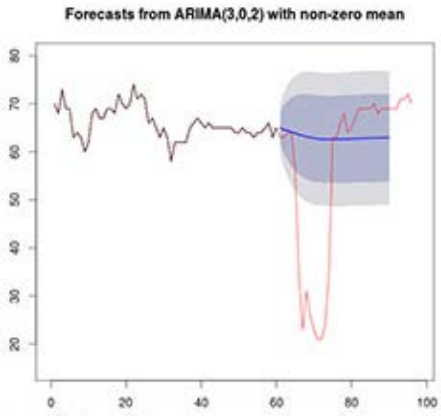

Figure 4: Autoregressive integrated moving average model (ARIMA); good for steady state, not good for transitions

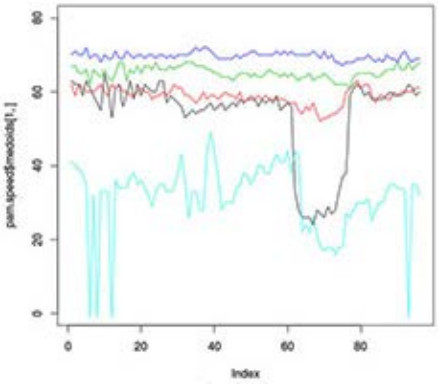

Figure 5: Speed medoids illustrating clustering by partitioning around medoids (PAM)

Accomplishments — Raw data, rolled up data, and other traffic information have been retrieved from files, databases and websites so that they can be combined and used for traffic profile prediction. Figure 3 shows the segment of I-4 from which the initial data was analyzed. The stars represent the locations of the detectors. An autoregressive integrated moving-average (ARIMA) model has been developed as a baseline for traffic profile prediction. Figure 4 illustrates the predictions of the ARIMA model selected. Data for I-4 in Orlando has been analyzed across lanes, in both directions and across various time periods (days, weeks, months, years). Sensor data has been analyzed and, where necessary, corrected to address anomalies found. Visualizations of traffic parameters, such as speed, volume, and occupancy across a set of detectors and time have been used to evaluate the impact of periodic and abnormal events. Data for different days of the week and different seasons, as well as those influenced by events, have characteristic shapes. Figure 5 shows the typical shapes (called medoids) of traffic speeds in a specific lane at a specific location. This type of analysis is called partitioning around medoids (PAM) and is useful in finding typical shapes from a collection of shapes. Analyses of the impact of rolling the data up to various time spans and impact of the length of data considered in making the models have begun.

2015 IR&D Annual Report

Automated Detection of Small Hazardous Liquid Pipeline Leaks, 10-R8552

Principal Investigators
Maria S. Araujo
Sue A. Baldor
Shane P. Siebenaler
Edmond M. DuPont
Daniel S. Davila

Inclusive Dates: 04/01/15 – Current

Background — The prevailing leak detection systems used today (e.g., computational pipeline monitoring) are simply unable to detect small leaks (less than one percent of the line throughput). False alarms of any leak detection system are a major industry concern, as they lead to alarms being ignored, resulting in leak detection systems that are ultimately ineffective. The focus of this research is to detect small leaks while also characterizing and rejecting non-leak events to significantly reduce false positive rates.

Approach — The objective of this project is to develop and evaluate a technology that can be suitable to meet the goals set by the Pipeline Research Council International (PRCI) for small liquid leak detection — Detect small leaks (1 percent of line throughput) in less than 5 minutes, with 95 percent confidence level, under all operating conditions (i.e. steady-state, pump start/stop, line pack, take-offs, etc.).

The approach is focused on fusing input from the different sensors in a variety of different combinations (hyperspectral, infrared, and visual), and use feature extraction and classifier training techniques to identify unique features that could provide a more reliable "fingerprint" of not only small liquid leaks, but also non-leak events in a variety of operating conditions, to substantially reduce false positive rates. Leaks considered in this research include crude oil and refined products such as diesel, gasoline, and jet fuel, which would cover a large percentage of hazardous liquid pipelines in the U.S. Leaks and non-leak events are being simulated in various lighting and weather conditions that would allow for signatures of leaks and non-leak events to be well characterized.

Accomplishments — Small leaks were simulated using various fluids (e.g., crude oil, kerosene, etc.) on a variety of representative surfaces (e.g., gravel, grass, dirt, etc.). All imagers recorded data simultaneously, so as to allow for the construction of a composite image using data from all or a subset of the sensors. Scenarios that could trigger false alarms (i.e., non-leak events) were also simulated and characterized. Focus was given to highly reflective and highly absorbent materials/conditions that are typically found near pipelines such as water pools, presence of highly-reflective surfaces (e.g., insulation sheeting on pipes), concentrated zones of heat (e.g., from the sun and other warm fluids).

Feature characterization is being performed via a set of feature characterization techniques running in parallel. The first of these, mean spectral vector analysis, is currently under development. The second characterization technique under development is textural analysis, which involves a three-dimensional generalization of the ubiquitous two-dimensional Gabor filters. These filters mimic the human visual system for the purpose of edge and texture detection.

SOUTHWEST RESEARCH INSTITUTE®

2015 IR&D Annual Report

Radio Frequency (RF) Detection of Fire Source, 10-R8556

Principal Investigators
Thomas C. Untermeyer
Sterling Kinkler
Jason Huczek

Inclusive Dates: 05/11/15 – 09/11/15

Background — SwRI previously developed radiometers to search for Radio Frequency (RF) signals occurring at the time of rocket launches. During this testing, SwRI discovered that the RF sensors detected the launch heat source through heavy smoke when infrared and visible cameras could not. Also, separate testing revealed that RF sensors could also detect burning black powder hidden behind a sheet of insulating material when infrared and visible cameras could not. Several potential clients have expressed interest in the need for having a different type of sensor to detect and locate the source of a fire for use during fire-fighting. Based on the results of the rocket launch testing and the insulation testing, it was believed that the same RF technology would provide a better method for detecting the source of a fire hidden by heavy smoke or behind walls. The main goal of this program was to determine whether or not a burning fire produced RF at sufficient energy levels to allow an RF sensor to detect and locate the source of a burning fire.

Approach — The SwRI team used an existing 35 GHz radiometer, an existing 94 GHz radiometer, and an existing 35 GHz radiometer array to measure and record RF emissions before and during a controlled burning fire located within a room enclosure constructed specifically for this purpose. In addition to RF emissions, the SwRI team recorded visible and infrared imagery during testing.

Accomplishments — The individual 35 GHz and 94 GHz radiometers provided inconclusive results while attempting to collect data during a burning fire. Either the radiometers did not properly function, or they did not have enough amplification. The other possibility is that a burning fire does not produce enough energy at those frequencies to detect the source of a fire at practical distances.

The 35 GHz radiometer array functioned well but also did not conclusively determine that a burning fire produced enough energy at this frequency to detect the source of a fire at practical distances.

Previous experience with detecting the fireballs of weapon launches at 35 GHz and 94 GHz indicated the possibility of detecting burning fires at appreciable distances. This research utilized existing radiometers originally optimized to detect the rather short duration of fireballs produced from the launching of weapons. The detection of the source of burning fires may rely on the design and development of new radiometers optimized for fires by increasing their integration time. Also, the type of burning material (wood versus chemicals) and the type of building wall material could also affect the ability of detecting the source of burning fires at practical distances.

2015 IR&D Annual Report

Select Superoptimization of Finite Element Analysis Tools, 10-R8563

Principal Investigators
Stephen A. Kilpatrick
Alex G. Youngs
Joel B. Allardyce
Stephen R. Beissel
Ben A. Abbott

Inclusive Dates: 06/24/15 – Current

Background — Some of the following problems are most cost-effectively solved using finite element analysis (FEA):

- Characterizing the ballistic limit of armored plating and composite fabrics
- Characterizing the performance of armored vehicles under blast and ballistic loads
- Characterizing the ballistic limit of materials with complex geometries

Ongoing work on these problems suffers from overly long computational times for the simulation runs. Significant additional project efforts would likely be funded if the simulation runtimes could be reduced by an order of magnitude.

SwRI currently has two methods of modeling these problems: 1) an externally available commercial software product and 2) internally developed software. Due to processing limitations, both modeling methods can only be employed on panels of extremely limited size. The desire is to achieve significant optimization of both sets of software to enable the simulation of more realistic panel sizes.

Approach — Superoptimization is the task of finding the optimal code sequence for a single, loop-free sequence of instructions. This effort attempts to apply superoptimization techniques to specific functions to significantly increase the performance of the overall program. Initially, a set of basic optimization techniques will be applied to the solution to provide a baseline set of performance enhancements. Once the baseline performance enhancements have been made, we hypothesize that the application of superoptimization techniques to selected hotspot functions in the code will reduce the execution time of this computationally intensive problem by an order of magnitude.

Accomplishments — Automated scripts were developed to benchmark and profile the two software products across a variety of input data sets. For the internally developed software product, improved execution times for the input sets have been realized through newer, faster hardware. Further improvements are expected to both products as we begin to understand the hotspot functions of interest and apply superoptimization techniques to those functions.

SOUTHWEST RESEARCH INSTITUTE®

2015 IR&D Annual Report

Subtle Anomaly Detection in the Global Dynamics of Connected Vehicle Systems, 10-R8571

Principal Investigators
Paul A. Avery
Adam K. Van Horn
Brian K. Anderson
Michael A. Brown

Inclusive Dates: 07/01/15 – Current

Background — Increasing connectivity among vehicles, roadside devices, and traffic management systems under the United States Department of Transportation (USDOT) Connected Vehicle (CV) program creates the potential for both novel benefits to society as well as novel risks. The vulnerability of individual vehicles for targeted disruption has increased as their control systems, and even their entertainment systems, have shifted towards computer control. This is compounded as vehicles begin receiving and acting upon messages within a CV system. The USDOT is actively funding research into the security algorithms, protocols, and procedures needed for the unique aspects of emerging vehicle and highway system technologies.

The concept of security for automated vehicles, especially ones that are connected to other information sources via over-the-air (OTA) messages, must go beyond message authentication to consider the broader issue of message trust by using a multi-factored approach. The global dynamics of a system comprised of individual and independent entities emerge as a result of the interaction of the individuals over time. The current project is investigating the algorithms and methods required to detect subtle anomalies in the behavior of a connected vehicle system at the system level.

Approach — The project team will utilize traffic data collected in District 5 (D5) of the Florida Department of Transportation (FDOT) to develop data-analytic methods for characterizing nominal traffic system behavior (behavior in the absence of anomalous CV messages). The team will then use a commercially available traffic modeling and simulation software product (TransModeler) to simulate and analyze the collective dynamics of traffic systems under various conditions where CVs are present. A classifier will be developed to detect subtle shifts in the global traffic behavior due to the presence of an anomaly.

Accomplishments — The project team identified specific and relevant CV operational scenarios and the requirements for implementation, in which the global dynamics of the system can be disturbed by OTA messages. A risk matrix was generated to score each of the identified threat scenarios according to their severity (S), probability (P), and ease of implementation (Ei) within the TransModeler software, according to the relationship of S*P/Ei. This exercise also helped the project team to determine an appropriate roadway to model within the FDOT D5. An approximately 17-mile segment of Interstate 4 in Florida, just north of Orlando was selected.

The project team also began work on the CV interface with TransModeler, which includes development of a socket communication layer between simulated vehicles based on dedicated short range communication (DSRC) standards. The team began testing this capability in TransModeler by injecting a "ghost vehicle" using an SwRI-developed graphical user interface (GUI). Basic safety message (BSM) data generated by the simulated vehicles was then analyzed using an SwRI-developed tool, which enables the rapid analysis of BSM data to determine the location and geometry of lanes. The errant BSM data from the ghost vehicle

is visible using this tool and is an example of the type of data available from CV systems that may indicate anomalous behavior.

SOUTHWEST RESEARCH INSTITUTE®

2015 IR&D Annual Report

Intelligent Propulsion System for Water-Borne Sensors, 20-R8431

Principal Investigators
Ronald Green
Phil West
Ben Abbott

Inclusive Dates: 12/13/13 – 12/13/14

Background — Original work on developing water-borne sensor (WBS) systems that utilize sensors for mapping the environment was undertaken at Southwest Research Institute in 2007. Past SwRI-funded research and development led to externally funded projects with the U.S. Army Corps of Engineers and the Federal Highway Administration. Current WBS technology consists of a self-contained sensor platform, equipped with ultrasonic sensors, that uses advanced data processing techniques to produce three-dimensional maps of cavities. The SwRI research team advanced the capabilities of the water-borne sensors by incorporating the following improvements:

- propulsion system
- improved sensor packaging
- radiation-hardened sensors
- remedial navigation system
- refined data communication capabilities
- improved data display capabilities

SwRI researchers are currently working to design and develop a next-generation WBS system with propulsion and navigation capabilities to enhance the utility of the technology. SwRI has already received expressions of interest from a broad variety of potential clients with different application requirements including routine maintenance inspections; high-risk, critical surveys (characterization of nuclear reactor containment vessels); and earth science exploratory surveys.

The overall objective of this project was to develop, demonstrate, and evaluate the use of an inexpensive propulsion and navigation system for enhanced utility of the WBS system. A propulsion system framework with navigation capabilities was planned for implementation on a WBS platform to which other environmental sensors (e.g., cameras, dosimeters, temperature probes) could be added. These combined capabilities provide for mobility and additional sensing capabilities that broaden the overall applicability of WBS. The new WBS is capable of collecting an array of data in both confined and large spaces. Adding a quasi-intelligent guidance system to the propelled sensor expands the range of applications of the WBS.

Approach — The specific research approach was to assemble and field-test a WBS with propulsion and a guidance system. The mobility platform is capable of delivering the sensor platform in a scientifically targeted manner to meet project objectives. Requirements and goals constrained by realistic needs were used to first select the mobility platform and then subsequently to evaluate its efficacy. A removable, off-the-shelf, propulsion system was added to the WBS. Initially, a tethered control system was implemented to allow an operator to remotely control the probe with real-time feedback. Current prototypes are now capable of non-tethered propulsion and navigation. Navigation algorithms couple input from ultrasonic and payload sensors (video, pressure, temperature, etc.) to make decisions about navigation. This technique allows an efficient physical search of a subject area by intelligently choosing which areas to map with greater complexity. The ability to simultaneously search a wide area and then focus sensor attention to areas that warrant more detailed evaluation through these techniques will speed reaction time, efficiency,

and effectiveness. This approach balances competing constraints (e.g., size, sensitivity, cost) while remaining flexible enough to fit to a broad range of applications.

Accomplishments — Construction of the prototype propulsion platform, a remotely operated vehicle, has been completed. The prototype has been tested in a water-filled tank. An autonomy plugin to the remotely operated vehicle platform has been developed. The goal of this autonomy plugin is to generate a global map of the environment, make decisions on where to explore, and be able to return the WBS to the point of deployment. The autonomy plugin uses simulated ultrasonic sensor data to map out and navigate a virtual world. Existing ultrasonic imaging capabilities were repackaged and attached to the propulsion unit. A general user interface has been implemented and basic two-dimensional mapping and return path planning has been implemented. Programmatic control of the remotely operated vehicle based on output from navigation algorithms has been accomplished. Current prototypes have greatly improved reliability and capacity and are available for advanced field testing and demonstration.

SOUTHWEST RESEARCH INSTITUTE®

2015 IR&D Annual Report

Defect Characterization Using Guided Wave Technology, 18-R8436

Principal Investigators
Jay L. Fisher
Adam C. Cobb

Inclusive Dates: 01/01/14 – 10/01/15

Background — Guided wave inspection technology is most often applied as an inspection survey tool, in which relatively low-frequency ultrasonic waves, compared to those used in conventional ultrasonic nondestructive evaluation (NDE) methods, propagate along the structure. Discontinuities cause a reflection of the sound back to the sensor for flaw detection. Although the technology can be used to accurately locate a flaw over long distances, the flaw sizing performance, especially flaw depth estimation, is much poorer than other, localized NDE approaches. Estimating flaw depth, as opposed to other parameters, is of particular interest for failure analysis of many structures. At present, most guided-wave techniques to estimate flaw depth require many assumptions to be made, such as weld geometry and flaw shape, and are highly dependent on the flaw reflection amplitude, which can vary based on many factors other than flaw depth.

Approach — To estimate flaw depth in a way that is not strictly amplitude-dependent, an approach based on a multimodal analysis was developed. The response of the fundamental shear horizontal wave mode (SH0), which is uniform through the part thickness, is compared with other higher order modes, primarily SH1, which are not uniform through the thickness. A specially designed meander wound electromagnetic acoustic transducer (EMAT) probe was used to generate SH0, SH1, and SH2 modes. Additionally, a model was developed to predict beam energy profiles (Figures 1 and 2) and flaw amplitude response based on part thickness, sensor size, probe distance to the flaw, and wave mode. This model was used to develop a relationship between the SH1 to SH0 mode amplitude ratio and the flaw depth, for a range of flaw widths.

Accomplishments — The approach was verified with a test set of 96 defects on plate specimens with flaws of different widths, depths ranging from 5 percent to 100 percent of total wall thickness, and different sensor-to-flaw spacings. Of these 96 flaws, 69 had SH1/SH0 amplitude ratios in a portion of the amplitude ratio curve that was not single-valued, so that they could be classified only as having depths greater than 40 percent of total wall thickness. Of these 69 flaws, five had depths that were in the range of 30 to 40 percent of wall thickness. Therefore for these 69 defects, 93 percent were classified correctly. Of the remaining 27 flaws, all had SH1/SH0 amplitude ratios in a single-valued portion of the curve, which meant that their depths could be estimated. Overall, the average depth sizing error of these flaws was only 4.3 percent, with a tendency to slightly oversize the flaw depth. The standard deviation of the error was 7.6 percent, and the maximum error was approximately 19 percent. In conclusion, this project showed that it was possible to characterize flaw depth independent of factors that cause the absolute amplitude of an individual wave mode to vary, such as non-uniform coupling of the probe to the inspection part surface, as well as (to a large extent) flaw width, and without the need for geometric reflectors for calibration. Figure 3 summarizes these sizing results.

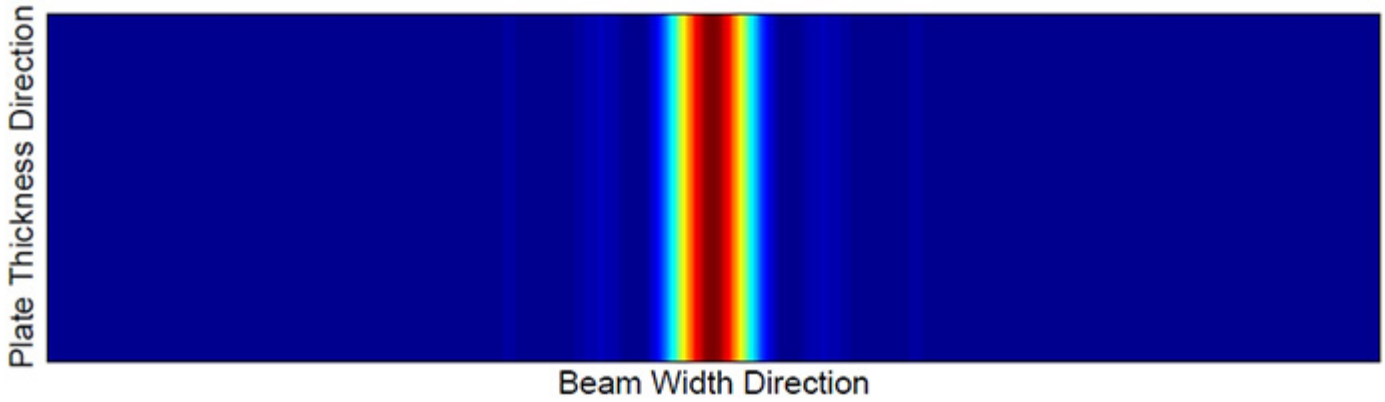

Figure 1: SH0 mode beam profile for a probe with a width of 38 mm and wavelength of 9.5 mm, at a distance of 34 cm from the probe.

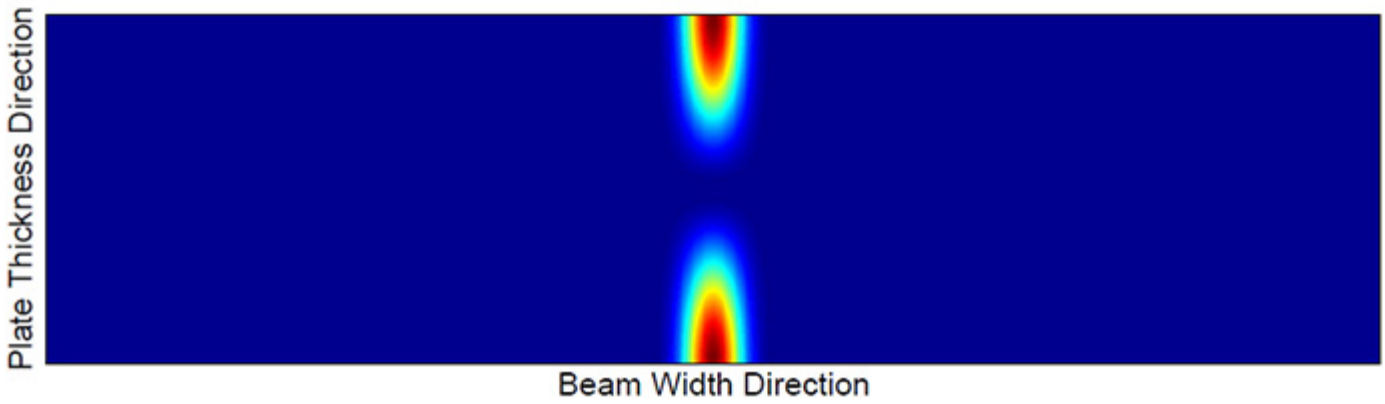

Figure 2: SH1 mode beam profile for the same conditions as in Figure 1.

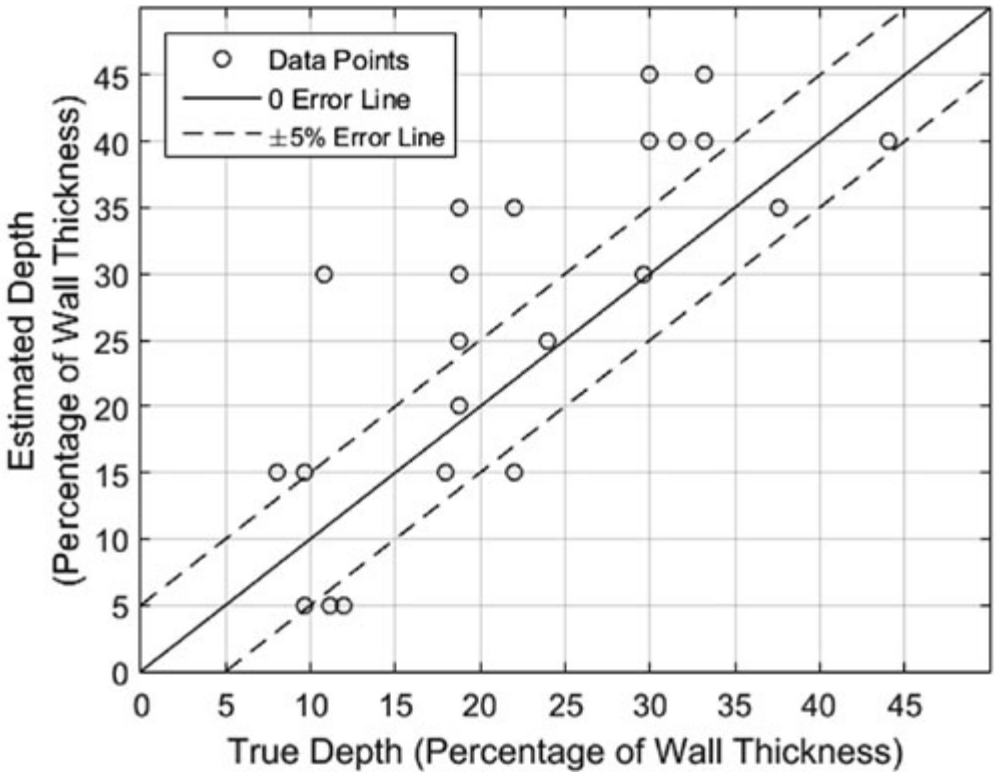

Figure 3: Depth sizing performance for flaws with an amplitude ratio greater than the

threshold.

SOUTHWEST RESEARCH INSTITUTE®

2015 IR&D Annual Report

FOCAS HGTR Design Evolution to a High Pressure Fully Transient System — Creation of the Full-Scale Gas Reactor, 03-R8427

Principal Investigator
Cynthia Webb

Inclusive Dates: 10/14/13 – 10/14/14

Background — The current emissions certification procedure for heavy-duty engines uses a transient test cycle and a ramped modal test cycle. The certification test cycles run at moderate-to-high loads, and do not weigh the cold portion of the test heavily (US HD-FTP is weighted 1/7 for cold-cycle emissions and 6/7 for hot-cycle emissions). Even with the low relative weighting factor, the emissions from the cold-start cycle still typically account for 40 to 50 percent of the total FTP emission. Due to the low weighting, the standards can be met with little or no emphasis on achieving high catalyst efficiencies at lower temperatures. However, beginning in 2013, the CA ARB funded a program that will focus on cold-start and low-temperature operation. The intended outcome of the study will be lower emissions standards, forcing the manufacturers to address and reduce cold-start emissions.

One major difficulty with studying cold-start emissions is that an engine is capable of only one cold-start a day (or perhaps two with aggressive forced cooling). Additionally, repeatability from day to day may make decisive comparisons difficult. These factors make studying cold-start emissions very time consuming and expensive.

The FOCAS® Hot Gas Transient Reactor (HGTR™) bench is a high-flow, diesel-fueled, burner-based catalyst performance evaluation and aging system that expands the capabilities of SwRI's FOCAS burner technologies. The reactor was sized to accommodate full-sized catalyst systems, allowing independent control of any combination of total exhaust flow, temperature, NO_x, water vapor, oxygen and HC concentration within the operating window of the device. Because the burner system provides independent control of temperature, it can simulate cold-start tests and cold-temperature operation, allowing many cold-start tests to be conducted in a day.

Approach — Through work conducted under two previous internal research projects, 03-R8372 and 03-R8427, the SwRI FOCAS HGTR diesel burner based catalyst evaluation test stand was modified to allow the burner to simulate the transient exhaust conditions generated by a diesel engine operating over a cold-start U.S. HD-FTP test cycle. All the simulated exhaust components were controlled independently, allowing the user to program any combination of variables. The independent control of variables allowed the measured exhaust gas conditions from the engine test to be input as a target cycle for burner, implying that the burner can be used to simulate any engine.

Accomplishments — The HGTR burner control range was greatly extended, and the transient control capability of all independently controlled subsystems was improved, allowing for very close simulation of engine conditions over the transient FTP cycle. This work produced very promising results and demonstrated that the FOCAS HGTR could be used for transient test cycle simulation. Figures 1 through 5 show comparisons to the burner simulation of the engine operation. In each graph, the setpoints (SP) were the data measured from the engine. The feedback (FB) or burner out (BO) conditions were measured from the HGTR simulation of the engine cycle.

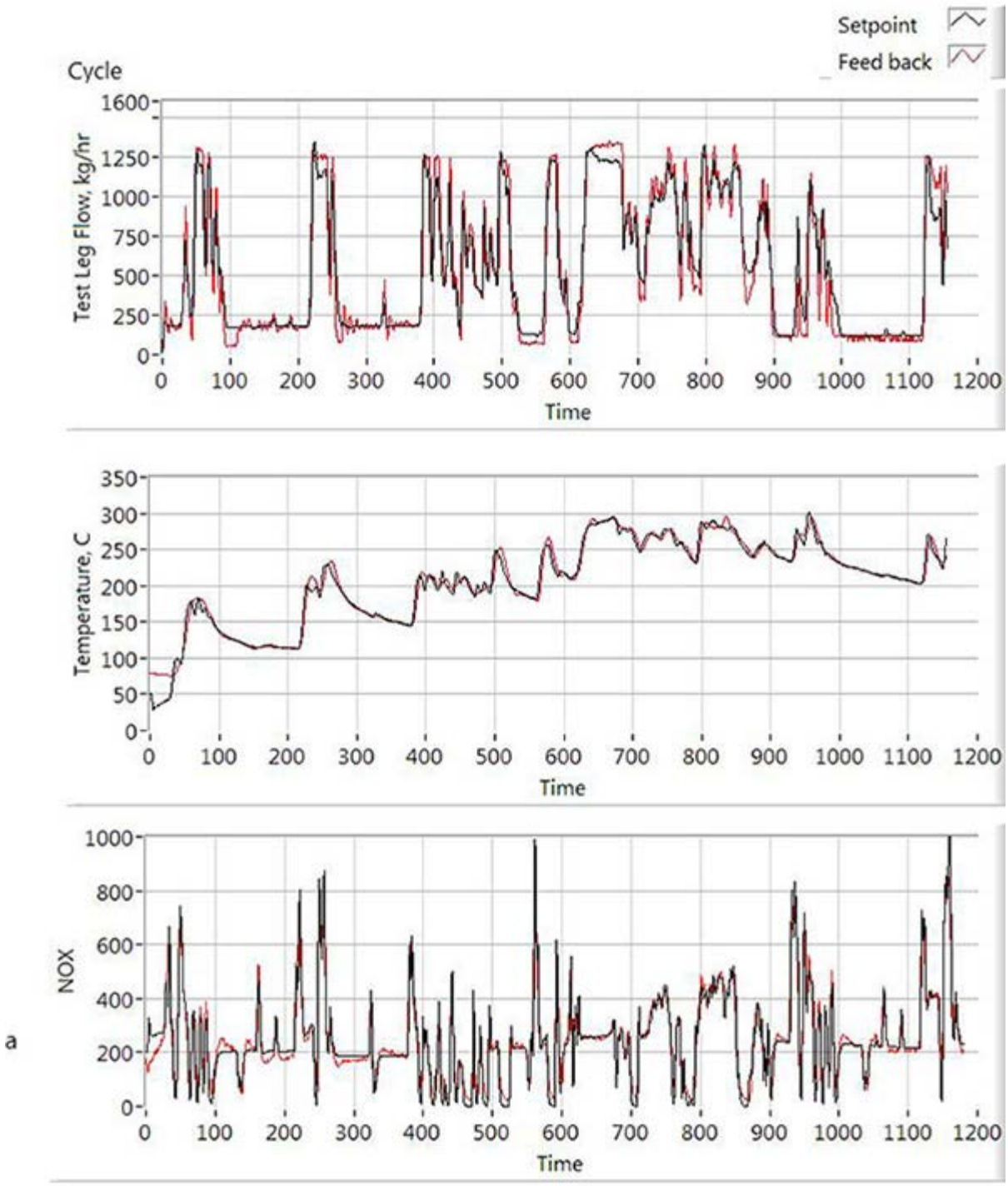

a

Figure 1. Comparison of flow, temperature, and NO_x between the engine and the HGTR simulation.

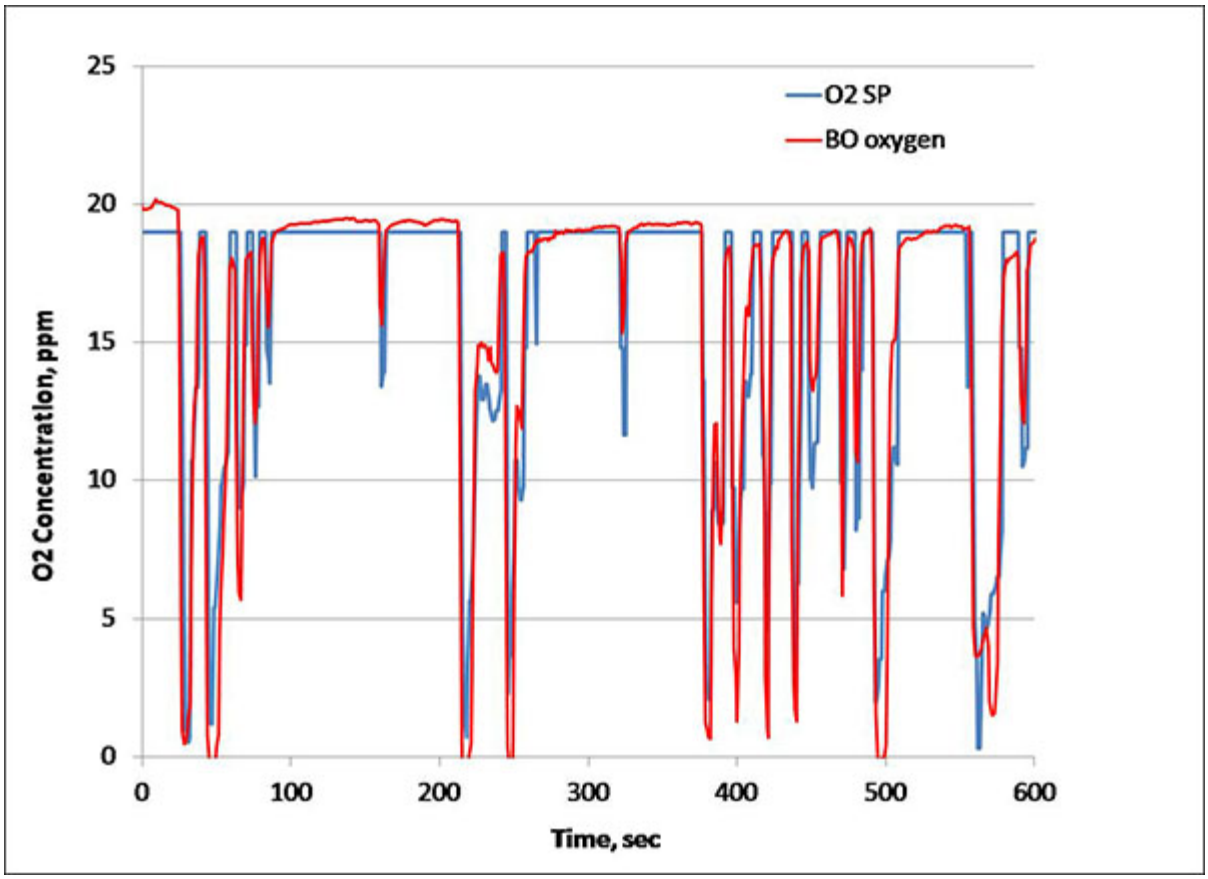

Figure 2. Comparison of measured exhaust oxygen concentration between an engine and HGTR over portion of cold-start FTP test cycle.

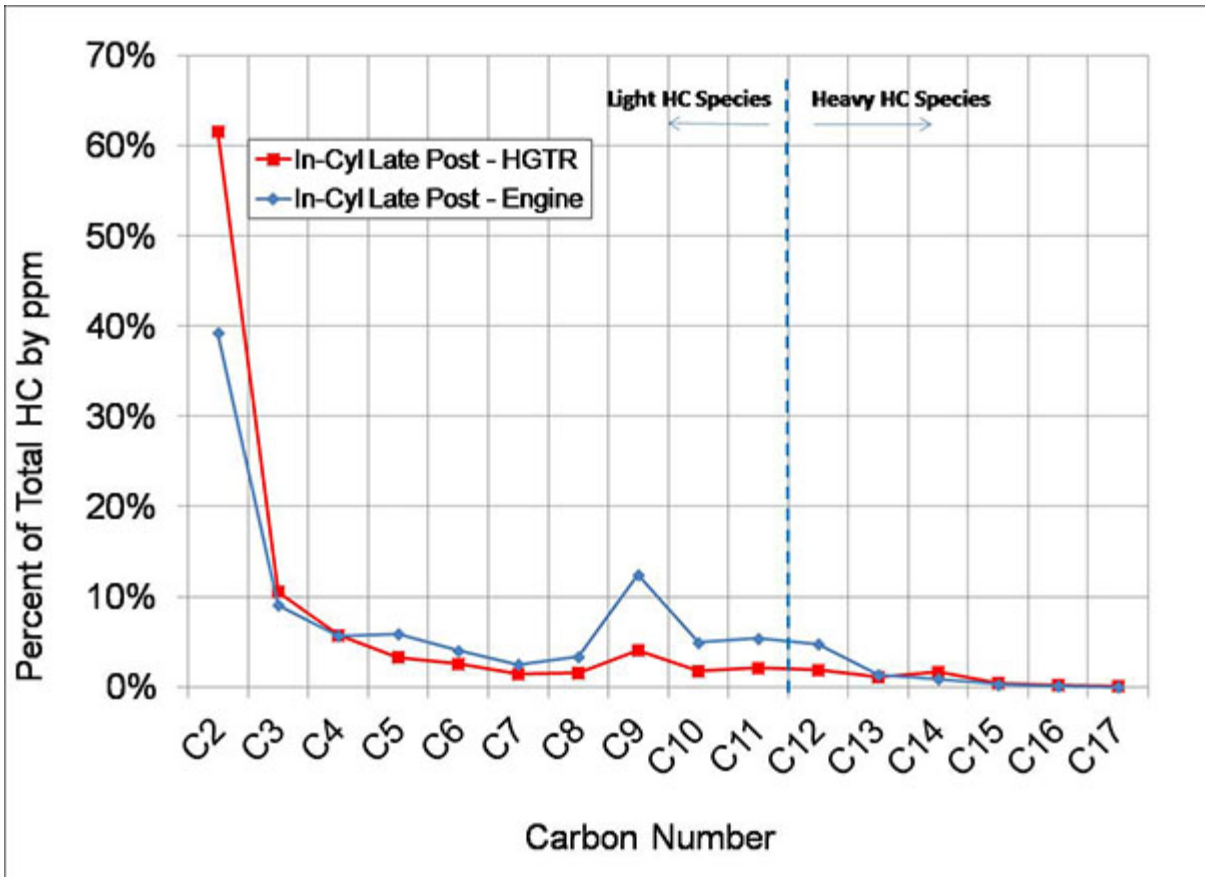

Figure 3. Comparison HC species generated by in-cylinder post injection on engine and in simulation

HGTR.

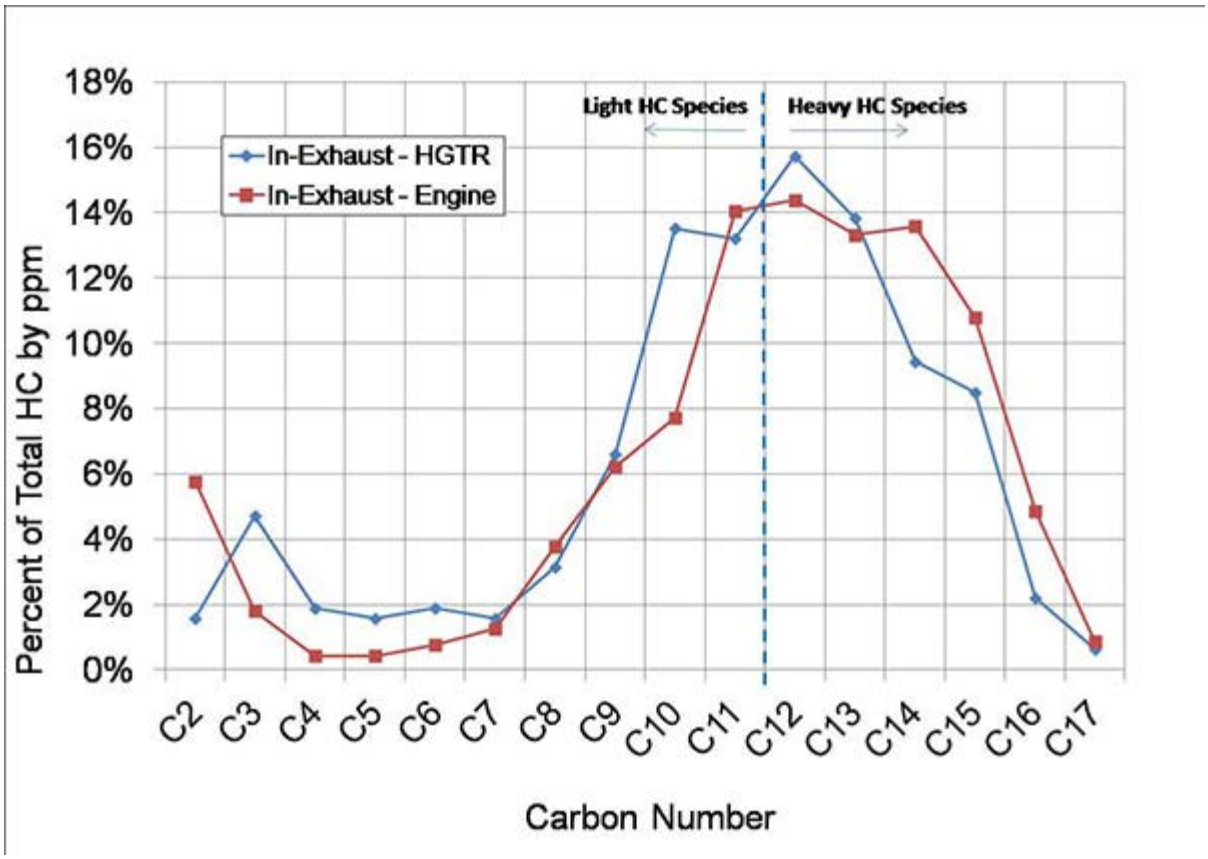

Figure 4. Comparison HC species generated by in-exhaust fuel injection on engine and in simulation HGTR.

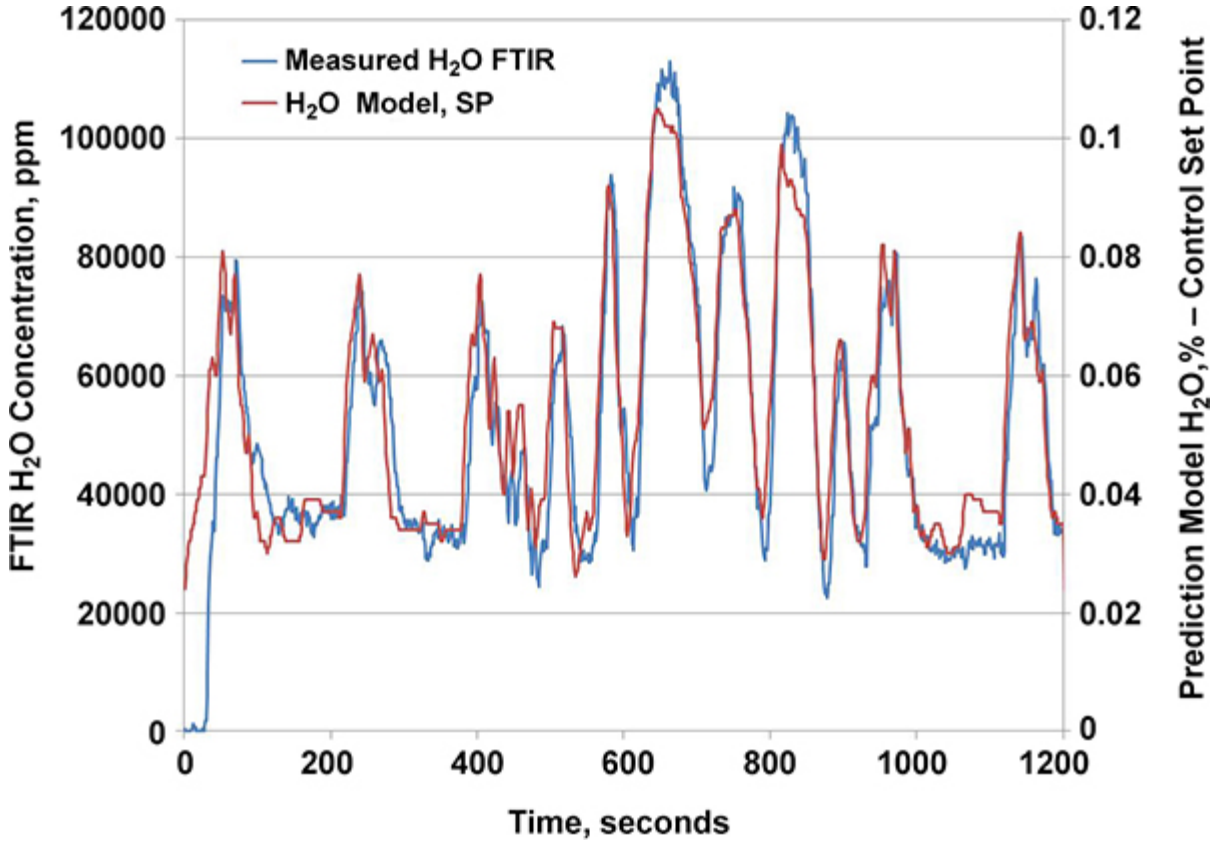

Figure 5. Measured and predicted water vapor over simulated cold-start FTP test cycle.

SOUTHWEST RESEARCH INSTITUTE®

2015 IR&D Annual Report

Identifying and Elucidating Low-Temperature Limiters to Catalyst Activity, 03-R8435

Principal Investigators
Gordon J.J. Bartley
Cary A. Henry

Inclusive Dates: 01/01/14 – 01/01/15

Background — The drive to more fuel efficient vehicles is underway, with passenger car targets of 54.5 mpg fleet average by 2025. Improving engine efficiency means reducing losses such as the heat lost in the exhaust gases. But reducing exhaust temperature makes it harder for emissions control catalysts to function because they require elevated temperatures to be active. Addressing this conundrum was the focus of this project.

Approach — The primary objective of this project was to identify low-temperature limiters for a variety of catalyst aftertreatment types. The approach was to determine the low-temperature limiters for all of the major emissions catalysts types, and to consider the mechanisms involved. Mitigation strategies were considered and some investigated.

Figure 1: SwRI's Universal Synthetic Gas Reactor®

SwRI's Universal Synthetic Gas Reactor® (USGR®) was the primary tool used to perform the testing, and catalysts tested were the three-way catalyst (TWC), the diesel oxidation catalyst (DOC), and ammonia selective catalytic reduction catalysts (NH_3-SCR), of which there are three base formulations: the lean NOx trap (LNT), the ammonia oxidation catalyst (AMOx), and the natural gas oxidation catalyst (NGOx).

Accomplishments — The project work is complete. Nitric oxide (NO) and unsaturated hydrocarbons were found to be significant low-temperature limiters to TWC activity.

Removal of the NO lowered the carbon monoxide (CO) light-off temperature from 229°C to 174°C, and the

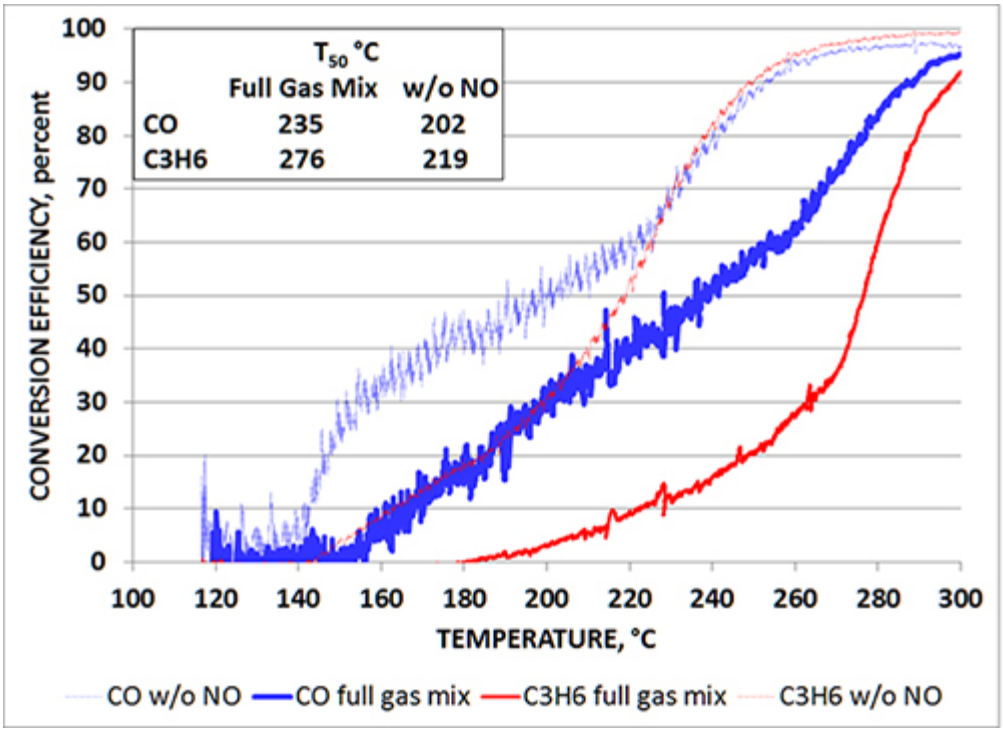

Figure 2: TWC with and without nitric oxide

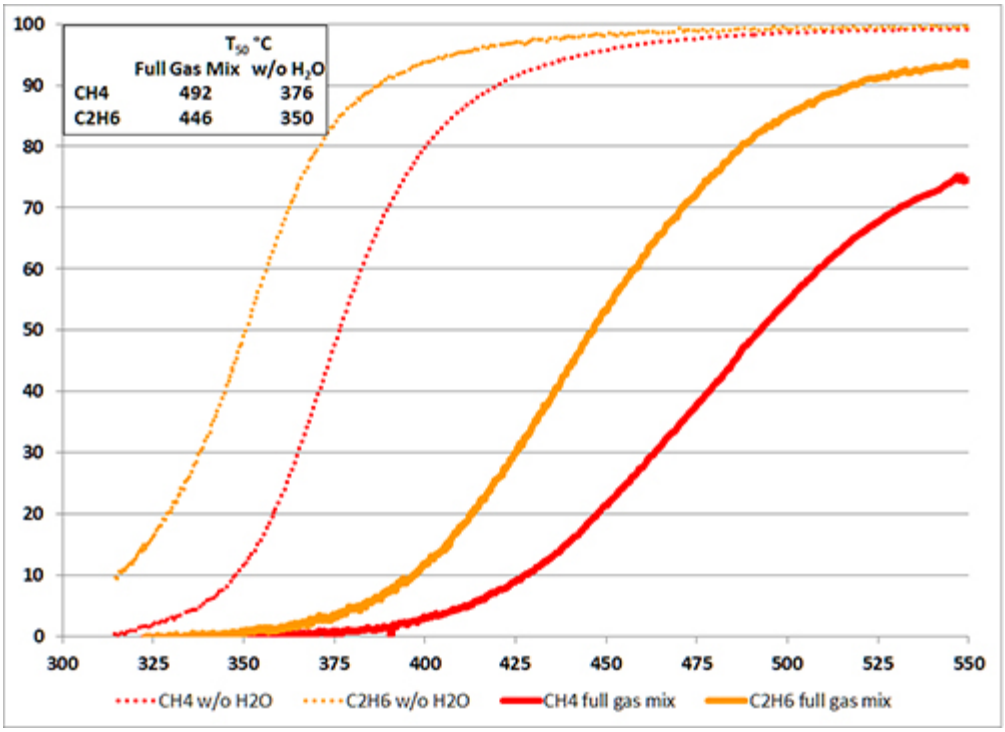

Figure 3: NGOx with and without water

propene (C_3H_6) from 257 to 203°C. Conversely, removal of C_3H_6 lowered the CO light-off temperature from 229 to 185°C, but significantly reduced NO activity. Thus, NO and C_3H_6 are limiters to CO light-off, but C_3H_6 is needed to promote NO light-off. This type of complex interaction is common throughout catalysis.

For the DOC, removal of NO dramatically improved the light-off of ethene (C_2H_4) from 248 to 179°C. Removal of hydrogen (H_2) slightly hurt C_2H_4 light-off, so NO is a limiter again, and H_2 is a mild promoter. For the Fe-Z NH_3-SCR catalyst, removal of nitrogen dioxide (NO_2) dramatically increased light-off temperatures. The latter is well known, as NO_2 is a powerful promoter of the NH_3-SCR reaction. None of the other gases had any marked effect.

For the Cu-Z NH_3-SCR catalyst, there were no limiters to performance, and only H_2O was shown to inhibit the V-SCR catalyst. For these catalysts, a different approach will be needed to improve performance, such as replacing the NH_3 reductant with a more effective reductant, possibly H_2. For the AMOx catalyst, removal of C_2H_4 lowered the NH_3 light-off temperature from 281 to 212°C, and removal of CO lowered it to 250°C. In contrast, removal of H_2 raised it to 298°C, so C_2H_4 and CO are both limiters, but H_2 is a promoter. For the LNT catalyst, removal of CO lowered the NO light-off temperature from 165 to 107°C. Confusingly, removal of C_3H_6 raised the NO light-off temperature from 165 to 205°C, and removal of

propane (C_3H_6) raised it slightly to 170°C, but removal of both C_3H_6 and C_3H_8 dramatically lowered it to 102°C. For the NGOx catalyst, removal of H_2O dramatically lowered the CH_4 light-off temperature from 492 to 376°C. To pursue further, H_2 was increased by an order of magnitude and the CH_4 light-off temperature reduced to 469°C, so increasing H_2 exposure may be a mitigation strategy for NGOx catalysis.

2015 IR&D Annual Report

Sampling System Investigation for the Determination of Semi-Volatile Organic Compounds (SVOC) Emissions from Engine Exhaust, 03-R8442

Principal Investigators
E. Robert Fanick
Svitlana Kroll
Chris A. Sharp
Shraddha Quarderer
John E. Gomez

Inclusive Dates: 01/01/14 – 12/31/15

Background — Semi-volatile organic compounds (SVOC) are a group of compounds that may form during combustion and/or are present in the unburned portion of the fuel and lubricating oil that ultimately becomes part of the exhaust. Many of these compounds are considered toxic or carcinogenic. Since these compounds are present in very low concentrations in diesel engine exhaust, the methods for sampling, handling, and analyzing these compounds are critical to obtaining representative and repeatable results. Engine testing is typically performed using a dilution tunnel method. With a dilution tunnel, the collection of a representative sample is important to ensure that the sample is representative of the actual exhaust. Experiments were performed to determine the equilibration time and other sampling parameters required for the measurement of SVOC. The results show that representative results can be obtained with this method.

Approach — The main objective of this project was to validate and qualify the SwRI dilute sampling procedures for use as a dilute exhaust sampling method. Some of the individual tasks included:

- Identifying and implementing possible refinements and improvements in SwRI's dilute-based sampling method
- Evaluating the constant volume system (CVS) tunnel soot equilibration variables (tunnel wall effects)
- Establishing the test to test repeatability for measuring SVOC
- Determining SVOC trap breakthrough
- Comparing collection efficiency of various sample media
- Validating procedures for sample media handling and media blanks
- Comparing solvents for removal of particulate- and volatile-phase compounds
- Optimizing the sampling system design

A 2012 Ford 6.7L engine was used to produce the engine exhaust throughout the entire experiment. The testing started with a "clean" dilution tunnel, and engine-out exhaust ("dirty" exhaust) was sampled to determine the equilibration time for the dilution tunnel. Tests using different filter media and trap breakthrough experiments were also performed. The exhaust was then changed to aftertreatment-out ("clean" exhaust), and the equilibration time was determined from a "dirty" tunnel to a "clean" tunnel. Figure 1 shows a schematic of the dilute exhaust SVOC sampling system. Samples were collected periodically throughout the tunnel equilibration period, and these samples were extracted and analyzed by gas chromatography/mass spectroscopy (GC/MS).

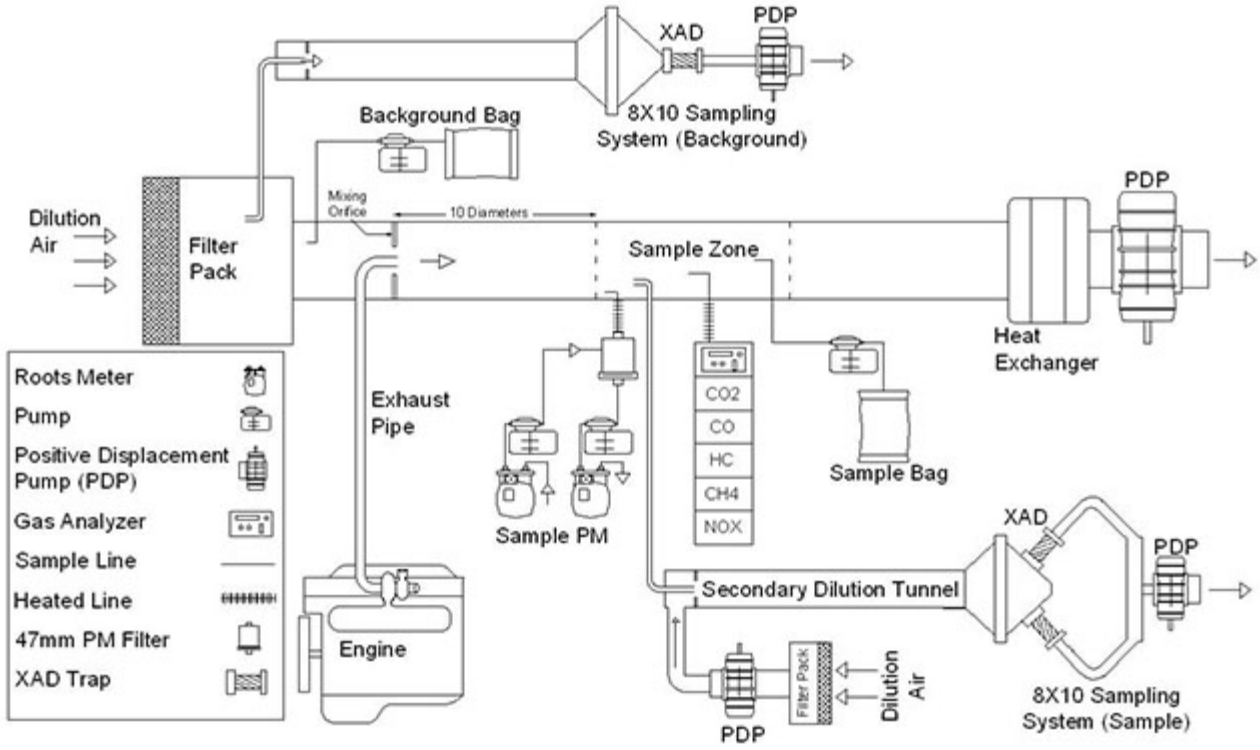

Figure 1: New sample system schematic for dilute exhaust SVOC measurements.

Accomplishments — As a result of this study, several accomplishments and improvements were made to the dilute exhaust sampling system. These improvements included:

- Implementation of a background air SVOC sampling system, in addition to the traditional tunnel blank
- Implementation of closed-loop control to maintain constant flow rate on the dilute exhaust SVOC sampling system
- Implementation of 8-x10 inch Zefluor™ filter instead of the traditional 20x20 inch Pallflex filter
- Elimination of polyurethane foam (PUF) in the SVOC sample train (use XAD porous polymer resin only)
- Installation of a heated blanket around the secondary dilution tunnel for the dilute exhaust SVOC sampling system
- Implementation of a field blank procedure for each day of testing to account for ambient air contributions
- Implementation of sampling surrogates and an internal, clean-up, and recovery standard to improve quantitation
- Improvement of solvent extraction techniques for extraction of XAD and filters
- Optimization of the solvent system to reduce losses in surrogate compounds
- Validation of sample media handling for both extraction and collection
- Evaluation of different filter media
- Determination of test-to-test repeatability
- Determination of the tunnel equilibration period
- Determination of trap breakthrough

In addition to the accomplishments listed above, the Environmental Protection Agency (EPA) agreed to allow this method to be introduced for a review and comment period in the Code of Federal Regulations. This accomplishment will allow the SwRI method to be used as an alternative for sampling and analysis of SVOC in dilute engine exhaust. Several papers were presented on this topic at Coordinating Research Council (CRC), Society of Automotive Engineers (SAE), and Emissions 2015 conferences; and the

method will be sent for the EPA review period in October 2015.

SOUTHWEST RESEARCH INSTITUTE®

2015 IR&D Annual Report

Battery Duty-Cycle Decomposition for Cycle Life Analysis, 03-R8480

Principal Investigators
Bapi Surampudi
Joe Steiber

Inclusive Dates: 07/01/14 – 12/30/15

Background — In a growing percentage of automotive applications, battery pack life is one of the most important attributes that impacts warranties from OEMs. Active life of electrochemical cell energy storage elements such as batteries is measured based on capacity degradation from 100 to 80 percent. The degradation of capacity is a function of temperature and operational duty cycle. Batteries are used in applications with diverse duty cycles. A few examples of such applications are hybrid electric vehicles (HEV), plug-in hybrid electric vehicles (PHEV), electric vehicles (EVs), frequency regulation in grid storage, renewable energy smoothing for solar/wind, peak shaving for grid storage, telecom UPS, hybrid earthmoving equipment, and military and space missions. The life of the same battery will be quite different for each of these applications. There is a strong need among all these industries to have a common life test procedure that can be utilized to better understand and predict cell life for their application.

Approach — A map-based testing procedure has been conceptualized and researched in order to attempt to measure cell degradation at various depths of discharge and current levels at different temperatures. The methodology is based on the premise that any duty cycle can be decomposed into a combination of interpolated weighted components, generated as part of a design of experiments (DOE) matrix near the boundaries of battery operating space. The boundaries mark the transition between normal operation and abuse, and are typically captured by variables such as nominal state of charge (SOC), peak-to-peak SOC variation, charge power, discharge power, and temperature. Each component of life measured is used to estimate the overall life of the battery for a given application duty cycle. This project generated test data for the components using three typical duty cycles to identify the effect of several cycling factors, ordering of the cycling, and key limiting/critical behavioral change triggers.

Accomplishments —

- Identified the impact of dominant factors of a cell's degradation process through DOE experimentation
- Identified critical influences during the cell aging that mark the onset of a major variation in a cell's degradation behavior
- Measured thermodynamic behavior of a cell under isothermal conditions (entropic variations during charge and discharge processes)
- Improved the periodic determination of cell capacity following cycling
- Established and validated the role of the cycling order (of various duty cycles) on the overall degradation of the cell
- Established the correlation of life degradation of a cell under a uniform cycle versus a randomized cycle
- Demonstrated an error in prediction of only 2.3 percent during composite profiles spanning more than 550 consecutive aggressive cycles

SOUTHWEST RESEARCH INSTITUTE®

2015 IR&D Annual Report

Development of New Ruthenium Catalysts for the Low-Temperature Reduction of NO_X Emissions from Vehicle Exhaust, 03-R8488

Principal Investigators
Gordon J.J. Bartley
Zachary Tontzetich (UTSA)
Ryan Hartley (UTSA/SwRI)
Mahesh Krishnan (UTSA)
Robert Fanick

Inclusive Dates: 09/01/14 – 08/31/15

Background — NH_3-SCR catalysts are commonly used to reduce NO_x emissions to N_2 from engine exhaust. Limiting factors are the thermolysis and hydrolysis of urea solutions for production of the NH_3, and the light-off temperatures of the catalysts used. A published paper indicated that very low-temperature NO_xSCR could be achieved using H_2 as the reductant and a Ru-based catalyst. This project investigated Ru-based catalysts for this reaction.

Approach — The primary objective of this project was to evaluate Ru-based catalysts for reduction of NO_x to N_2, and further develop them for practical applications. The approach taken was to start with a Ru-Al_2O_3 catalyst, prepared by a commercial manufacturer specifically for this project, and characterize its catalytic properties. The next step was to determine how best it may be employed, and further develop Ru-based catalysts to improve performance characteristics in the chosen applications. Coated core samples were prepared at The University of Texas at San Antonio (UTSA), and SwRI's Universal Synthetic Gas Reactor® (USGR®) was the primary tool used to perform the testing.

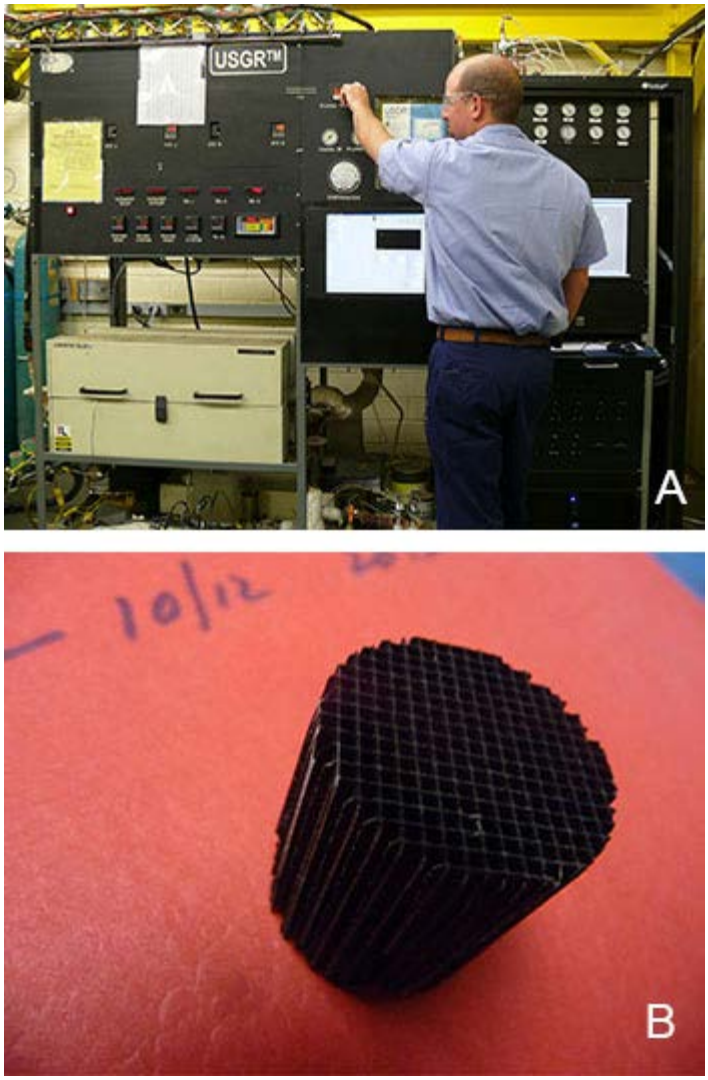

Figure 1: Synthetic gas reactor and test core

Accomplishments — The project work is complete. The project began by testing the reference catalyst in a simulated diesel lean exhaust gas mixture using H_2 as the reductant. It was immediately apparent that the catalyst was very effective at preferentially oxidizing H_2 to H_2O, CO to CO_2 and NO to NO_2. No NO_x SCR was apparent.

The original research paper was studied, and the test conditions recreated. Under the simplified, rich gas mixture referenced in the paper, the catalyst performed similarly to the paper results. However, using a simplified gas mixture for the SwRI D-EGR engine exhaust, the catalyst exhibited 100% NO_x conversion with 99+% selectivity to N_2 and a low light-off temperature of 195°C. With a fully formulated gas mixture, the light-off was inhibited by H_2O to 272°C. Different support metal oxides were explored with the purpose of reducing the Ru-NO bond strength, thereby lowering the catalyst light-off temperature. The order of performance was TiO_2 (250°C T_{50}), SiO_2 (258°C T_{50}), Ce_2O_3 (275°C T_{50}), and Al_2O_3 (284°C T_{50}). Both the TiO_2 and SiO_2 supported catalysts performed markedly better than the reference, with TiO_2 the best, in line with the finding of others under different testing conditions.

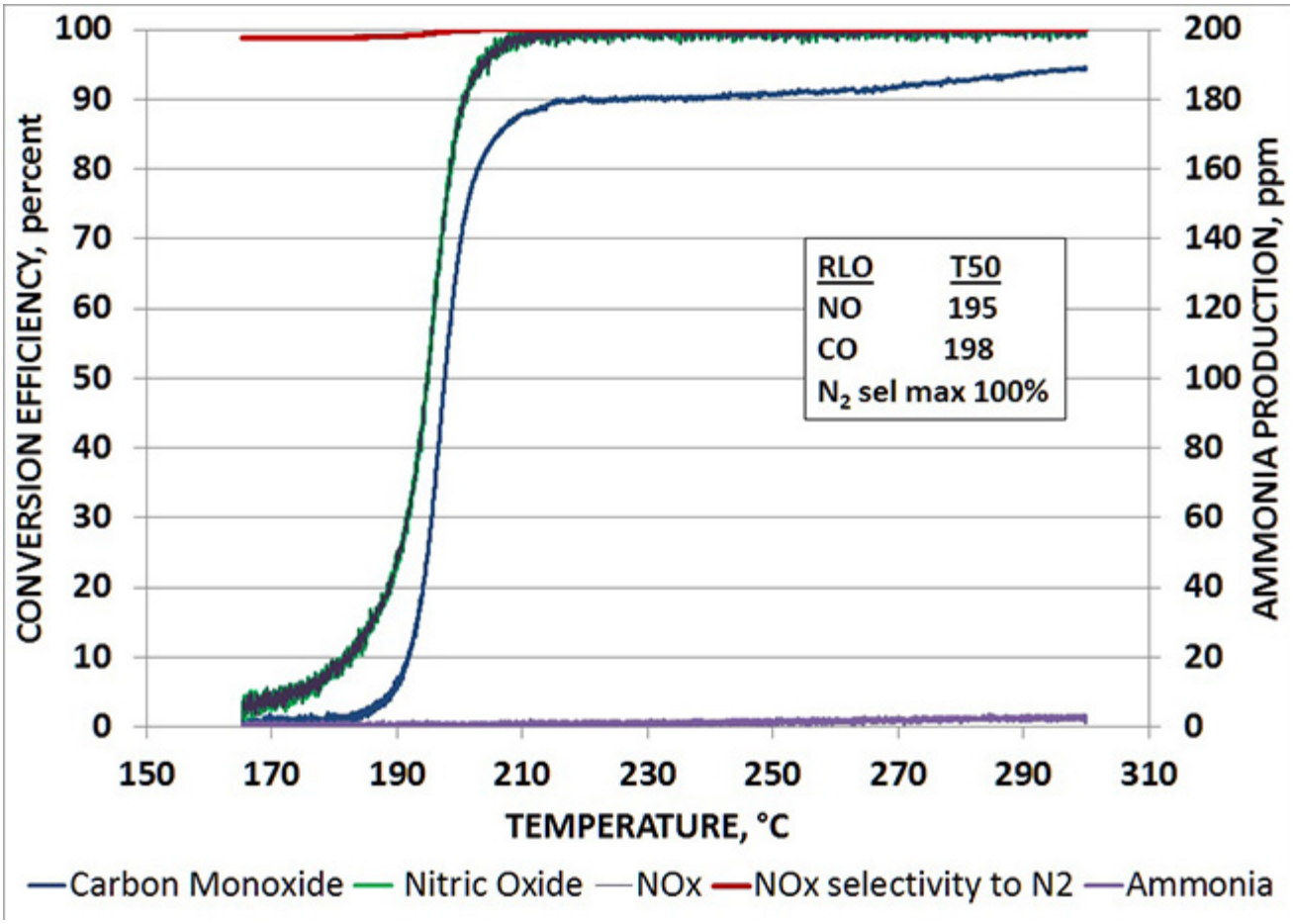

Figure 2: Ru-Al_2O_3 in simplified D-EGR gas mix

SOUTHWEST RESEARCH INSTITUTE®

2015 IR&D Annual Report

Methodology Development for I.C. Engine Tumble Port Evaluation, 03-R8494

Principal Investigators
Kevin Hoag
Anthony Megel

Inclusive Dates: 09/29/14 – 01/29/15

Background — The purpose of this project was to develop tools to aid in the design of tumble flow intake ports for spark-ignition engines. Tumble is the bulk flow that enters a piston engine cylinder, rotating about an axis perpendicular to the cylinder centerline. As the piston begins moving up at the end of the intake, and beginning of the compression stroke, the flow field breaks down into small scale turbulence. The turbulence in turn works to increase the flame speed during combustion, improving engine efficiency and reducing the tendency to auto-ignition. Various flow benches have been designed in attempts to characterize tumble, but with limited success. Until now computationally intensive, dynamic (moving piston and intake valve) models have been required. The only acceptable experimental alternatives require optical access and are difficult to implement. The objective of this research was to develop a simple, steady-flow computational model that could be applied at discrete points in the intake process to characterize the tumble flow provided by various intake ports.

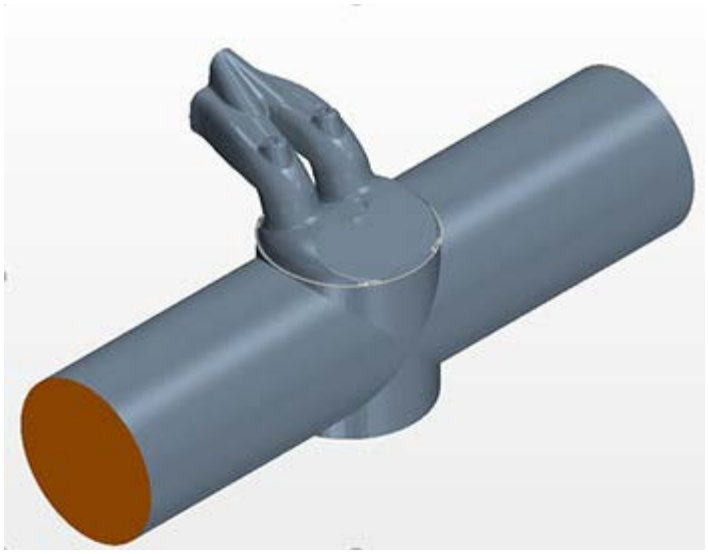

Figure 1: Three-dimensional computational fluids model

Approach — A steady-flow, three-dimensional computational fluids model was constructed, as shown in Figure 1. The model uses an intersecting tee that can be moved to mimic piston position, while the intake valve lift is indexed to the position corresponding to that of the piston, based on event timing in the engine. Discrete points in the intake process can be selected as required for a particular study, and the pressure drop that would be seen across the intake valve at that point in the process can be specified as boundary conditions. The three-dimensional flow field is then computed for each steady-state case.

Results from this simplified model were compared to those obtained from a dynamic simulation of the same engine. Comparisons were made at selected crank angle positions; an example is provided in Figure 2.

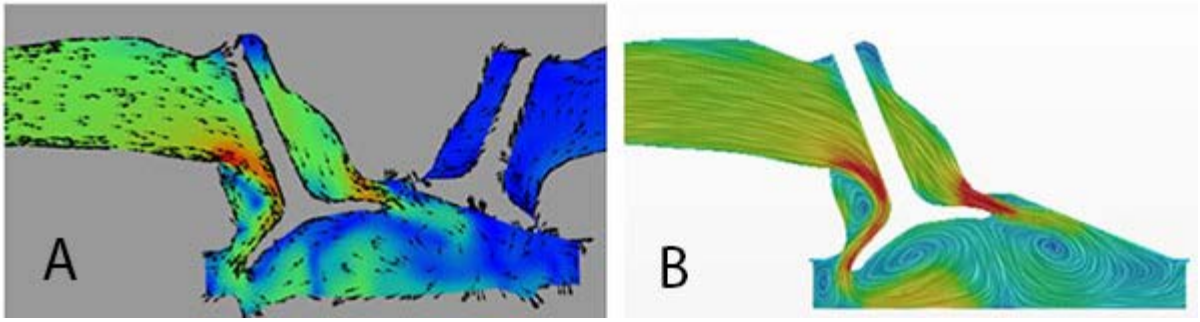

Figure 2: A) Moving boundary - 30 degrees ATDC; B) Steady Flow 31 degrees ATDC

Accomplishments — Comparisons between the simple tool and the full dynamic simulation have been made for two different engine designs to date, with very good agreement. The purpose of the model has been to correctly order various possible designs in terms of the resulting tumble flow at the end of the intake stroke. In each comparative study the ordering has been exactly correct. Model building and computational times have been compared, and the simple tool developed on this project requires just over 20 percent of the resources required for the full, dynamic analysis.

2015 IR&D | IR&D Home

2015 IR&D Annual Report

Effect of Jet Fuel Properties on Soot Mass and Solid Particle Number Emissions from Aircraft Engines: Development of a Fuel Particulate Matter (PM) Index Concept, 03-R8497

Principal Investigators
Imad A. Khalek
Nigil Jeyashekar

Inclusive Dates: 10/01/14 – 10/01/15

Background — Jet engines will be subject to a new particle emissions regulation likely to start in 2022. Health effects of ultrafine particles emitted from gas turbine engines and the potential of black carbon effects on climate change are the major driver for the regulation. The regulation focuses on soot or black carbon mass and solid particle number emissions down to very small particles, 10 nanometer in diameter. Jet fuel properties are expected to have a strong impact on particle emissions from gas turbine engines. There is an industry need for a consistent fuel metric that can be used as a predictor for jet fuel particle forming potential in gas turbine combustion. This is important both on the national and international level due to the global nature of the aerospace industry.

Approach — The project was initiated to better understand the effect of fuel properties on particle emissions from gas turbine engines. The work was performed in our laboratory using a simulated gas turbine combustor and five different jet fuels with different aromatic contents. Particle measurement included total (solid + volatile) particle number and size, solid particle number and size, and soot mass. Combustor operation included simulated idle, takeoff, and cruise conditions. As a part of this investigation, we developed and used a singular jet fuel particle index (JFPI) as a means to differentiate fuels for their soot formation tendencies. The JFPI included more than 800 measured fuel species and combined both the physical and chemical characteristics of fuel properties.

Accomplishments — The work demonstrated that jet fuel properties have a drastic influence on the size, number, and mass of particles emitted from gas turbine engines. Most importantly, we were able to demonstrate that the JFPI developed in our work can be used as an excellent indicator of jet fuel soot forming tendency in gas turbine combustion. For example, good linear correlation (R^2 ~0.93) was observed at cruise condition between solid particle number and soot mass and the JFPI. The JFPI can be used as an important indicator to differentiate jet fuel soot forming tendency worldwide. We plan to write a paper for the 2016 ASME Turbo Expo. We also plan to launch an industry consortium in 2016 to expand the development of the JFPI to more fuels and various combustion system designs.

SOUTHWEST RESEARCH INSTITUTE®

2015 IR&D Annual Report

Lubricant Impact on Fuel Economy — Correlation between Measured Engine Component Friction and Vehicle Fuel Economy, 03-R8502

Principal Investigator
Peter Morgan

Inclusive Dates: 10/01/14 – Current

Background — Friction reduction is one of the primary methods to improve vehicle fuel economy with future lubricants. Many lubricant manufacturers are targeting low viscosity lubricant formulations in combination with friction modifier (FM) additive chemistry to reduce friction losses in modern engines. Low viscosity formulations can reduce friction losses in areas where hydrodynamic lubrication is prevalent, such as crankshaft or camshaft main bearings, as well as components that operate with hydraulic pressure, e.g., camshaft phaser actuators. Friction modifier additives often serve as a means to reduce friction losses in components that encounter various lubrication regimes due to rapid changes in the directions and speeds of the two sliding surfaces, e.g., interaction between piston or piston rings and cylinder liner surfaces.

Approach — SwRI has been working with many lubricant manufacturers to quantify the effects of lubricant formulations on engine and component friction or vehicle fuel economy. However, data that clearly correlates how specific lubricant properties or compounds impact engine component friction (e.g., piston-liner friction) and vehicle fuel economy measurements have not been generated. By using the two established test methods (engine motoring friction measurement and vehicle fuel economy measurement), SwRI will be able to demonstrate how specific lubricant properties or additive chemistries impact the friction of various engine components and how those impacts translate into changes in vehicle fuel economy.

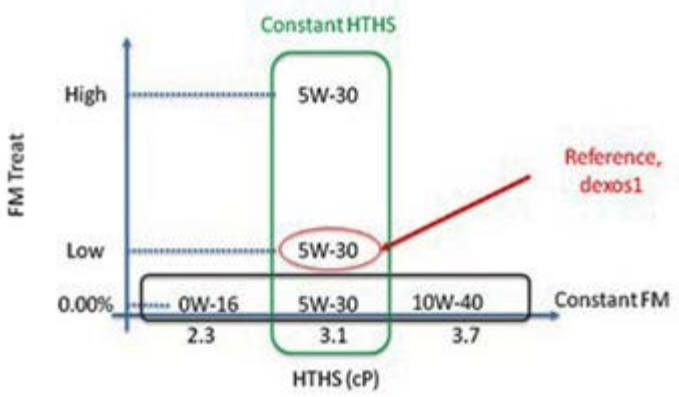

Figure 1: HTHS vs. FM Treat

The five test lubricants illustrated in Figure 1 were identified by SwRI and prepared by a major oil company. This matrix of lubricants allows us to look at both the effect of viscosity and FM on the vehicle fuel economy.

The lubricants were tested in a 2012 Chevy Malibu to determine gaseous exhaust emissions and fuel economy. The vehicle was installed in SwRI's light-duty vehicle chassis dynamometer test facility and operated over the Federal Test Procedure (FTP-75) and Highway Fuel Economy Test (HwFET).

Following the vehicle fuel economy measurements, the engine will be removed from the vehicle and used for the engine motored friction measurement. Detailed information about engine and engine component friction can be obtained from the motoring friction testing. However, we still cannot measure component friction when the engine is running (fired conditions). In order to bridge this gap, a commercial engine simulation code will be used to provide this insight. This simulation is able to predict the forces at each

friction joint and give feedback about the trends for fired operating conditions. This simulation tool is being used to correlate the data generated through the motoring friction testing (motored engine) with the results obtained from the vehicle fuel economy testing (fired engine).

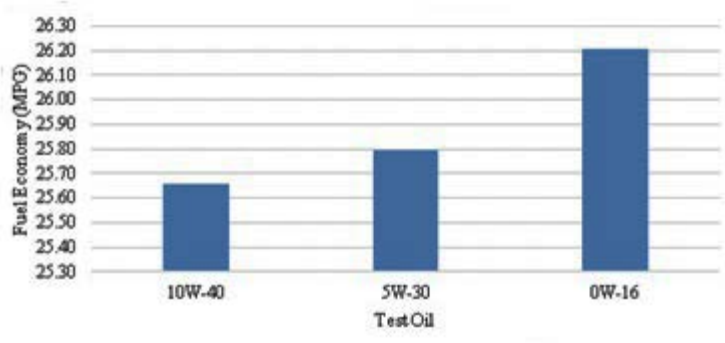

Figure 2: Lubricant viscosity impact on combined vehicle fuel economy

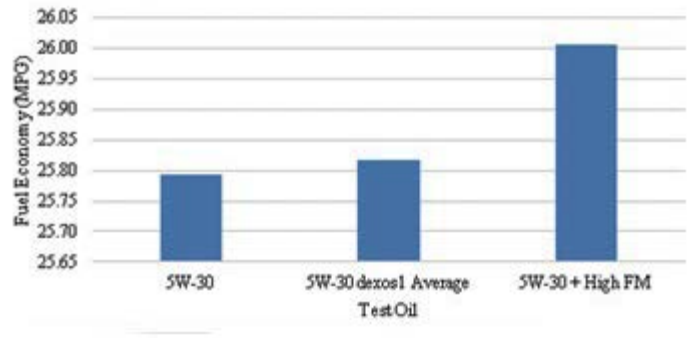

Figure 3: Impact of FM treat rate on combined vehicle fuel economy

Accomplishments — The oil company funded the testing for several additional lubricants beyond the original test matrix, so this program is still ongoing. Vehicle testing has concluded, and the engine is in the process of being removed for motored friction testing. Because the friction testing has yet to be completed, only limited conclusions can be drawn.

Figure 2 shows the viscosity impact on combined fuel economy from the three lubricants (10W-40, 5W-40, and 0W-16) with no FM. As expected, operating the engine with high-viscosity lubricant showed a decrease in vehicle fuel economy and low-viscosity lubricant showed an increase in vehicle fuel economy. This change in fuel economy is primarily evident for drive cycle conditions that include significant amounts of low-load engine operation and/or cold operating temperatures (e.g. cold start) since the impact of lubricant viscosity on friction is amplified at those conditions.

Figure 3 shows the change in combined fuel economy on the three lubricants (no FM, commercial FM dose, and large FM dose) with the same viscosity. The lubricants allow us to look at the impact of operating the engine with differing levels of FM treat rates in the lubricant. As expected, operating the engine with increased levels of FM in the lubricant showed an improvement in vehicle fuel economy.

More meaningful trends in the relationship between lubricant properties and vehicle fuel economy will be derived using the GT simulations once the test results can be coupled to the motoring friction test data.

SOUTHWEST RESEARCH INSTITUTE®

2015 IR&D Annual Report

Experimental Investigation of Co-direct Injection of Natural Gas and Diesel in a Heavy-duty Engine, 03-R8522

Principal Investigators
Dr. Radu Florea
Gary Neely

Inclusive Dates: 01/01/15 – 12/31/15

Background — For the U.S. market, an abundant supply of natural gas (NG) coupled with recent greenhouse gas (GHG) regulations have spurred renewed interest in dual-fuel combustion regimes that use NG for the heavy-duty truck market. The GHG regulations stipulate that by 2017, truck engines shall emit 6 percent lower CO_2 emissions than the reference 2010 engines with an additional 4 percent reduction required by 2027. Combustion of methane (CH_4), the main constituent of NG, produces up to 20 percent lower CO_2 emissions due to its higher hydrogen content compared to diesel. However, because the NG is injected into the intake manifold, a homogeneous NG and air charge is subject to the compression process, packing some of the charge into piston crevice regions, which are difficult to oxidize during the combustion process. These crevice losses lead to reduced engine efficiency and unburned CH_4 emissions, which essentially offset the benefit of reduced CO_2 emissions of NG combustion, as methane is thought to have a strong global warming potential.

Approach — This project is aimed at leveraging the unique co-direct-injection capability of the Westport™ High Pressure Direct Injection (HPDI) system to reduce the fuel penalty and methane emissions associated with traditional introduction of natural gas (NG) in dual-fuel engines. The HPDI system was used to control the amount of NG pre-mixing by injecting NG during the compression stroke, which reduced the crevice packing issue of fumigated NG. The injection strategy investigated in this project, called DI^2, differed from the production HPDI strategy. These strategies are illustrated in Figure 1.

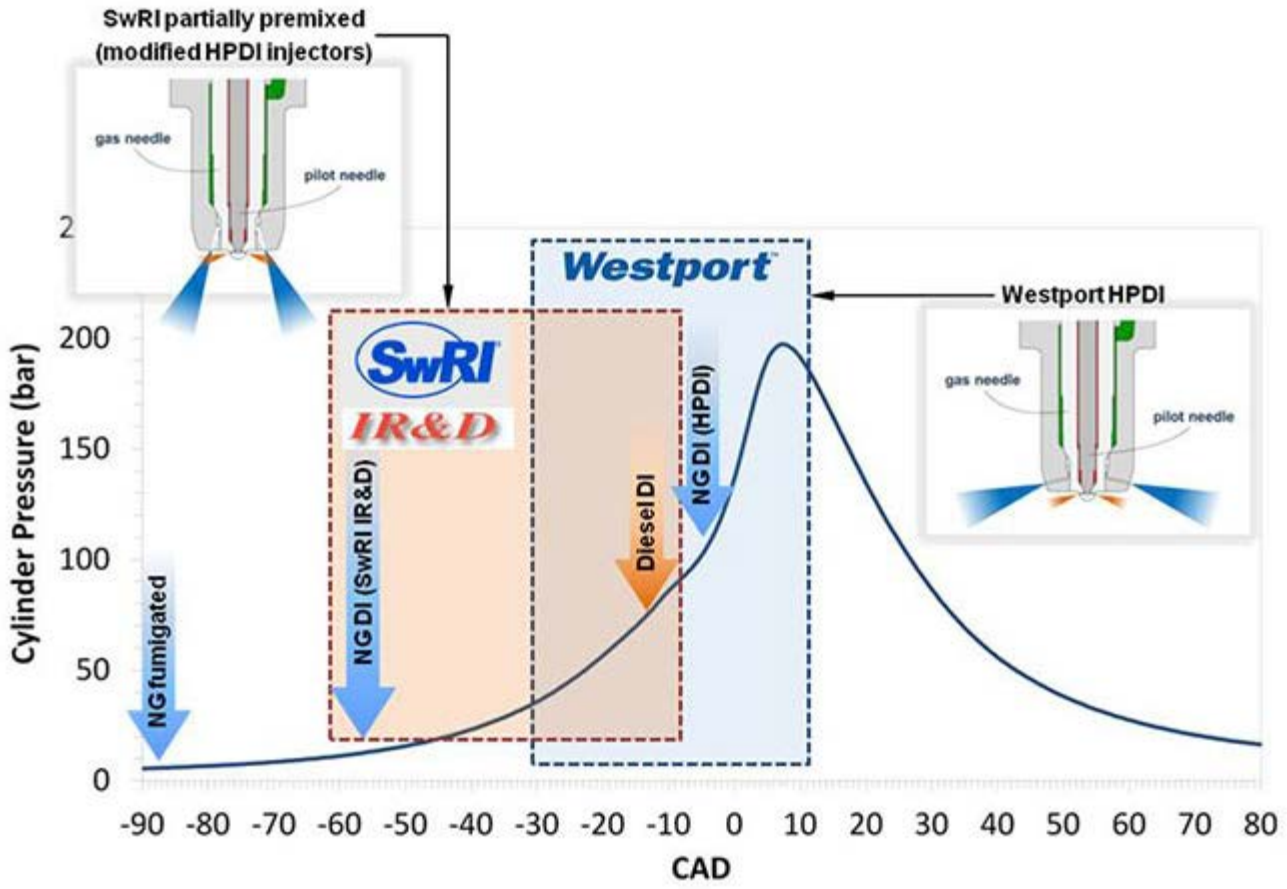

Figure 1: Dual-fuel Injection strategies. HPDI is production strategy while DI^2 is the strategy studied in this project.

Accomplishments — By operating in the DI^2 combustion mode, the engine efficiency was improved by more than 2.5 brake thermal efficiency points compared to the most efficient operation using the HPDI combustion strategy. At the same time, the measured combustion efficiency was improved to 98.6 percent, up from 97.1 percent measured for an equivalent fumigated combustion strategy. The improved combustion efficiency led to a 50 percent reduction in unburned CH_4 emissions compared to fumigated engine operation. The results confirm that significant reductions in unburned CH_4 emissions can be achieved for dual-fuel combustion with advanced injection technologies and positions the dual-fuel engine well for meeting future GHG regulations.

SOUTHWEST RESEARCH INSTITUTE®

2015 IR&D Annual Report

Detailed Characterization of Emissions from D-EGR Vehicle, and Evaluation of Synergistic Control Technologies, 03-R8547

Principal Investigator
Cary Henry

Inclusive Dates: 04/01/15 – Current

Background — The EPA drafted legislation regulating greenhouse gas (GHG) emissions from mobile sources, and in concert, the National Highway Transportation Security Administration also regulated Corporate Average Fuel Economy (CAFE) standards for light duty automobiles. These changes pose both a challenge and numerous opportunities for the emission control system. Both regulations require a 35 percent reduction in fuel consumption from 2016 to 2025. In parallel to this, the California Air Resource Board (CARB) recently adopted more stringent criteria pollutant regulations to reduce emissions of carbon monoxide (CO), oxides of nitrogen (NOx), and hydrocarbons (HC). CARB and the EPA have both drafted legislation mandating an 80 percent reduction in NOx and HC emissions from 2015 to 2025.

SwRI has been developing the D-EGR concept for several years as a part of the HEDGE consortium and internally funded programs. Recent work has yielded important information indicating fuel consumption reductions of 15 percent are possible for U.S. certification cycles. There is 25-percent re-circulated exhaust gas in the D-EGR application and peak combustion temperatures are much cooler, which results in a reduction of CO and NOx emissions. With the 25 percent dilution, however, laminar flame speeds are significantly lower, and HC emissions can increase, posing a challenge given that exhaust temperatures of the D-EGR engine are lower and more in line with a diesel engine. Due to the unique nature of the D-EGR architecture, there exist new opportunities to utilize catalysts in the EGR stream to provide reformate to improve the combustion characteristics of the engine.

The objective is to investigate the emissions chemistry of the D-EGR architecture by performing a detailed characterization of both particulate and gaseous criteria pollutants. Additional steps include the proposal and evaluation of synergistic emission control technologies, which can enable improved fuel efficiency while still meeting the legislated criteria pollutant standards.

Approach — In Phase 1 of the project, a detailed characterization of the criteria pollutant species (PM/PN, NO_X and HC) was conducted, and the emission control system operating conditions were documented.

Emissions were characterized over several regulatory light-duty vehicle drive cycles, as shown in Figure 1. Emissions were characterized for both the D-EGR vehicle and a production 2012 Buick Regal with the stock turbocharged, direct-injected, non-EGR engine. Because of the unique nature of emissions from the D-EGR application, knowledge gained from Phase 1 of the project will be used to develop and evaluate new emission control strategies, which may be used to provide further reductions in fuel consumption of the D-EGR concept. The development and evaluation of synergistic emissions will be conducted in Phase 2 of the program, and will focus on new and existing exhaust emission control strategies that may be better suited to the unique exhaust conditions for the D-EGR application. These new strategies will first be evaluated in controlled catalyst reactor facilities, and then will be installed for evaluation on the D-EGR vehicle.

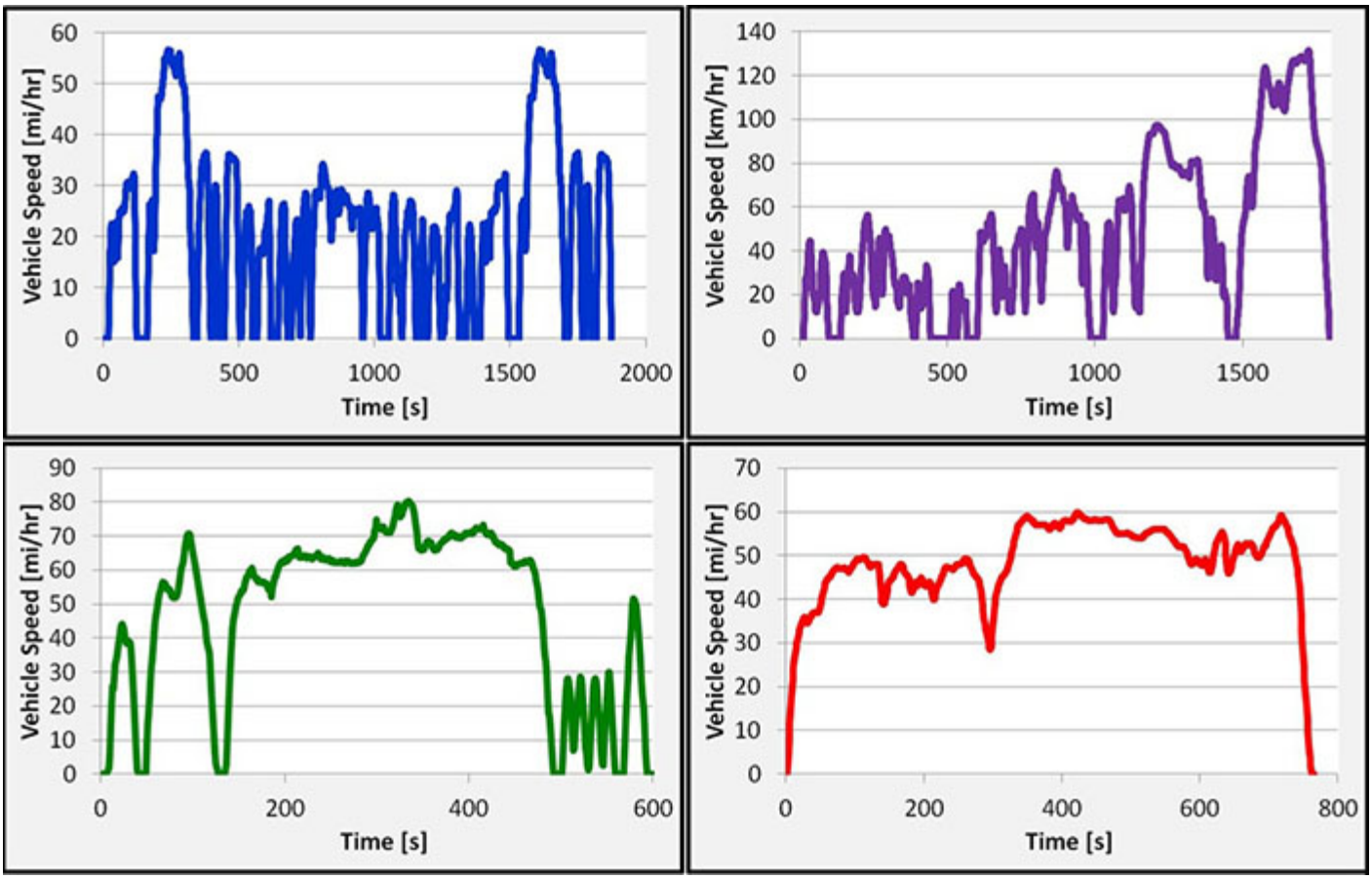

Figure 1: Global light-duty vehicle regulatory drive cycles: a) FTP-75, b) WLTP, c) HWFET, d) US06

Accomplishments — Phase 1 of the program was completed. Gaseous and particulate emissions were characterized for both vehicles over the four light duty vehicle drive cycles shown in Figure 1. HC speciation for the FTP-75 and WLTP is shown in Figure 2. When comparing the Stock GDI and D-EGR vehicles, a noticeable shift in HC species was observed. Specifically, an increase in Ethanol emissions and C5to C8 class HC was noted. This inherent difference in HC species likely would benefit from alternative catalyst designs. Phase 2 will focus on developing and evaluating these new catalyst strategies.

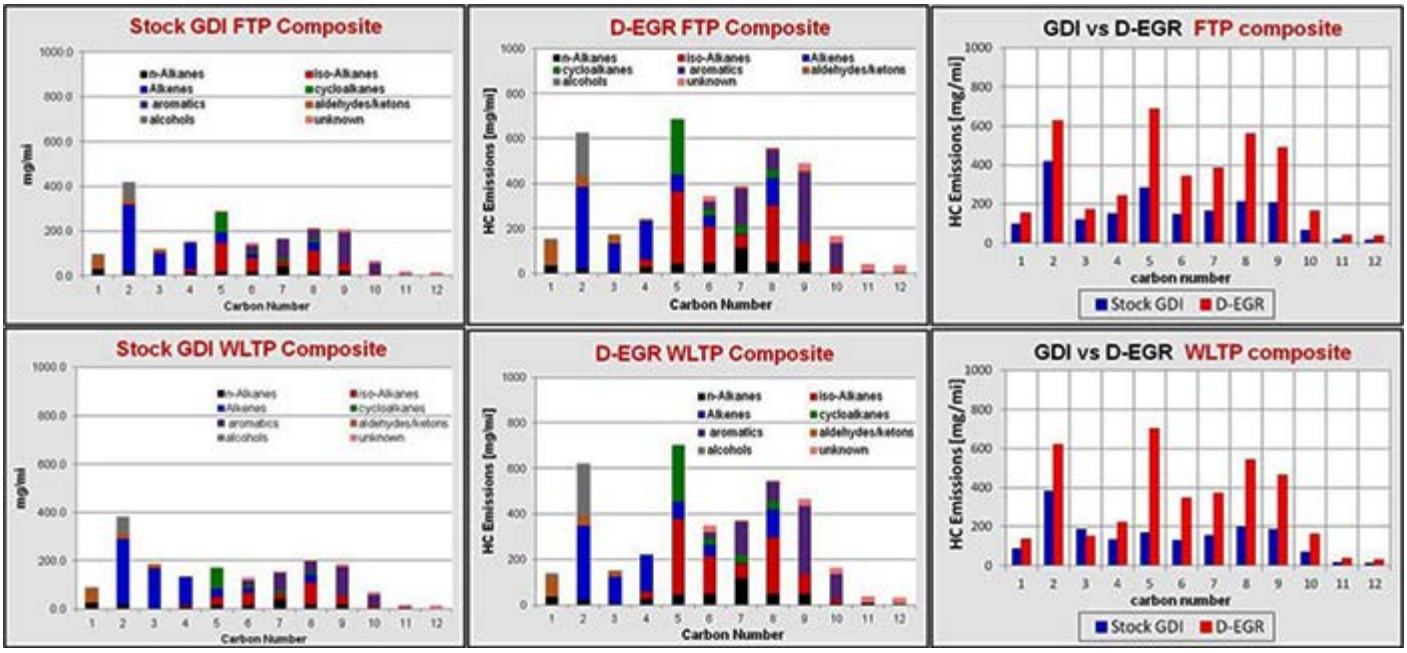

Figure 2: Comparison of HC emissions between the D-EGR and stock GDI vehicles for the FTP-75 and WLTP regulatory cycles

---

2015 IR&D Annual Report

Combustion Chamber Design Optimization for Advanced SI Engines, 03-R8551

Principal Investigators
Kevin Hoag
Terry Alger
Chris Chadwell
Chris Wray
Mark Walls

Inclusive Dates: 04/01/15 – Current

Background — Advances in spark-ignition engine combustion systems increasingly require excess oxygen or a diluent (typically exhaust gas recirculation, or EGR). Either of these approaches holds the advantages of reduced heat rejection, and improved compression and expansion efficiency. However, the resulting reduced flame temperature and the presence of the diluent both serve to slow down the flame speed. The slower flame speed adversely impacts efficiency, and increases the propensity for auto-ignition. Prior experiments conducted at SwRI, as well as results reported in the literature suggest that reducing the bore-to-stroke ratio provides some compensation by shortening the flame travel distance required for complete combustion. Turbulence is also known to increase flame speed, and tumble intake flow provides a strong lever for increasing turbulence. The intent of this research is to expand the known matrix of these important combustion chamber design parameters, quantifying their impact on key performance and efficiency measures.

Approach — A single cylinder research engine developed under a previous internal research project was selected for this project. Three configurations will be tested: the baseline configuration using components and dimensions from a production engine, and two test configurations in which the stroke has been increased and the cylinder head modified for increased tumble. Each configuration will be tested, and measurements will be taken

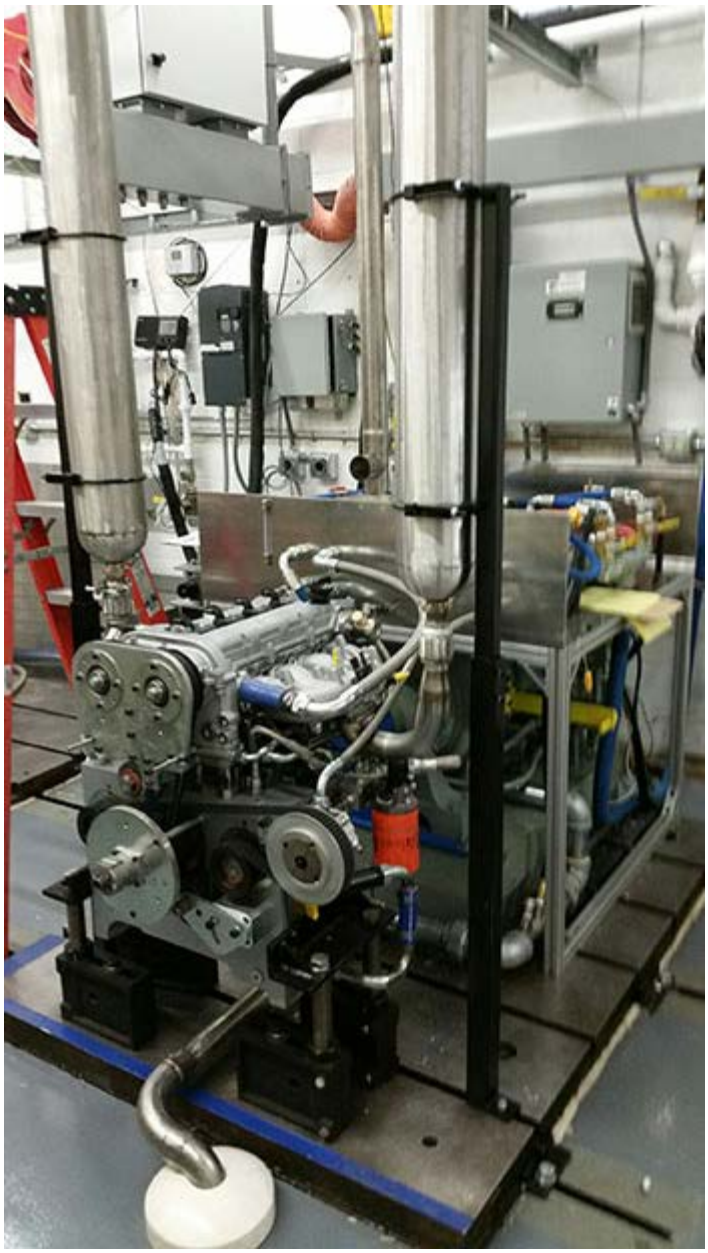

Figure 1: Test cell installation

regarding fuel efficiency, burn duration, and resistance to auto-ignition. Data analysis will be complemented with combustion chamber computational fluid dynamic (CFD) modeling to draw conclusions regarding the impact of tumble flow and bore-to-stroke ratio on combustion performance and efficiency.

Accomplishments — This research project is currently underway. The baseline engine has been assembled, and installation in the test cell is currently underway. The test cell installation is shown in Figure 1. All parts have been procured for the remaining engine builds. Instrumentation and the test cell control system are now being completed, and testing is expected to begin in late November 2015.

SOUTHWEST RESEARCH INSTITUTE®

2015 IR&D Annual Report

Octane Index Effects on Fuel Economy, 03-R8555

Principal Investigators
Peter Morgan
Peter E. Lobato
Ian B. Smith
John K. Brunner
Robert R. Legg

Inclusive Dates: 07/01/15 – 10/01/15

Background — Many original equipment manufacturers (OEMs) have begun to bring direct-injected engines to the marketplace. These systems have been designed with fuel efficiency in mind, but their efficiency is limited by knock. These new engines seem to respond to changes in research octane number (RON) and motor octane number (MON) differently than previous port-fuel injected (PFI) engines. Fuel sensitivity (S) may be an alternate metric to either RON or MON for predicting the ability of a fuel to mitigate knock. The fuels for this project had constant RON and spanned a range of sensitivities (0, 5, and 10).

Approach — SwRI's Direct Electronic Vehicle Control (DEVCon) is an enabling technology to evaluate the impact of fuel sensitivity on fuel economy. DEVCon is different from robot drivers because it takes the pedal actuators out of the equation and allows us to drive the vehicle by feeding a voltage straight into the engine control module. With this and our internally designed control strategy, it has allowed substantially better repeatability when measuring the fuel economy of a vehicle operating on a chassis dynamometer. This is a novel way to drive a vehicle while on the dynamometer, for which a patent application has been initiated.

A 2014 Ford Focus with a gasoline direct injected 2.0 liter naturally aspirated engine was procured from a rental fleet for testing. This vehicle was hot-start tested in triplicate over the US06 driving cycle with three different fuels. Three different fuels were blended using SwRI's fuel blending facilities. These fuels all had a 91 RON and were differentiated by their sensitivity (0, 5, and 10).

Accomplishments — Utilizing this approach and the results, SwRI has been able to demonstrate its leadership when repeatability is necessary to statistically differentiate small fuel economy differences. We have been able to show an average coefficient of variance for vehicle fuel economy over the US06 of 0.21 percent, which is nearly an order of magnitude better than what we have historically achieved with human drivers over this aggressive test cycle. We were able to quantify how a fuel's sensitivity translates to vehicle fuel economy test results. As shown in Figure 1, the zero sensitivity fuel resulted in the

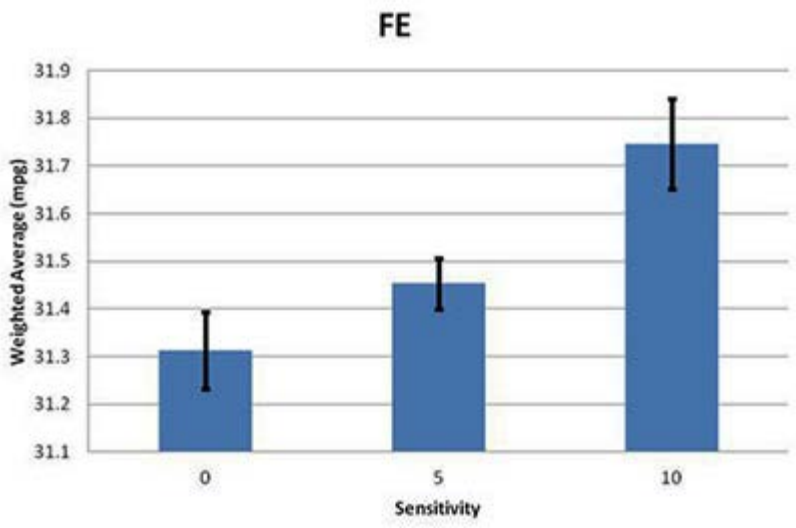

lowest fuel economy, while the 10 sensitivity fuel resulted in the highest fuel economy. We generated experimental data to strengthen SwRI intellectual property (IP) on DEVCon and how it can detect small changes in fuel economy over the US06 cycle. We generated experimental data that has already been used to promote SwRI's capabilities in vehicle fuel economy testing.

Figure 1: Averaged fuel economy results.

2015 IR&D Annual Report

Determination of PAHs in Tires by GC/MS and NMR — A Method Comparison in Regards to Meeting the EU's PAH Standards for the Tires, 08-R8402

Principal Investigators
Joseph Pan
Gillian Soane
Ka See

Inclusive Dates: 07/01/13 – 12/31/14

Background — In 2007, the European Union (EU) issued 1906/2007/EC (REACH), a regulation requiring that as of January 1, 2010, all process oils isolated from tire treads contain less than 1.0ppm benzo(a)pyrene (BaP), and that the sum of eight specified polycyclic aromatic hydrocarbons (PAHs) be less than 10ppm. ISO 21461, the EU's official method for meeting this regulation, uses NMR to determine whether a tire meets these new standards. The EU regulation states that if the Bay-H NMR signal of the process oil isolated from the tire treads is <0.35% of the total H NMR signal, the tire is regarded as having met the EU's original PAH standards. Little research had been done showing that the ISO 21461(NMR) method upholds the EU's original PAH standards for the tires.

Approach — The first objective was to develop a GC/MS method that would accurately and precisely determine each individual PAH concentration in the process oils isolated from tires. The approach included using the GC/MS with isotope dilution technique, studying the effects of the sizes of the rubber bits on PAH extraction efficiency, comparing various solvents to determine maximum efficiency for extracting PAHs from rubber bits, fine tuning the sample extract cleanup procedures with liquid-liquid partition and silica gel liquid column chromatography, and studying the accuracy and precision of the developed GC/MS method. The second objective was to compare GC/MS and NMR methods in regards to tires meeting the EU's PAH standards. Fifty commercial passenger car tires (including 11 EU-made tires) were purchased and analyzed for PAHs using the developed GC/MS and the ISO 21461 (NMR) methods. Results were compared for each tire. Pass/fail decisions were made for each tire using the EU's PAH standards of BaP concentration, sum of the 8 PAHs, and the NMR data.

Accomplishments — Using the GC/MS method rubber bit sizes within the range of 0.125-2.8mm had no effects on the extraction efficiency of PAHs from the tire rubbers using toluene as extracting solvent. The solvent extraction efficiencies of the 5-ring PAHs from the rubber bits were: toluene > carbon disulfide > acetone = 1,4-dioxane > propionic acid > carbon tetrachloride > cyclohexane. DMF (N,N-dimethylformamide) or NMP (N-methyl-2-pyrrolidone), each with 10 to 15 percent water, extracted PAHs well from hexanes, separating PAHs from the non-PAH hydrocarbons. The liquid chromatography columns packed with activated silica gel also separated target PAHs well from the non-PAH hydrocarbons. The method average accuracy for the determination of 18 PAHs and the 5-ring PAHs in the process oils isolated from custom-made rubber were 52.1 and 48.5 percent, respectively. The method's average %RSD for the determination of 18 PAHs and the 5-ring PAHs in the rubber process oils were 15.3 and 18.8 percent, respectively.

For the comparison of PAH results using GC/MS and ISO 21461 methods on 50 tires, ISO 21461 passed 82 percent (41/50) of the tires, of which 85 percent (35/41) were considered "false negatives" based on the GC/MS results of BaP and "sum of EU 8 PAHs." This trend is seen in the 11 EU-made tires. In

conclusion, the ISO 21461 (NMR) method does not produce data proportionally reflecting the concentrations of BaP or "sum of 8 PAHs" in the tires. A PAH method developed by SwRI using GC/MS determines individual PAH levels in the tires well and should be adopted as the official method for upholding the EU's original PAH standards for the tires.

2015 IR&D Annual Report

Determining the Sensitivity of Fuel Lubricity Additive Concentration on Test Parameters and Contact Geometry, 08-R8513

Principal Investigators
Peter Lee
Greg Hansen
Steve Westbrook
George Wilson

Inclusive Dates: 01/05/15 – 05/05/15

Background — In diesel engines, the fuel pumps and fuel injectors are subjected to tremendous pressures, upward of 30,000 psi in modern systems. To generate and maintain this level of pressure, the internal pump and injector components are made to an exacting standard. The drawback is that the moving components are largely lubricated with only the diesel fuel. If the diesel fuel has insufficient lubricating quality, catastrophic wear and subsequent failures can occur. This work was undertaken in an attempt to improve the correlation of the high frequency reciprocating rig (HFRR) wear scar results with pump test results for a series of fuels with varying levels of lubricity additive.

Approach — It was known from the beginning of this work that the point contact generated by the ball-on-disk contact was likely the largest contributor to the insensitivity of the HFRR test. The first, and ultimately only, change to the standard test conditions was to replace the ball test specimen with a cylinder (pin) to generate a line of contact. The increase in surface area would allow the surface active molecules in the lubricity improver a chance to work from the very first stroke, and would give lower contact stress, pushing the lubricating regime towards the hydrodynamic and away from the adhesive wear conditions typically seen in poor HFRR results.

Accomplishments — A series of standard tests were done on the HFRR using fuel blended with a commercially available lubricity improver. Seven blends were made ranging from 0 to 400 parts per million (ppm) treat rate. The fuel was tested with no additive, and the wear scar measured just over 900 microns in mean diameter. At the 12.5ppm treat rate, a 1.2 percent decrease in wear scar was observed. At the 25ppm treat rate, a 7.1 percent decrease in wear scar was observed. When the standard ball (point contact) was changed to a pin (line contact), a dramatic change in additive response was observed. The fuel with no additive measured about 450 microns in mean width. At the 12.5ppm treat rate, a 20 percent decrease in wear scar was observed. At the 25ppm treat rate, a 48 percent decrease in wear scar was observed.

SOUTHWEST RESEARCH INSTITUTE®

2015 IR&D Annual Report

Validating Using Laser Scan Micrometry to Measure Surface Changes on Non-Concave Surfaces, 08-R8562

Principal Investigators
Eric Liu
Sean C. Mitchem
Kerry J. McCubbin

Inclusive Dates: 06/22/15 – 11/04/15

Background — Contact stylus profilometry is a staple instrument in the field of surface metrology due to its high sensitivity to detect sub-micron level surface deviations in the vertical plane. To evaluate changes in surface topography caused by wear phenomena, contact stylus profilometry requires accurate overlays of the worn surface profile relative to that of the original unworn surface profile using common unworn surface features that are present in both worn and unworn surface profiles. This limits the articles that can be measured and is not applicable to newer engine technology, where previous parts designs only had partial contact between two surfaces but now involve contact that causes wear across the entire surface and eliminates the unworn reference edges that were previously available. SwRI developed a method documented in U.S. Patent Application 14-620,020 utilizing laser scan micrometry (LSM) to measure wear on cylindrical objects that have no unworn features on the surface. The focus of this research involved proving equivalency of the SwRI-developed technique LSM method with the industry-accepted technique of contact stylus profilometry for measuring wear on camshafts that have undergone lubricant testing. For clients to feel comfortable with our new measurement technique, it was important to produce data and demonstrable testing results that showed a level of equivalency in wear measurement results.

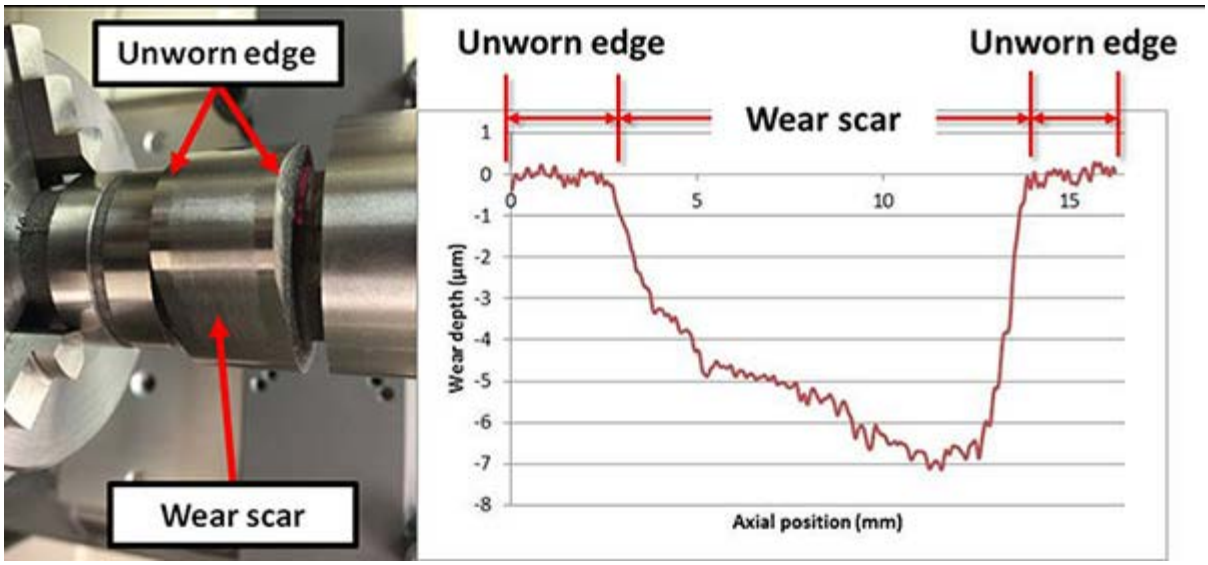

Figure 1: Worn cam lobe test specimen (left) and example of surface profile obtained by contact stylus profilometer (right)

Approach — Our approach involved measuring wear on cam lobes with different wear severities using both methods and then comparing the wear measurement results to determine equivalency (see Figure

1). To validate the accuracy of our method, we needed to improve the angular positioning accuracy over our existing proof-of-concept system (see Figure 2). This was accomplished by integrating an absolute encoder on the rotational axis and developing motor drive algorithms that use encoder feedback to provide precise and repeatable angular positioning. By being able to validate the accuracy of our angular positioning at each measurement point, we were able to compare the measurement data with data collected from measuring the same part on the contact stylus profilometer.

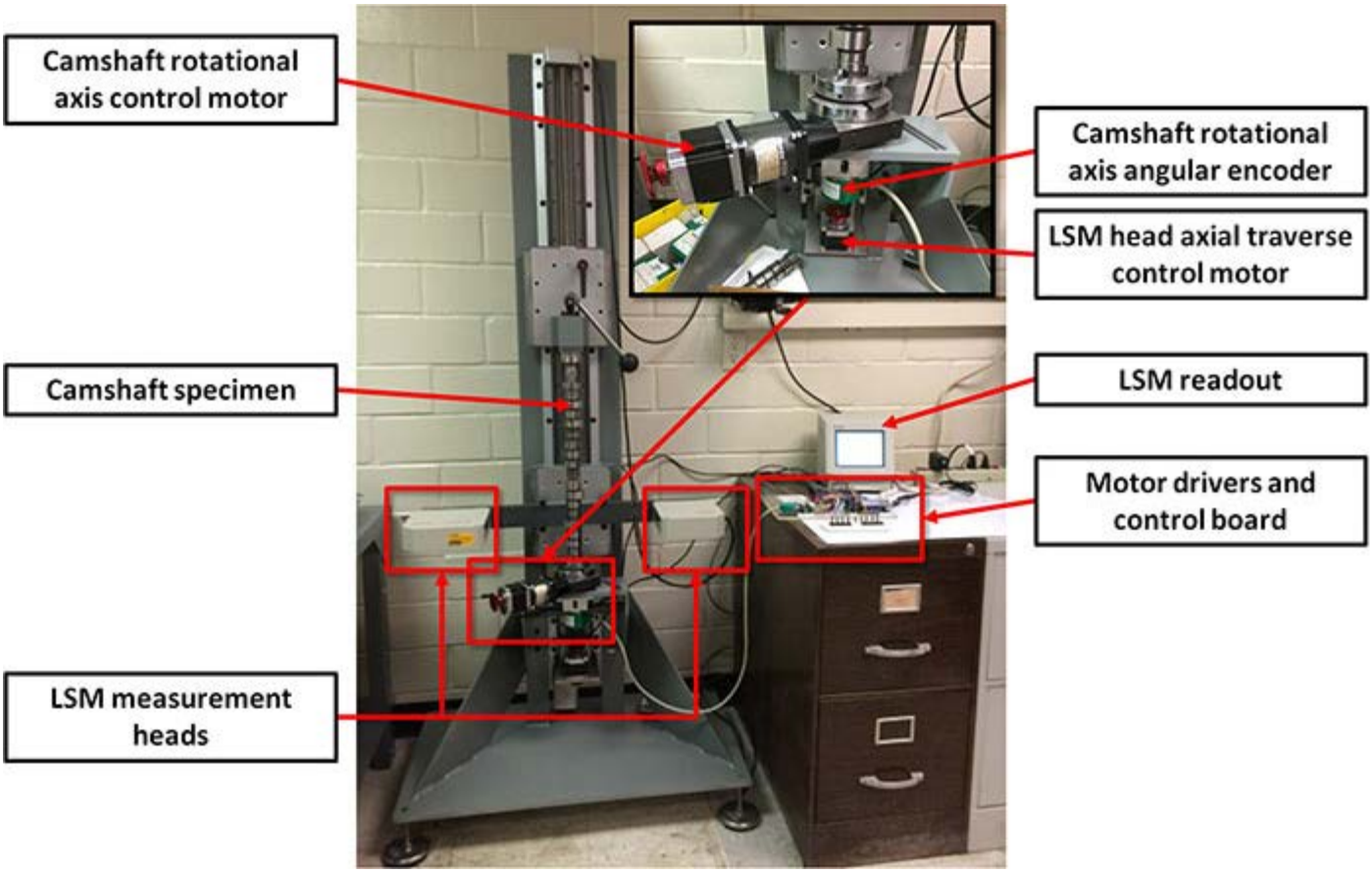

Figure 2: Components of LSM measurement apparatus

Accomplishments — Our results in achieving precise angular positioning by using the encoder feedback were 100 percent. We were also able to improve the motor controls to eliminate any potential issues with backlash or partial steps. Measurement results showed that we were able to achieve a measurement equivalency of 81.4 percent on a 10µm-deep wear scar, and 76.5 percent on a 20µm-deep wear scar, well within what would be acceptable to our client base (see Figure 3). Additionally, we were able to validate that we can achieve a 93.4 percent repeatability of ±2µm between two separate measurements of the same test sample, a major goal of the research. With the additional capability to measure surfaces that have worn reference surfaces, which contact stylus profilometry cannot measure, we feel confident that we now have a measurement technique that our clients will seek to use in their testing needs.

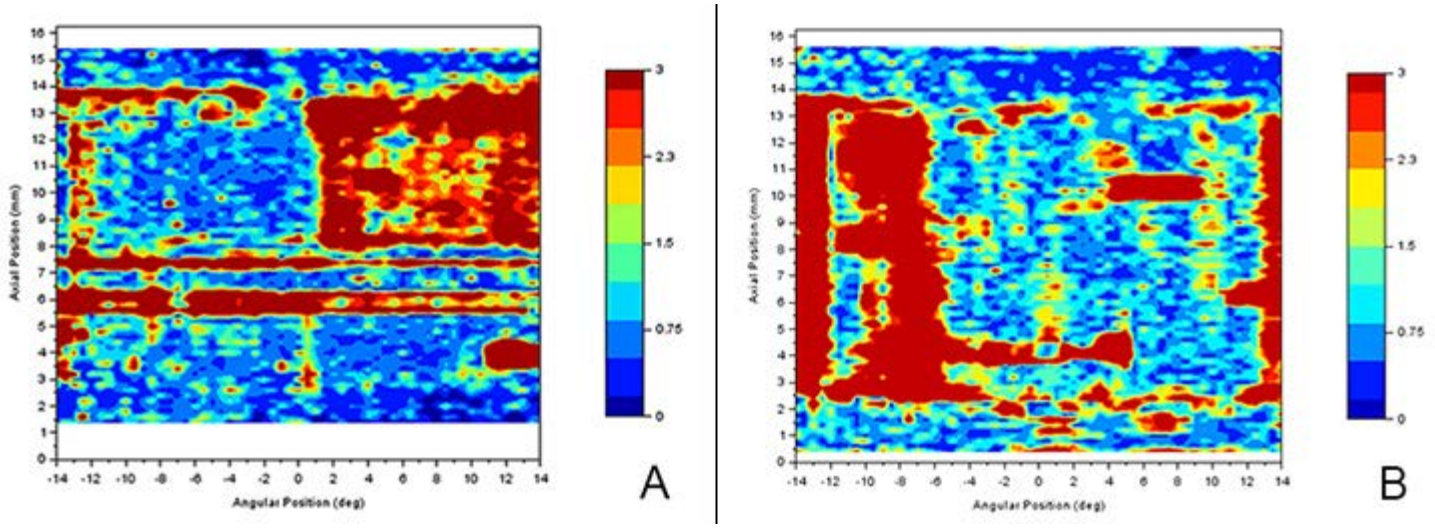

Figure 3: Map of difference between contact stylus profilometer and LSM measurements of cam lobe surface with approximately 10µm-deep (A) and 20µm-deep (B) wear scars within range of -14° to +14° of the zero point

---

2015 IR&D | IR&D Home

SOUTHWEST RESEARCH INSTITUTE®

2015 IR&D Annual Report

Microwave Methods for Enhanced Combustion in Natural Gas Engine Applications, 10-R8408

Principal Investigators
E. Sterling Kinkler Jr.
Christopher Chadwell
Barrett W. Mangold
Russell K. Barker

Inclusive Dates: 07/01/13 – 12/31/14

Background — Internal combustion engines (ICE) are used to convert energy stored in fossil fuels to usable power for transporting people and accomplishing work in an astonishing array of applications and industries. Planes, trains, and automobiles have been the most visible platforms using ICE technologies since the early 1900s, and the energy crises of the 1970s initiated much interest in higher fuel efficiencies. Accompanying the vast growth of operating ICE products, environmental issues are also major concerns. Current and especially future, economic, regulatory, and social pressures are fueling significant research in cleaner, higher efficiency combustion processes. Exhaust gas recirculation (EGR) techniques are frequently found in modern gasoline engines to help reduce harmful emissions and improve efficiency. High levels of EGR dilution can result in slower combustion and related ICE performance problems.

Enhanced combustion of gaseous fuels has long been observed when electric fields are applied. Microwave (MW) techniques can produce very high intensity electric fields within an enclosed volume and are often used to develop intense electric fields that accelerate sub-atomic particles to near-speed-of-light velocities for modern physics research. International regulations allocate multiple MW frequency bands for use in industrial applications. Previous work at Southwest Research Institute®, coupling MW power into an existing spherical chamber during combustion of gasoline/air mixtures, has produced promising experimental results.

Approach — We seek to effectively couple MW power into an enclosed metallic chamber emulating the combustion chamber (CC) of modern ICE products. Design and test of fundamental methods and techniques to develop intense electric fields within a modern ICE CC is an enabling step toward implementing running ICE platforms that can facilitate performance testing with MW-enhanced combustion (MEC) techniques applied.

Our approach to this program is to research, fabricate, and test experimental MW coupling methods that can achieve significant MW fields within a CC and accommodate the many constraints imposed by the design and operation of modern commercial ICE products. The ICE CC is generally in the shape of a cylinder with variable height and contains a harsh internal environment, including cyclic high temperatures and pressures. Our research goals include implementation of high intensity internal electric fields for a range of ICE products and operating conditions. The large-bore natural gas ICE class was chosen due to physical and dimensional characteristics and the potential for relatively significant economic and environmental impact of improvements in efficiency and emissions, as engines in this class typically run 24/7 at high loads.

Accomplishments — The team performed research and preliminary design and analysis for a number of experimental MEC implementation methods and selected an initial design using a coaxial MW delivery system coupled to a small circular dielectric-filled MW waveguide. The filled waveguide is intended to

couple and excite a desired MW field structure within the CC, maintain the necessary pressure envelope of the CC, and facilitate future MEC integration within commercial ICE products. The team completed design and fabrication of a filled waveguide, including features needed to efficiently transition between a coaxial MW feed and the waveguide. The team also completed design and fabrication of the laboratory CC fixture that mimics selected commercial CC shapes and sizes, and can facilitate MW system function, performance, and sensitivity experiments. The coaxial-fed filled waveguide and CC fixture were combined, and system test and refinement work followed. Independent experiments were conducted to verify that the desired MW field structure within the CC was accomplished. An agreement with a major engine manufacturer was concluded, providing the team with design information for current ICE products. Teaming with a large original equipment manufacturer provided realistic constraints on the design of the MEC system to accelerate acceptance of MEC technology in the large bore natural gas engine industry.

2015 IR&D Annual Report

Hypothesis Testing for Subfreezing Mass Movements, 20–R8407

Principal Investigators
Donald M. Hooper
Cynthia L. Dinwiddie

Inclusive Dates: 07/01/14 – 07/01/15

Background — Debris flows, some seasonally recurring, are known to be present on dune slopes in several mid- to high-latitude dune fields on Mars. Mass movement signatures are among the best records of historical and ongoing geologic activity on Mars, and seasonally recurring debris flows on Martian sand dunes therefore imply modern, ongoing alluvial activity. We observed analogous debris flows consisting of a sand and liquid water mixture that cascaded down leeward dune slopes under subfreezing conditions in March 2010 at the Great Kobuk Sand Dunes (GKSD), Alaska (internal research project 20-R8136). For this project, field work was conducted at Great Sand Dunes National Park and Preserve (GSDNPP) in Colorado to examine subfreezing debris flow initiation and development.

Approach — Project team members conducted field work at GSDNPP during February 10–19, 2014, to test the hypothesis that relatively dark sand lying on bright snow may cause local hot spots to form where solar radiation can be absorbed by the sand and conducted into the snow, enabling meltwater to form at subfreezing air temperatures and sand to mobilize through alluvial processes. The team chose to focus instrumentation and data collection on a sinuous transverse-to-barchanoid dune at a site that the National Park Service calls “Sand Pit.” Field data was acquired from SwRI meteorologic and hydrometeorologic stations. Sedimentologic samples collected during GSDNPP field work were required for granulometric and particle analyses, oven-dried porosity/density analyses, and laboratory-measured hydraulic properties and total water content. Our thermal properties analyzer, heat-dissipation probe, and dual probe heat-pulse sensor were used to measure thermal conductivity, specific-heat capacity, and thermal diffusivity of the principal sand units both *in situ* and in the laboratory. A network of temperature loggers was deployed during field work to record spatial and temporal distributions of dune surface temperature to characterize topographically and insolation-controlled microclimates. A thermal infrared imaging camera was used to measure the surface temperature distribution across a grid prepared to capture various soil moisture conditions.

Accomplishments — A wide variety of active denivation features and niveo-aeolian processes was observed at GSDNPP, but field team members did not observe any naturally occurring debris flows at Sand Pit. Dry sand avalanching on the slip face was common, however, especially when the wind was from the west or southwest. An artificial debris flow was initiated on the dune brink by pouring measured volumes of water down the slip face. Only two liters of water was required to produce a debris flow that resembled those observed at the GKSD. This suggests that even a small volume of liquid water may mobilize a debris flow on an aeolian dune slope and these small debris flows resemble the small-scale, defrosting-associated “Dark Dune Spot” seepage-like flow features observed on Mars. Localized heating and thawing at scales too small for orbital sensors to identify may yield Martian debris flows at current climate conditions.

To better understand how debris flows fed by liquid water form when ambient air temperatures are subfreezing, we performed meteorology-driven, cryohydrologic numerical modeling using a commercially available, finite-element, geotechnical engineering code. We used 15 years of climate data recorded in Kobuk Valley near the GKSD augmented by site-specific weather data that we measured in the field

during March 2010. Simulations of a generic, approximately 20-meters high sand dune at the GKSD illustrate the seasonal freezing and thawing of an approximately 3-meter-thick active layer; short-lived, syngenetic permafrost developing dynamically below the active layer as the dune slowly migrates forward; and a layer of unfrozen water sandwiched between the seasonally frozen active layer and the frozen permafrost. During some years this layer of unfrozen water is partially saturated having some air in the pore spaces, and during other years it has a fully saturated base with partially saturated liquid water above it. In no simulated year during the timespan from 2000 to 2015 did the seasonally frozen active layer penetrate completely to the top of the permafrost. Furthermore, there is a complete pathway for liquid meteoric water to be transported in small quantities all the way down to the top of the regional groundwater table at the base of the dune system (i.e., approximately 2 meters below the interdunes).

Simulations resulted in ice-rich, pore-water pressures at the dune surface during the March 17–30, 2010, timeframe, consistent with field observations of debris flows that required the presence of significant water in order to form. However, matching simulated ground temperatures in the near surface to those measured in the field proved to be a significant challenge. Simulated temperatures were warmer than measured within the first meter below ground, and the volumetric water content may be overestimated during this timeframe, leading to too much thermal buffering in the upper 20 cm of the simulated soil column compared to that suggested by ground truth temperature data. The current conceptual model and model parameters apparently result in excess heat in the upper layers of the model domain, translating to simulation output that suggests the perched water layer occurred 2 meters deeper than we observed in the field and in geophysical data in March 2010. Future direct measurement of GKSD sand material properties under external funding should produce more representative simulation results that provide better matches to field observations both in terms of ground temperature in the first meter below ground level and also in the position of the perched water layer identified in the field through hydrogeophysical interrogation, while still revealing the presence of enough near-surface soil moisture and snow to effectively produce debris flows on sunward-facing lee slopes during the heat of the day, even under ambient subfreezing conditions.

2015 IR&D Annual Report

Investigation Using Satellite-Acquired Multispectral and Synthetic Aperture Radar Data to Detect and Monitor Road Degradation for Heavy Truck Traffic, 20-R8413

Principal Investigators
Gary R. Walter
D. Marius Necsoiu

Inclusive Dates: 09/15/13 – 06/15/15

Background — Accelerated road degradation resulting from a high level of heavy truck traffic has been identified as a significant impact associated with the development of unconventional oil and gas resources using hydraulic fracturing technology. These impacts are a concern not only in the area of the Eagle Ford or Permian plays in south and west Texas, but also in other plays throughout the United States, such as the Marcellus Formation in the eastern United States, the Bakken Formation in North Dakota, the Niobrara Formation in Colorado, and the unconventional oil/gas plays in California.

Surveying and monitoring the condition of roadways can be both time consuming and expensive. The Eagle Ford Play in south and southwest Texas covers an area that is approximately 20,000 square-miles. Analysis of satellite-acquired remote sensing data would provide a way to rapidly survey road conditions over large areas to identify road segments that potentially require repair or at least onsite inspection of their condition. This would allow state and county transportation departments to prioritize inspection and repair efforts as well as allocate financial resources accordingly.

Approach — The objective of the project was to develop and demonstrate a methodology for using satellite-acquired multispectral and synthetic aperture radar (SAR) data to detect and monitor the conditions of roads. Typical road damage associated with heavy truck traffic consists of cracking, rutting, and raveling. The extent of our analyses was limited by the temporal and geographical availability of data that could be obtained within the time and budgetary limitations of the project. Initial investigations focused on the analysis of WorldView-2 high-resolution optical satellite data acquired for roads in Karnes County, Texas, affected by heavy truck traffic. Several geocoded image products were analyzed and compared with road conditions, such as damaged pavement, changes from old to new pavement, changes in pavement type, traffic volume, and dirt on pavement.

Due to lack of SAR satellite data for Karnes County, work was refocused on the area near SwRI, where pavement age was known and roads could be inspected, and in Brazoria County, where SAR satellite data were available. TerraSAR-X staring spotLight satellite data (HH and VV polarization) were used to correlate radar backscattering and polarimetric coherency response to pavement age and condition of the roads on and near SwRI. The roads near SwRI were affected by heavy truck traffic. They were easily inspected, and the age and construction of the pavement was known. Finally, the analysis of historical TerraSAR-X spotLight data (HH polarization) for roads in Brazoria County was used to investigate the potential radar backscattering and multitemporal filtering techniques to reveal changes in road pavement conditions.

Accomplishments — The qualitative results provided important insights into the types of satellite remote sensing data and data analysis techniques that could be used successfully for monitoring road pavement conditions over relatively large areas. Specifically, analyzing high-resolution visible and near-infrared imagery acquired by WorldView-2 satellite has potential for revealing changes in asphalt pavement

conditions. The spectral response of asphalt pavement, particularly in the near-infrared data, shows changes as the asphalt ages due to loss of volatile hydrocarbons. TerraSAR-X radar satellite data seem to be useful for detecting changes in pavement type, damage to pavement, such as cracking and scaling, and occasionally severe rutting. Further development of an automated approach to detect road degradation and other manmade surfaces (e.g., airport runways) using a fusion of high resolution optical and radar satellite imagery may be possible.

2015 IR&D Annual Report

Developing Methodologies for Gravity-Assisted Solution Mining, 20-R8423

Principal Investigators
Gary R. Walter
Kevin Smart

Inclusive Dates: 10/01/13 – 09/30/15

Background — The objective of this project was to develop a numerical approach for geomechanical analyses of solution mining activities by combining modeling of the evolution of a horizontal solution cavity with a model that predicts the onset of caving and the extent of caving. This approach can be used to design and optimize undercut solution mining projects in bedded evaporites, particularly for trona deposits such as those in the Green River Basin of Wyoming. This new simulation approach can help mine operators in designing and operating solution mining projects of this type rather than relying on intuition and experience from conventional underground mining.

Approach — The project produced a simplified cavity development model for simulating the gross aspects of evolution of the solution cavity geometry. The model can be used as input to the geomechanical model of the caving process. The model assumes a well-mixed fluid at each cross section of the cavity so that the fluid flow rate can be computed from the known injection-extraction rates and the cross-sectional area of the cavity. The one-dimensional advective-dispersion equation is used to compute local, average concentrations. Cavity wall dissolution rates are based on published, empirical relationships between fluid concentrations and dissolution rates. Changes in cavity geometry are simulated using geometric relationships between evaporite dissolution and cavity wall geometry. Two approaches were used to simulate cavity stability and fracturing. In the first approach, a caving model was developed to simulate the gross aspects of caving initiation and cave front progression. The evaporite mass above the undercut was discretized into Voronoi blocks. In addition to gravity-driven deformation, these blocks can undergo creep-related deformation, which is simulated by assigning viscoplastic material behavior to these blocks. The second approach used a finite-element-based modeling technique to simulate cavity wall creep and development of fractures in the overburden.

Accomplishments — A computer code capable of simulating the evolution of a solution cavity for time periods up to approximately three years was developed. This code was then used to generate representative solution cavity geometries for simulating the stability of the cavity and fracture development. Combining solution cavity evolution simulations with geomechanical modeling provided valuable insights into the processes important to solution mining of bedded evaporite deposits. In addition to developing the solution cavity evolution modeling code and testing the efficacy for the geomechanical modeling approaches, this project produced two manuscripts for presentation at Solution Mining Research Institute technical conferences. The first manuscript focused on development and collapse of solution cavities in thin trona beds. The second addressed the stability of solution cavities developed in thick potash deposits.

2015 IR&D Annual Report

Dynamic Response of Steel-Plate and Concrete Composite Small Modular Reactor Structures Under Explosive and Seismic Loads, 20-R8433

Principal Investigators
Asadul Chowdhury
Kevin Smart

Inclusive Dates: 12/13/14 – Current

Background — Conventional reinforced concrete structures for nuclear facilities are designed using the American Concrete Institute code. This code is based on extensive experimental, analytical, and numerical studies, as well as observations of the performance of reinforced concrete structures under loads from actual natural hazards, such as earthquakes, high winds, floods, or tsunamis. There is considerable interest in the United States, Japan, and Korea to build nuclear power plants using steel-plate and concrete (SC) composite structures, herein called SC structures, in which concrete is sandwiched between a pair of surface steel plates and the traditional rebar inside the concrete is replaced by steel members of different shapes, sizes, and spatial distribution. The interest in SC structures stems from their improved performance, reduced cost, shorter modular construction period, and less onsite work.

Approach — The primary aim of this project is to gain a better understanding of dynamic behavior and responses of shallow-buried SC small modular reactor (SMR) containment dome structures subjected to explosive loads and earthquake ground motion through numerical modeling, starting with an existing constitutive relationship — concrete damaged plasticity (CDP) — and selecting a modified set of material input parameters and without explicit modeling of some steel members embedded inside concrete. A three-step approach is used: (1) numerical simulations of experimental tests of SC structures with explicit inclusion of concrete and steel components and comparison of simulation results with those from the experimental tests, (2) repeat simulations using a CDP constitutive relationship with modified properties to capture the overall behavior of the SC structure without explicitly simulating the steel components, and (3) test the modified constitutive model against an independent set of experimental results to gain confidence in model validity. The modified constitutive model will be used to study the response of underground SC SMR containment structures subjected to selected explosive and seismic loads, including soil-structure interaction without explicitly modeling each embedded steel and concrete constituent of the SC SMR containment structures.

Accomplishments — Numerical simulations of in-plane cyclic shear tests, out-of-plane shear tests, and cyclic unconfined compression tests of steel-concrete composite structures through detailed modeling of concrete and steel components have been completed. Comparisons between numerical simulation results and experimental observations (e.g., load versus displacement, maximum strength) demonstrated the adequacy of the models in reproducing the experiments. Numerical simulations using simplified models of steel components also have been completed. Results based on simplified models of steel components compare reasonably well with those based on detailed modeling. Numerical modeling of a hypothetical containment building of a SC SMR is in progress.

2015 IR&D Annual Report

Assessment of Thermal Fatigue in Light Water Reactor Feedwater Systems by Fluid-Structure Interaction Analyses, 20-R8434

Principal Investigators
Kaushik Das
Debashis Basu
Mohammed Hasan

Inclusive Dates: 12/13/14 – Current

Background — In a nuclear reactor, thermal striping, stratification, and cycling take place as a result of mixing pressurized hot and cold water streams. The fluctuating thermal load generated by such unsteady mixing may result in fatigue damage of the associated structures. The mixing is often caused by faulty valves and can potentially affect safety-related lines such as the pressurizer surge line, emergency core cooling injection lines, reactor clean-up systems, and residual-heat removal systems. Generally, thermal fatigue is considered to be a long-term degradation mechanism in nuclear power plants. This is significant, especially for aging power plants, and improved screening criteria are needed to reduce risks of thermal fatigue and methods to determine the potential significance of fatigue.

Though fluid mixing and thermal fatigue have been studied separately, a number of issues related to complex interaction between turbulent mixing and the mechanical structure of the light water reactor (LWR) have not yet been resolved. Key uncertainties in this area include the effects of solid walls on variations in the thermal load amplitude and frequency (often referred to as filtering). These effects determine the temperature spectrum transmitted from the fluid to the structure.

The primary objective of this ongoing project is to advance the use of numerical modeling techniques for reactor safety determination. This objective is being achieved by developing a proof-of-concept benchmark simulation that demonstrates that computational methods can be used to resolve the turbulent mixing-induced thermal fatigue in the context of LWR operations.

Approach — The project uses computational fluid dynamics (CFD) and numerical techniques to achieve the objectives. In particular, the modeling efforts primarily focus on the following:

- Using CFD tools to resolve the turbulent thermal mixing process, to have accurate knowledge of the thermal processes in the fluid field,
- Performing conjugate heat transfer (CHT) calculations within the fluid and surrounding solid structure to obtain a realistic estimate of the fluctuating heat load to the solid and assess the effect of a solid wall on thermal load modification,
- Evaluating thermal stress, and
- Estimating the structure fatigue based on the calculated thermal stress using an analytical approach.

Initially, the flow field is calculated using a CFD solver. At this stage the flow solution is compared against available experimental data for model confidence and benchmarking. Subsequently, temperature fluctuations on the structure are calculated using a CHT solver, and the thermal stresses are calculated from the temperature fluctuations. The CHT analysis is used for predicting fluid field and solid thermal fluctuation. The approach involves coupling the fluid and solid domains to predict the thermal stress generated by the thermal turbulence mixing phenomena. In this approach, the fluid field is modeled with the temperature-dependent incompressible Navier-Stokes equations. Turbulence is simulated using the

standard Smagorinsky sub grid scale Large Eddy Simulation model. The heat equation is used to model heat transfer in the piping system. For thermal fatigue analysis, the temperature, thermal stress, and stress intensity factor are calculated separately. These variables are used to find the structure degradation (number of cycles to failure and crack length propagation) by applying fatigue crack propagation correlation.

Accomplishments — Numerical simulations of the T-junction experiment carried out at the Älvkarleby Laboratory of Vattenfall Research and Development AB were performed to validate the numerical simulation results. Excellent agreement was achieved between the simulated results and the experimental data. A technical paper was presented at the American Nuclear Society annual meeting in San Antonio in June 2015, and another paper will be presented at the American Society of Mechanical Engineers International Mechanical Engineering Congress and Exposition in Houston in November 2015. A MATLAB® code was developed for the fatigue analysis. The project developed a robust integrated computational methodology to assess thermal fatigue damage in T-junction configurations that involve mixing hot and cold fluids. A reduced order model proper orthogonal decomposition was used to capture the coherent structures and turbulence scales.

2015 IR&D Annual Report

Developing Methods for the Rapid Evaluation of Pore Fluid Effects on Induced Seismicity, 20-R8456

Principal Investigators
Alan P. Morris
Gary R. Walter
David A. Ferrill

Inclusive Dates: 03/01/14 – 10/01/15

Background — Induced seismic activity has become a focus of media attention. Scientific investigations have linked felt earthquake activity with fluid injection into the Earth's crust, and this has been portrayed in popular media as a potential disaster scenario whereby damaging earthquakes are caused by human activities. Although the link between pore fluid pressure in rocks and seismic activity has been recognized since the 1960s, induced seismicity is often a surprise both in its occurrence and location. This illustrates our lack of understanding of the evolution of pore fluid pressure fronts generated by fluid injection, which stems from uncertainty regarding the permeability architecture of an injection site.

Approach — Despite the difficulty of predicting induced seismicity, Southwest Research Institute's (SwRI's) 3DStress® software has been used successfully in Europe to analyze the seismicity resulting from a stimulation program and to predict a magnitude 3.5 earthquake resulting from an emergency fluid injection to control a gas kick. Our objective is to improve the predictive capability of 3DStress by adding a pore fluid pressure analytical tool to model stress field perturbation caused by fluid injection. Developing and testing this new approach will improve our understanding of the interaction between human-induced pore fluid pressure changes and complex geological settings.

Accomplishments — We show that slip tendency analysis is an effective way to evaluate the likelihood of induced seismicity on known or suspected faults. Scenario analyses using established models of well hydraulics to generate pressure histories throughout a rock volume characterized by anisotropic permeability architecture and containing faults indicate that key variables are ambient stress state, size and geometry of existing faults, and permeability architecture surrounding the injection site. Our new approach can be used to evaluate the likelihood of induced seismicity given sufficient geological knowledge of the injection site and injection histories or plans. The 3DStress software has been updated to include this newly developed methodology. A new version of the code is scheduled for release by early 2016.

SOUTHWEST RESEARCH INSTITUTE®

2015 IR&D Annual Report

Mechanical Stratigraphy and Natural Deformation in the Permian Strata of West and Central Texas and New Mexico, 20-R8511

Principal Investigators
David A. Ferrill
Sarah Wigginton
Kevin J. Smart
Ronald N. McGinnis
Alan P. Morris

Inclusive Dates: 01/05/15 – 05/05/15

Background — With rapid development of self-sourced (often referred to as "shale") and low-permeability reservoirs, work focusing on mechanical stratigraphy, structural geology, and geomechanical analysis of these plays has expanded. With a shift in emphasis from drilling and production from the highly productive Eagle Ford Formation to the Permian Basin, there is a growing need to understand the Permian reservoir strata, specifically, the mechanical characteristics, natural deformation, and tectonic setting of relevant strata within the production areas. This information is important to making cost-effective decisions regarding vertical placement, direction, spacing, and completion strategies of horizontal wells ("laterals").

Approach — The objectives of this project were to locate geologic outcrops of Permian strata that could serve as suitable analogs for reservoir intervals and deformation styles within the Permian Basin, and conduct reconnaissance-level field characterization activities to generate a data set suitable for demonstrating the outcrop-analog relevance to potential joint industry project member companies and for use in field seminars for the oil industry. We started by compiling data on geologic outcrops of Permian strata in Texas and New Mexico along with structural and tectonic data throughout the region. Reconnaissance-level characterization was then conducted at suitable outcrop exposures to document lithology and thickness of bedding; collect representative Schmidt hammer rebound measurements to represent mechanical stratigraphy; and measure structures such as bedding, faults, folds, and fractures.

Accomplishments — Project accomplishments included developing an overview presentation summarizing the suite of geologic outcrops, including key stratigraphic and structural features; building an ArcGIS database of outcrop locations and data as the foundation for a new joint industry project; and preparing regional deformation maps showing the distribution of fault, joints, and folds and their geologic context. Surface exposures of lithologically varied Permian strata around the southern, western, and eastern margins of the Permian Basin in west Texas reveal a broad spectrum of bore-hole scale deformation styles that reflect their tectonic histories and that apply to both conventional (limestone and sandstone) reservoirs and unconventional (fine-grained mudrock) reservoir facies of the Permian Basin.

Collectively, data gathered from these exposures document that structural styles vary with tectonic context around the margins of the Permian Basin, and document a systematic 30-degree rotation of dominant strike trends around the basin. These results are directly relevant to predicting the distribution and style of sub-surface, small-scale deformation features that influence the permeability architecture and the potential for induced hydraulic fracturing of hydrocarbon reservoirs throughout the Permian Basin. An invited abstract and oral presentation were prepared for the West Texas Geological Society 2015 Fall Symposium (Midland, Texas), and an abstract was prepared and submitted for the 2016 Annual Conference and Exhibition of the American Association of Petroleum Geologists (Calgary, Alberta).

SOUTHWEST RESEARCH INSTITUTE®

2015 IR&D Annual Report

Testing and Analysis of Acoustically-Induced Vibration Stresses in Piping Systems, 18-R8478

Principal Investigators
Tim Allison
Brandon Ridens
Nicholas Niemiec
Jeffrey Bennett

Inclusive Dates: 07/01/14 – Current

Background — Acoustically induced vibration (AIV) is the phenomenon of high-frequency piping vibration downstream of a high-amplitude noise source, potentially leading to fatigue failure of the piping at a branch or welded support. Although AIV has long been a concern in high-capacity gas piping systems, recent capacity increases to aging systems and debottlenecking operations, as well as the development of new higher-capacity systems, have led to renewed interest in AIV mitigation strategies. Existing methods of AIV analysis used to predict if a weld failure is likely to occur are based on an incomplete historical dataset that does not properly address the fundamental physics of AIV, the high flow rates and pressure ratios encountered in modern blowdown systems, or the increasingly larger pipe sizes that are being implemented. In many cases, these methods are considered to be overly conservative and costly. Furthermore, AIV mitigation options are limited for existing systems that are predicted to fail. Therefore, a physics-based approach that is calibrated to physical measurements is needed for improving the accuracy of AIV failure predictions as well as accurate performance modeling of AIV mitigation strategies.

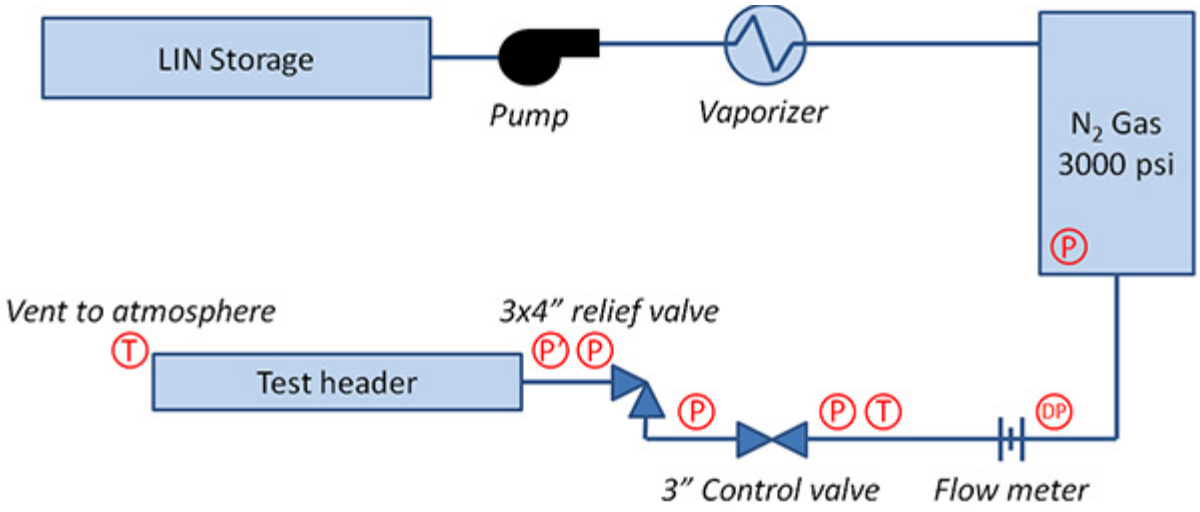

Figure 1: Experimental setup

Approach — The objective of this project is to gather experimental AIV data during blowdown testing of several piping samples that span a wide range of diameter and wall thicknesses (Figure 1). Data from this testing, performed at

SwRI's Gas Blowdown Facility (Figure 2), includes dynamic pressure and stress measurements to validate models of the noise source, internal piping acoustics, and piping stress response for several representative configurations of gas blowdown piping. Several AIV remedies including damping wrap, stiffening rings, and acoustic attenuators were also tested to quantify the stress reduction provided by each method.

Accomplishments — Test data for all piping configurations have been acquired and analyzed to quantify baseline AIV stresses and stress reduction performance of each AIV mitigation for the various piping geometries. Application of these experimentally obtained stress reductions to existing analysis methods enables SwRI to offer AIV analysis services with improved accuracy, and test data for various remedies increases the pool of available design and retrofit options. The test data are also analyzed to improve SwRI's capabilities for physics-based modeling of AIV. Detailed structural and acoustic finite element models were developed and analyzed for comparison with test data to determine combinations of acoustic and structural modes that lead to peak stress frequencies. An example comparison of test data with simulated mode shapes and frequencies is shown in Figure 3. Continued analysis of this data is in progress to determine possible methodologies for efficient physics-based AIV analysis.

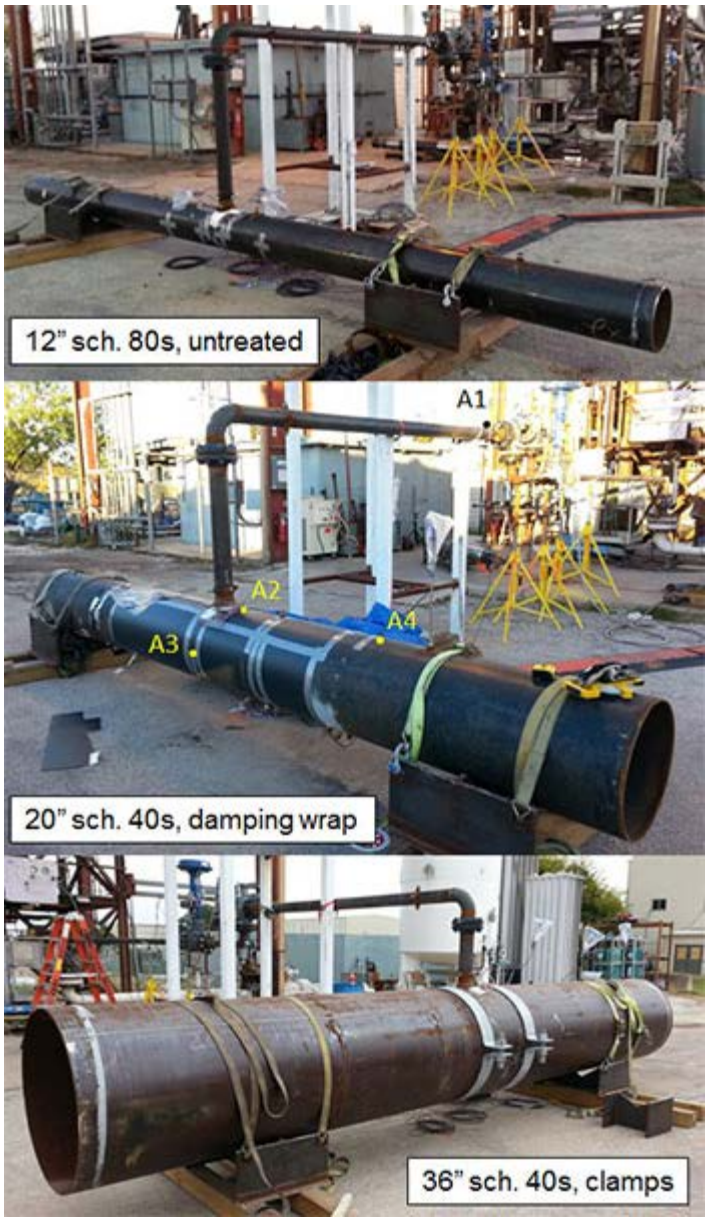

Figure 2: Test header configurations

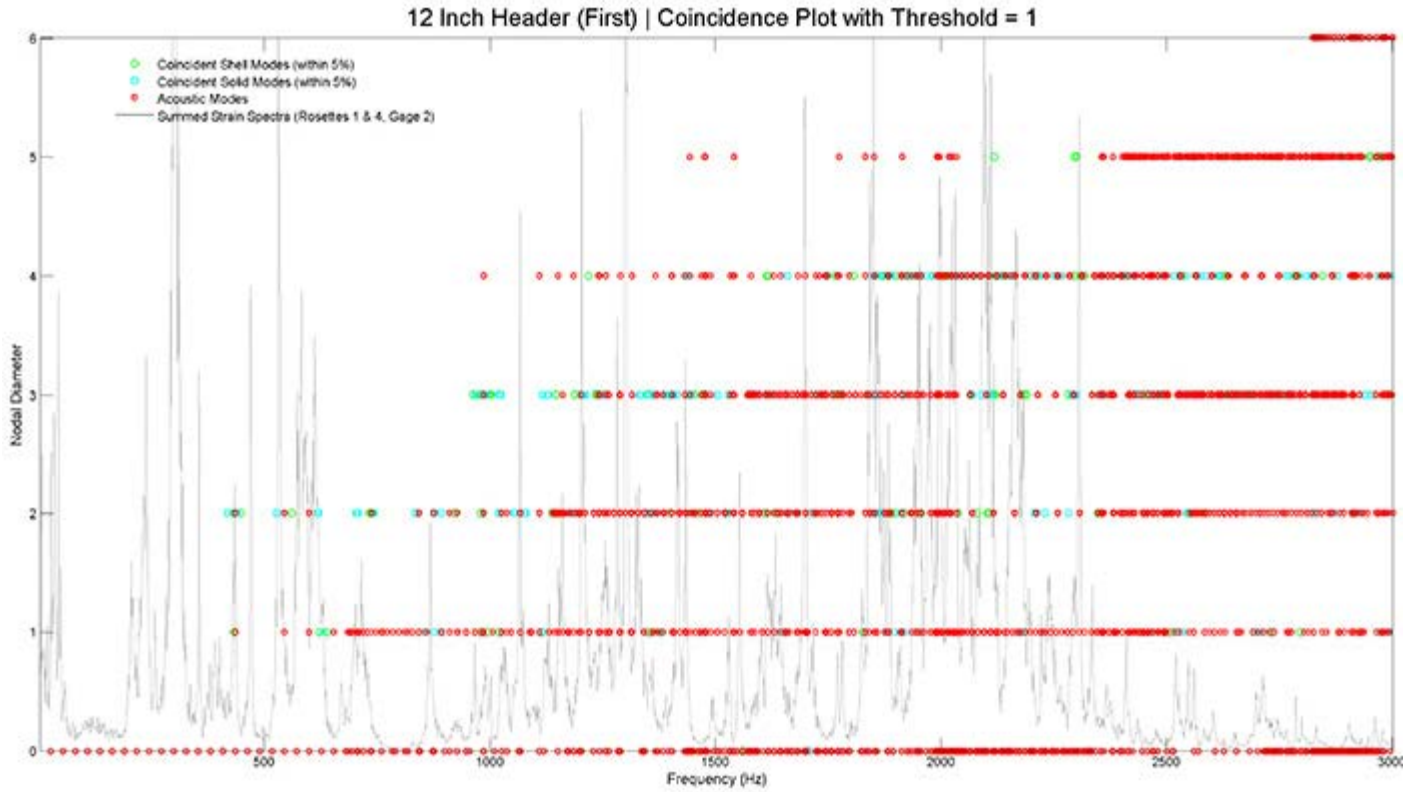

Figure 3: Example AIV coincidence plot with experimental data overlay

---

2015 IR&D | IR&D Home

2015 IR&D Annual Report

Desired Computational Enhancement for Our In-House Lattice-Boltzmann Method-Based Numerical Model for Applications in Oil and Gas Exploration and Biomedical Fields, 18-R8515

Principal Investigators
Hakan Başağaoğlu
John T. Carrola Jr.
Nicholas J. Mueschke
Nathan F. Andrews

Inclusive Dates: 12/15/14 – 05/31/15

Background — Over the past several years, we have developed a new numerical model based on the lattice-Boltzmann method. The model is equipped with a series of new algorithms to simulate inert or reactive nano-size or micron-size particles in transient shear flows in geometrically complex flow domains. The model is formulated for diverse applications involving, but not limited to:

- Determining rock permeability based on transient flow characteristics in three-dimensional microchannel networks in large reservoir formations for applications in oil and gas production and developments
- Optimizing size, shape, and surface characteristics of engineered particles with embedded nanodrugs designed for more efficient targeted deliveries to diseased sites (e.g., tumor) in the human body, and
- Assessing thrombotic risk in diseased hearts by analyzing transient microvortex developments in blood flows

We published new modeling features as well as model validation and verification tests via benchmark problems, theoretical results, and measurements from our in-house microfluidic experiments in a series of peer-reviewed journal articles. While we have demonstrated that the model successfully simulates various challenging problems, the code's computation efficiency for large-scale production runs requires improvement. These computational efficiency improvements are critical for near-term business development efforts.

Approach — The original code, written in Fortran 90/95 in a non-modular structure, was converted into a modular structure to enhance its readability and traceability. The code was translated into MATLAB and vectorized for the solutions teams, who were more comfortable with MATLAB than Fortran 90/95. Four benchmark problems with different levels of complexities were prepared for the solution teams to ensure that computationally optimized codes would produce the same results. The benchmark problems were accompanied with easy-to-follow input data structures to avoid any mistake in data entry and/or modifications. The code was compiled using Portland, Intel, and GFortran compilers on both Linux clusters and a PC. All compiler-specific error and warnings have been removed before the code was released to the solution teams.

Accomplishments — Three solution teams showed interest in enhancing the computational performance of our model. These three solution teams proposed completely different approaches, involving a new programming language, implementation of new parallelization techniques, novel code-restructuring approaches, and new random number generator functionalities. The new structure of the code and input files allowed each solution team work on code optimization with minimal input and guidance from the

principal investigators. All solution teams are currently working on the code optimization and reportedly making progresses on the computational performance of the model.

SOUTHWEST RESEARCH INSTITUTE®

2015 IR&D Annual Report

Methodology for Qualifying Flow Regime of Two-Phase Flow within a Pressurized Compressor, 18-R8521

Principal Investigators
Melissa Poerner
David Ransom
Ryan Cater
Grant Musgrove
Craig Nolen

Inclusive Dates: 01/01/15 – Current

Background — Wet gas compression has become a topic of increasing significance with the advent of subsea compression on oil and gas production streams. In subsea production facilities, the process natural gas from the wellhead can contain up to 5 percent liquid volume fraction (LVF), and centrifugal compressors are being designed to operate with this two-phase flow. Research to date has shown this small amount of liquid has a significant effect on the compressor performance, causing deviations as much as 200 percent from the dry operation. Industry has focused on using thermodynamic models and simulations of wet gas flow in computational fluid dynamics software to attempt to predict this change in compressor performance. These efforts have given results that are still largely different from the measured compressor performance. This project focuses on the aerodynamic aspect of compressor operation by using flow visualization to qualify the flow regime inside the compressor inlet, blades, and diffuser.

Approach — The objective of the research is to develop flow characterization methods on an ambient pressure compressor test stand for viewing two-phase flow that can later be used on a full-size, pressurized compressor. This includes developing two separate methods: an optical method for visualizing the flow at the inlet and exit of the compressor, and electrical resistance probes for quantifying the liquid film thickness on the compressor impeller blades. The data on the flow at the inlet and exit of the compressor impeller will help to define boundary conditions for modeling and give insight into the asymmetry that exists in the flow inside the compressor. Film thickness measurement will provide data to estimate the influence of the liquid on the aerodynamics of the compression process.

Accomplishments — Several accomplishments have been made in the current research. These accomplishments include:

- System design: The test system comprises a compressor, an airflow control system, a water supply and return system, and a measurement system. The design of the compressor (Figure 1) and water system are nearing completion.

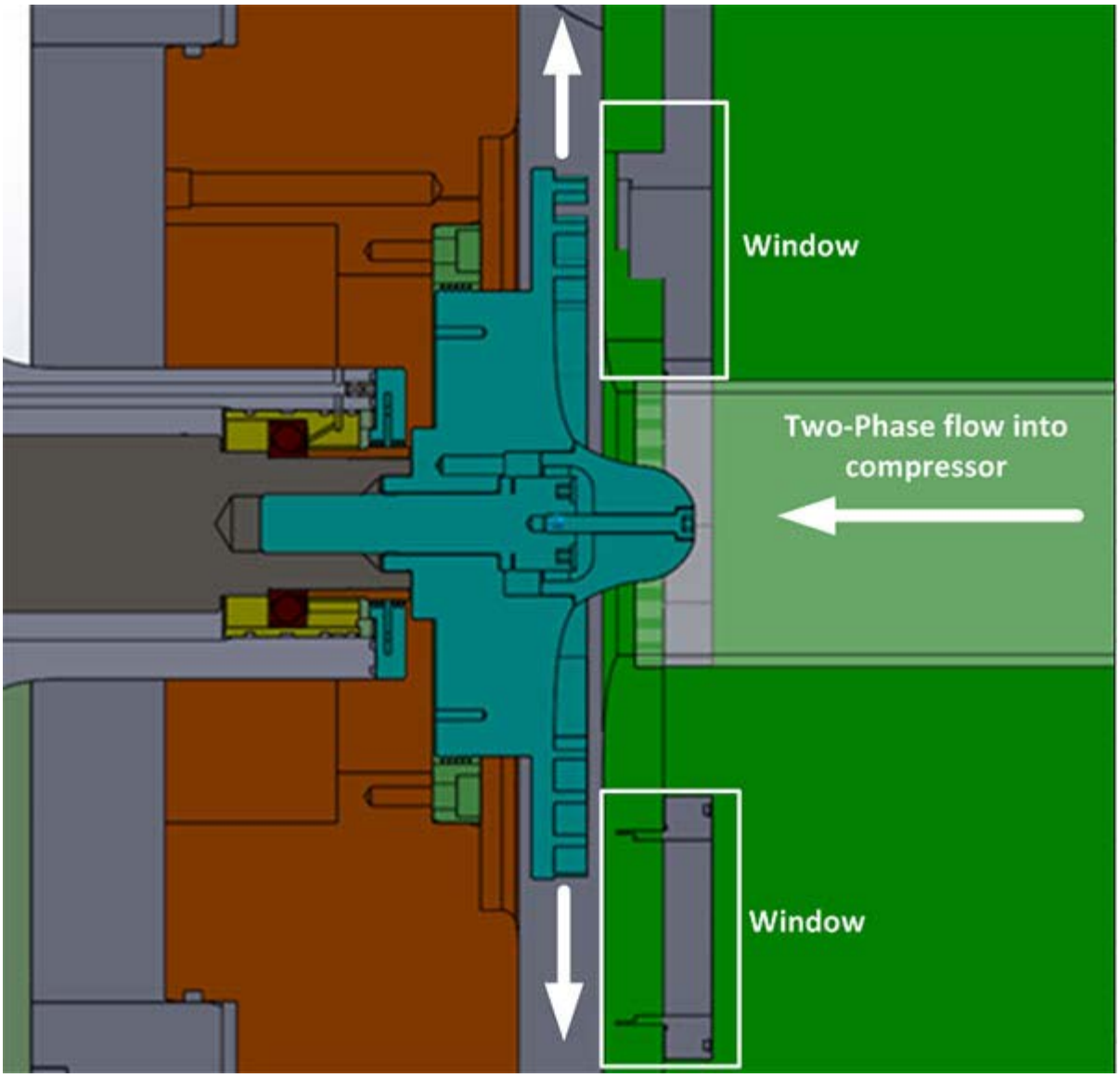

Figure 1: Cross section of test compressor showing location of windows

- Visualization system design: The flow visualization system consists of a series of windows where high speed photography will be used to capture images of the flow. For this system, a lighting study was conducted to find the optimal light setup for the image recording. In addition, a bench-top flow visualization study is currently in progress (Figure 2). This study is being used to test several window configurations to find the optimal method to view the flow inside the compressor.

Figure 2: Bench-top test of window configuration for visualizing two-phase flow

- Resistance sensors: Resistance sensors are being used to measure the liquid film thickness in the diffuser of the compressor. A bench-top test of the sensors is in progress to verify sensor design and operation and to calibrate the sensors (Figure 3).

Figure 3: Electrical resistance sensor bench test setup and calibration

In the following months, the compressor will be constructed, and all flow visualization and measurement equipment will be installed. After this, the wet gas flow visualization data will be collected.

SOUTHWEST RESEARCH INSTITUTE®

2015 IR&D Annual Report

Algorithms to Improve the Speed of the Numerical Model Based on the Lattice-Boltzmann Method, 18-R8541

Principal Investigators
Grant Musgrove
Shane Coogan
Shahab Saleh

Inclusive Dates: 03/01/15 – Current

Background — This work solves the second problem of the first call for the Computational Optimization Focused Internal Research Program, "Desired Computational Enhancements for Our In-House lattice-Boltzmann Method-Based Numerical Model for Applications in Oil and Gas Exploration and Biomedical Fields." Because the solver was developed through the solution of physical problems, computational efficiency was not a primary developmental concern. As the solver capability continues to expand with more complexity, computational efficiency is becoming increasingly important. The objective of the problem statement for this program is to improve the speed of the time-consuming computations of the lattice-Boltzmann (LB) solver. In the posed problem, four computationally intensive issues are requested to be improved to shorten solution time:

- Reduce computation time for the streaming algorithm
- Reduce computation time to search for the particle boundary and nearby solid nodes
- Reduce computation time to generate normally distributed random numbers and predict an average nanoparticle trajectory from many simulations
- New methods to scale or run the code in parallel with CPUs, GPUs, or a combination of both

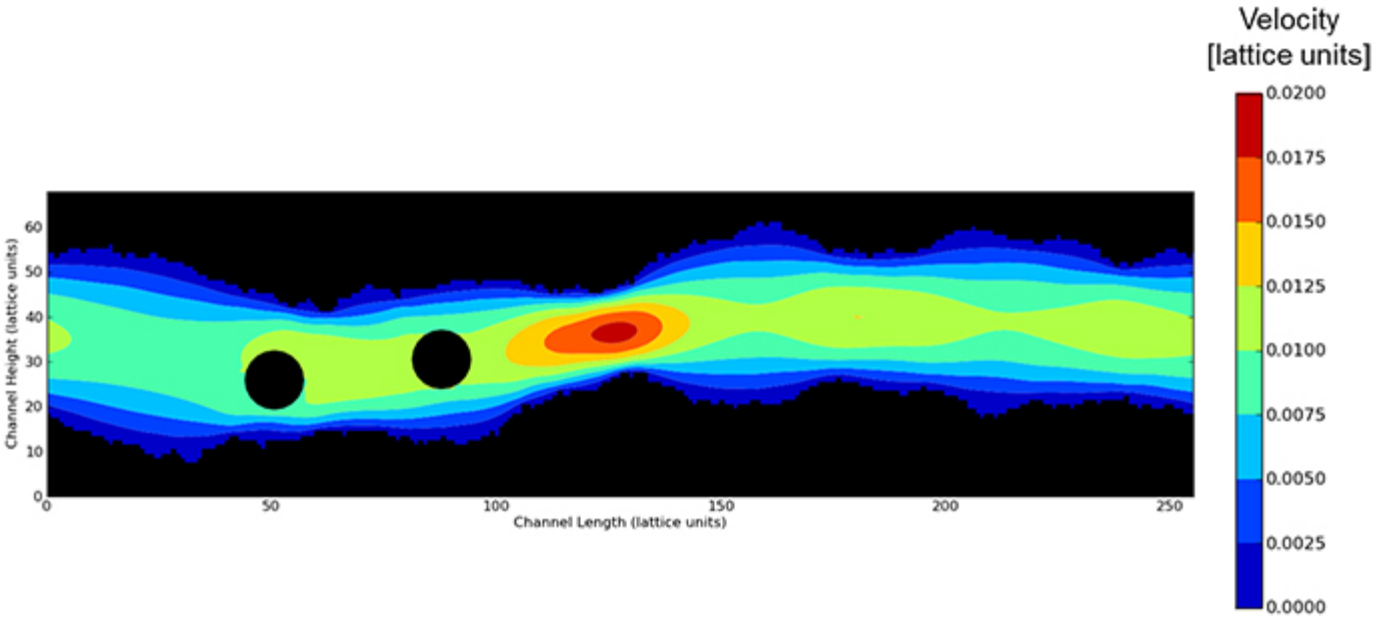

Figure 1: Two nanoparticles flowing through a domain with complex wall boundaries.

Approach — This project is intended to solve the first three issues by using efficient algorithms to speed up the computations of the current LB solver. The primary approach to improving computation speed is eliminating repetitive computations in the code for which the result does not change or changes very little. Additionally, the solution approach to predict nanoparticle trajectories requires random number generation and uses a Monte Carlo sampling method, both of which are improved upon by using probabilistic methods.

Accomplishments — The computational speed of the solver has increased between 40 and 75 percent for four benchmark problems by reducing or eliminating the repetitive calculations within the code. Two approaches to replace the Monte Carlo sampling method are being evaluated, a Latin-hypercube-sampling method and a matched-moment method. The goal of the Latin-hypercube-sampling method is to reduce the total number of solutions necessary to predict an average nanoparticle trajectory, while the matched-moment method is a computationally faster alternative than the generation of random numbers used in the LB solver.

2015 IR&D Annual Report

Space-Based Communications Processing, 15-R8469

Principal Investigators
Jennifer L. Alvarez
Larry T. McDaniel

Inclusive Dates: 05/01/14 – 07/01/15

Background — Satellite communications (SATCOM) providers are seeking to expand content distribution, especially of Internet content, to mobile users. Traditionally, SATCOM companies focused on fixed satellite services, which distribute content to users in fixed locations with dedicated, often large, terrestrial equipment. The push to provide mobile satellite services is unsurprisingly motivated by the booming market of smartphones and tablets. SATCOM providers are interested in becoming a part of the mobile data infrastructure by making SATCOM data transmission mechanisms transparent to mobile users. The expansion into mobile satellite services requires the capability to serve large user populations at extremely high data rates. The intent of this research is to develop foundational and cross-cutting technologies that would position us to provide hardware, algorithms, and intellectual property to SATCOM service providers and the spacecraft and component manufacturers that serve the SATCOM industry.

Approach — The project objectives were to develop an end-to-end satellite payload architecture that uses adaptive control algorithms and the next-generation, high-rate signal processing algorithms and hardware needed to achieve the required level of service. These underlying technologies can then be applied to SATCOM technology innovations, including adjustable antenna spot beams, adjustable multi-carrier amplifiers, radio frequency (RF) channelizers, advanced modulation/demodulation methods, and multiple access and routing mechanisms. Each of these technology elements will eventually contribute to space-based systems that can be dynamically optimized based on changing usage profiles over varying geographic area. We developed foundational technologies that are applicable to each of the potential SATCOM technology innovations.

Accomplishments — We have developed an initial, high-level model of an intelligent communications manager that uses knowledge of spatial characteristics, communications resources, and data flows to manage communication network resources. The network resources include the signal processing components on the spacecraft. The on-orbit data processing throughput goals of the project require a multi-processor architecture that is flexible and scalable to suit low-cost, low Earth orbit satellites, in addition to large, geostationary orbit satellites, and to allow optimization of services over time and market applications. We developed functional models of the required processing and estimated the necessary performance in operations per second. We mapped the processing and throughput requirements against processing architectures and advanced interconnect standards, and we prototyped one type of high-speed interconnect to prove performance. Thermal management of high-throughput processors is a key concern, and investigations and experiments were performed to quantify the performance of micro heat pipes suitable for use in space.

Based on this research, we received a $60,000 contract from a commercial client.

SOUTHWEST RESEARCH INSTITUTE®

2015 IR&D Annual Report

Susceptibility of Processor Memory to Radiation Induced Faults, 15-R8531

Principal Investigators
Jennifer L. Alvarez
Paul Riley

Inclusive Dates: 02/02/15 – 06/02/15

Background — SwRI low-cost avionics solutions are built around a radiation-hardened microprocessor, the Aeroflex/Gaisler GR712RC. The GR712RC was developed as an embedded processor architecture for applications that can be exposed to significant levels of radiation, which can affect the performance of the device. Of particular interest in our applications is single event upset (SEU). SEU is a soft error caused by the signal induced by a single energetic-particle strike. Effectively, an SEU causes a bit error in memory. Even with error detection and correction measures in place for processor memories, implementation-specific variables such as orbital characteristics, processor operating frequency, and software application details affect the robustness of the described techniques. This project addressed the execution of avionics software on a GR712RC-based processing platform when it is exposed to various levels of radiation, but without undergoing costly radiation testing. We provide a thorough analysis of error mitigation performance of processor memory at a system level for a GR712RC-based processing architecture.

Approach — The first objective of the research was to estimate, using radiation analysis tools and statistical methods, the likelihood of occurrence of functionally significant radiation upsets in volatile processor memory over a variety of orbit conditions. This served as the foundation for the experimental objectives, which involved injecting bit errors in memory in quantities and distributions representative of those expected under various mission conditions. Using an available test platform, we then evaluated the performance of application software representative of functions generally common to avionics to empirically understand the implications of radiation upsets in memory on real-world operations.

Accomplishments — A key product of this effort is a means to empirically understand the implications of radiation-induced bit errors on real-world operations without the need for actually conducting costly radiation testing of the devices. This is a valuable asset, because radiation testing on a single function device, such as a MOSFET, is approximately $30,000. Radiation on a complex device that has many functions and modes of operation, such as a microprocessor, can be several hundred thousand dollars depending on the scope of the testing.

SOUTHWEST RESEARCH INSTITUTE®

2015 IR&D Annual Report

Low Cost Lighter-than-Air Flight Control System, 15-R8574

Principal Investigators
Barbara Anderson
Bill Perry
David Lopez
Ethan Chaffee

Inclusive Dates: 07/01/15 – Current

Background — We identified a need for a new low-cost, lightweight, flight-control system with state-of-the-art electronics, large memory, and improved sensor capacity. Lighter-than-air flight control systems require a wide variety of sensors, actuators, and other hardware capabilities including Global Positioning System (GPS), cameras, accelerometers, gyroscopes, pressure sensors, temperature sensors, and local communication to other devices, all of which are items available in an Android® smartphone.

Approach — The purpose of this project was to determine if the advanced technology in an Android® smartphone is capable of providing data acquisition and flight-control capability in an extreme near-space environment. In order to achieve this, several items were identified that would be required to build a smartphone-based avionics system:

- Smartphone Custom App and External Hardware: A smartphone custom app was created in the Java Language, which was used as the basis for an LTA data acquisition and flight control avionics system. The custom app also communicated with a Texas Instruments® (TI) Sensor Tag communicating to the smartphone via Bluetooth®, and iridium short-burst data (SBD) over serial for long-range communication capability. A Lithium battery pack provided power to both the phone and a USB hub (via a DC-DC Converter), which ultimately powered the iridium SBD. The assembled components are shown in Figure 1.
- Thermal Analysis and Chassis

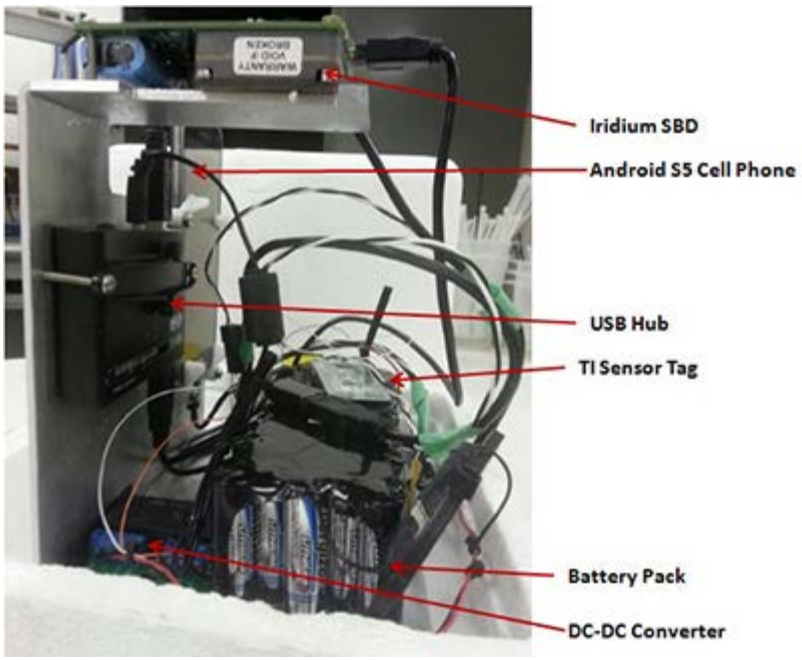

Figure 1: Assembled smartphone-based avionics system

Figure 2: Closed foam container showing visible heat sink plate and camera lens

Design: The thermal analysis performed for this project involved determining an approximate size of a heat sink window required to maintain the temperature of the flight package to within normal operation conditions. Thermal heat loads for radiation to space from both the package and heat sink, radiation to Earth, solar radiation, conduction through the container, and the heat generated by the electronics were all included in the model. The heat sink radiator was designed as an aluminum plate with a mount for the phone. A simple parametric analysis for the area of the heat sink window was performed to achieve a steady state operating temperature within the range the phone would normally see on the ground. The components were determined to be able to survive the pressure changes that are part of LTA balloon flights, as long as the heat sink continued to provide sufficient heat dissipation. To provide thermal incubation, components for the data acquisition and flight-control system were packaged inside a lightweight, painted foam container with custom cutouts for the heat sink radiator and the cell phone camera lens, as shown in Figure 2.

- Ground Station: Ground station equipment (GSE) consists of a standard laptop with an attached iridium SBD. Software was created in the C programming language and performed tasks including receiving messages from and sending commands via the iridium gateway to the smartphone avionics system, as shown in Figure 3.

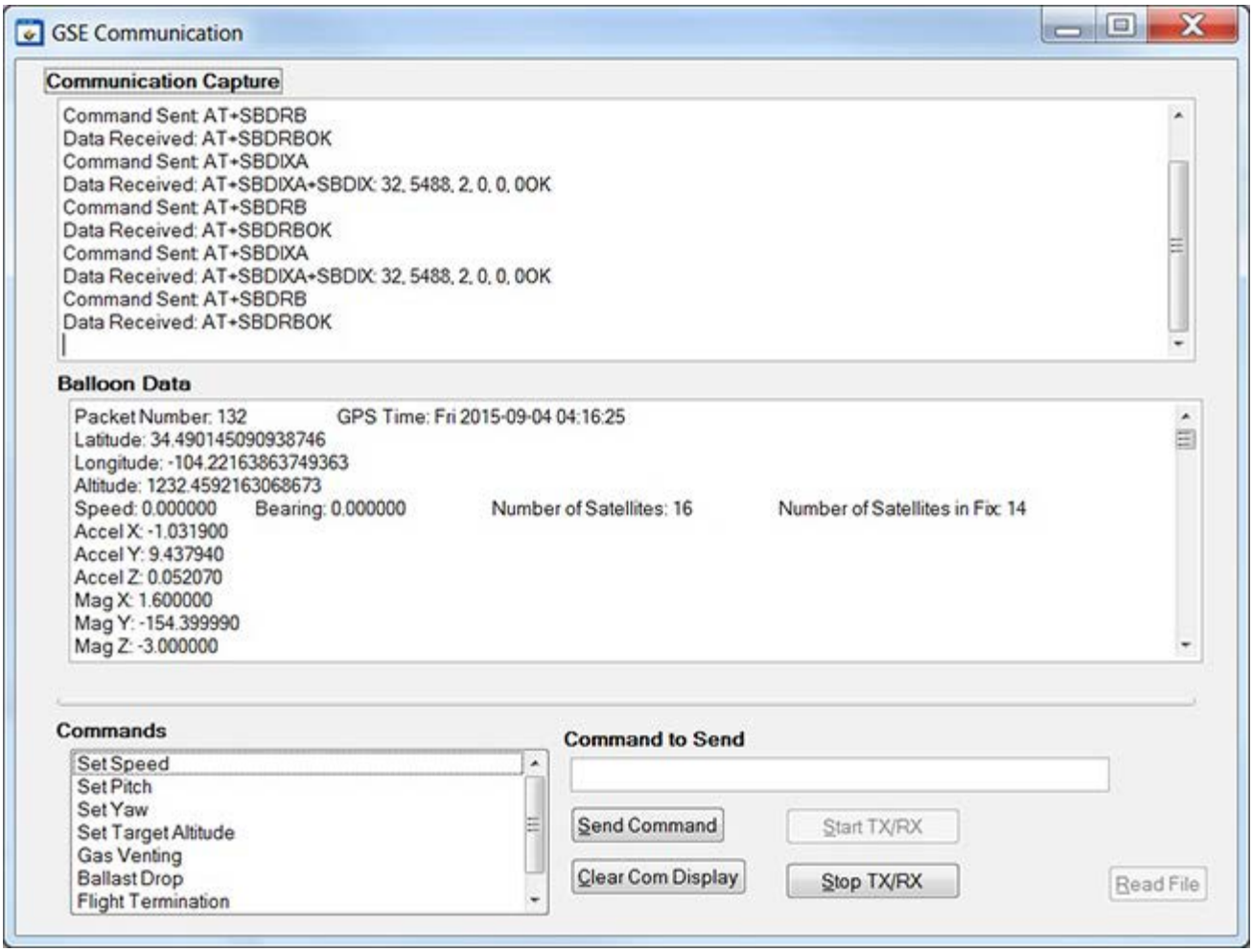

Figure 3: Ground station equipment main screen display

The complete system was evaluated by testing the smartphone avionics system as part of a NASA balloon flight that launched in New Mexico while the ground station communicated with the smartphone avionics system on-board the balloon, from SwRI in San Antonio. The following items were successfully evaluated to establish the feasibility of a smartphone-based avionics system:

- Compatibility to other functions
- System power
- System mass
- Thermal range
- System reliability
- Cost

Accomplishments — The results from the flight test of the smartphone avionics system successfully demonstrated that a commercial-off-the-shelf cell phone can be used as the basis for an LTA avionics system. The smartphone avionics system was able to acquire, record, transmit, and receive data for an entire flight lasting a total of 7.5 hours, including 2.5 hours of ascent, 4.5 hours of float hours at ~37,000 meters (~124,000 feet) and 0.5 hours of descent. Data sent to the ground station every 15 seconds included readings for gyroscopes, accelerometers, pressure, temperature, and GPS. The phone also took high resolution (16 Megapixel) photographs once a minute for the duration of the flight. Figure 4 shows a photograph taken by the smartphone avionics system during the float portion of the flight, at an altitude of 124,000 feet.

Figure 4: Photograph during float at 124,000 feet

Data recorded by the smartphone avionics system and transmitted to the ground station during flight was accurate and informative. Examples of the data include Figure 5 and Figure 6, which show that the GPS data collected by the smartphone avionics system aligns with data collected by the balloon vector navigation (VectorNav) System: a miniature, surface-mount, high-performance GPS-aided inertial navigation system, which was used to collect GPS data for a separate flight system.

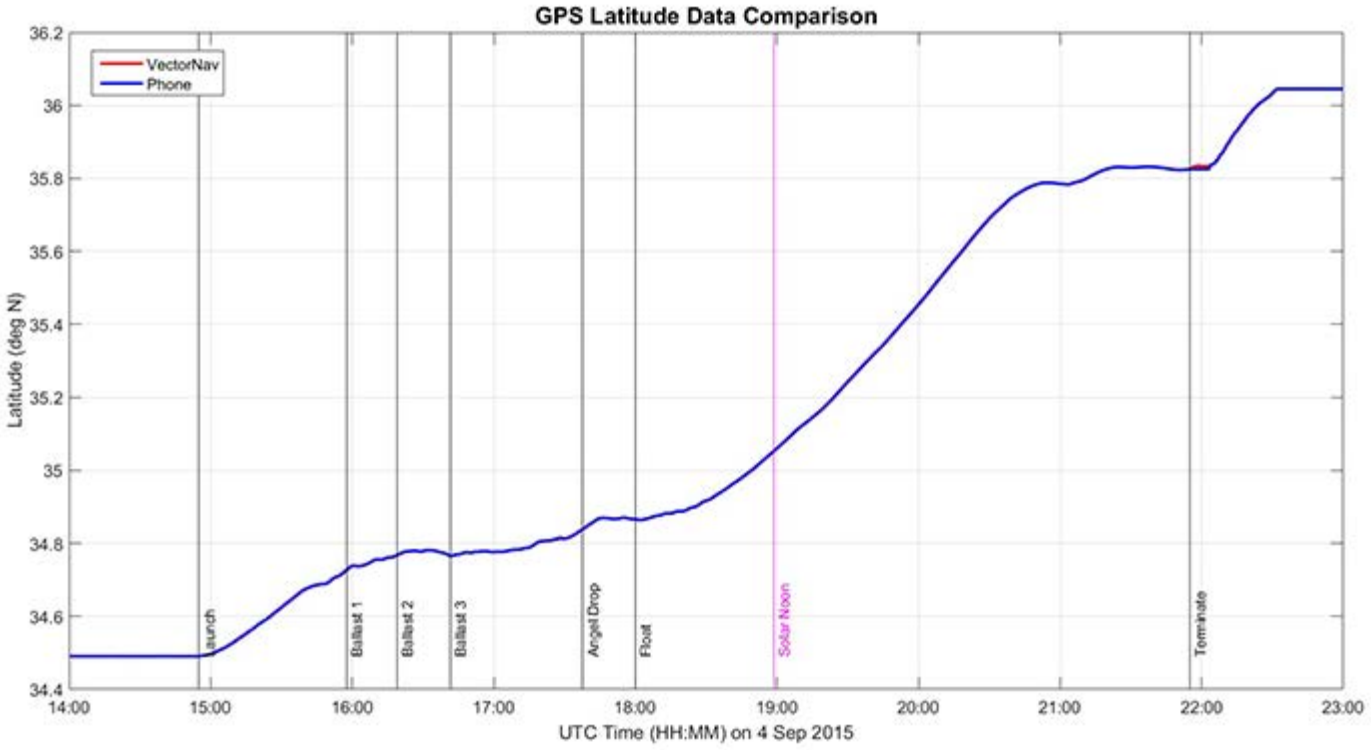

Figure 5: GPS latitude-smartphone avionics system vs. vector nav system

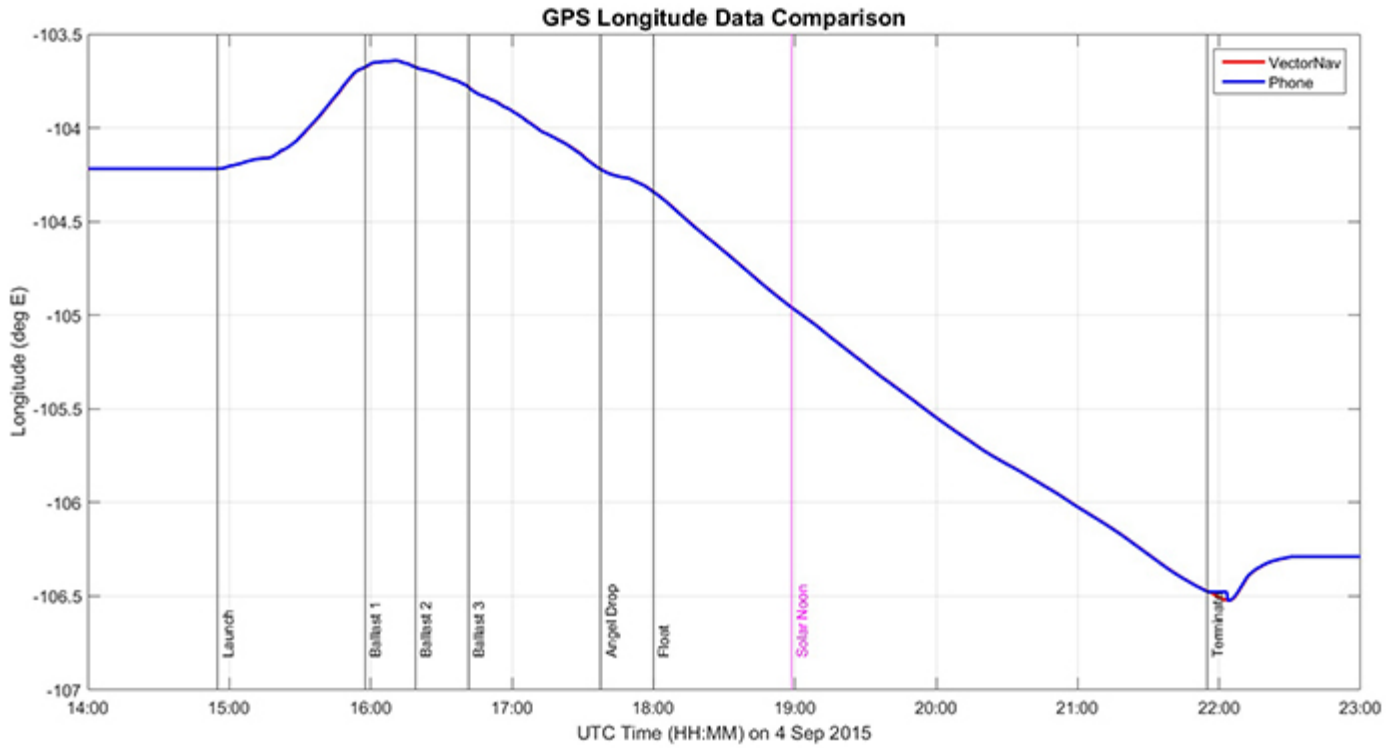

Figure 6: GPS longitude-smartphone avionics system vs. vector nav system

Figure 7 shows the relationship between the battery temperature acquired by the smartphone avionics system against the altitude and time of flight. The data clearly shows that while the balloon ascended through the troposphere, the temperature of the phone battery dropped, but stayed within operational temperature range, which can be attributed to the system chassis and foam container designs, which allowed for heat dissipation without allowing the hardware enclosed in the container to become too cold to function.

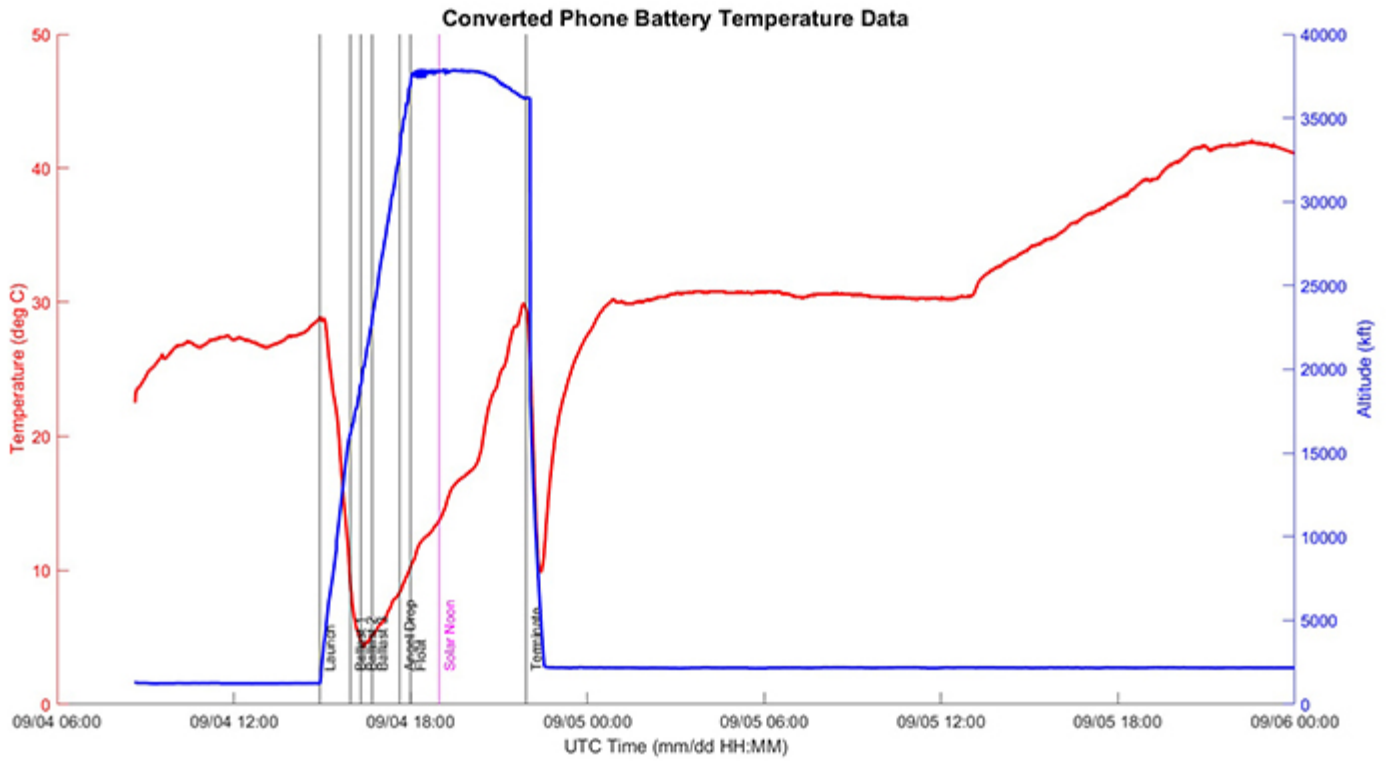

Figure 7: Battery temperature-smartphone avionics system vs. vector nav system

Flight testing also demonstrated that the GSE was able to successfully send commands to the smartphone avionics system, even when the balloon was at 124,000 feet. The overall results of this project show that a smartphone avionics system is a viable option for the future of high-altitude ballooning.

2015 IR&D | IR&D Home

2015 IR&D Annual Report

High Octane Number Gasoline Production from Lignin, 01-R8384

Principal Investigators
Maoqi Feng
Darius Daruwalla

Inclusive Dates: 04/01/13 – 12/31/14

Background — Biofuels production from lignocellulosic biomass would reduce the nation's reliance on imported fossil fuels while yielding economic benefits. Of the three major components in lignocellulosic biomass — celluloses, hemicelluloses, and lignin — lignin is the most difficult to convert. The objective of this project was to develop chemical methods for processing lignin through the steps of dissolution, depolymerization, deoxygenation, and separation to yield hydrocarbons in the gasoline boiling point range.

Figure 1: Batch reactor for lignin depolymerization

Approach — Ionic liquids were used as solvent, and lignin was catalytically depolymerized in a hydrogen environment generated *in situ* from formic acid decomposition to prevent repolymerization of the fragmented molecules. There were two steps in the process: depolymerization and hydrodeoxygenation. The oxygenates produced by depolymerization in Step 1 are not good fuels; the subsequent Step 2 catalytic hydrodeoxygenation of the substituted phenolic compounds in hydrogen could produce hydrocarbons.

Two kinds of lignin were used as the feed: kraft lignin from a commercial source and organosolv lignin extracted from wood chips. Three ionic liquids, 1-n-butyl-3-methylimidazolium chloride, 1-ethyl-3-methylimidazolium chloride, 1-n-butyl-3-methylimidazoline trifluoromethanesulfonate, and two deep eutectic solvents were used as solvents in the study. Figure 1 shows the reactor for the Step 1 tests.

Accomplishments — Kraft lignin was successfully depolymerized to phenols, anisole, and substituted phenols at reasonable yields (~60%) at 200°C in ionic liquids. Organosolv lignin (acid soluble) extracted from pine wood was successfully depolymerized to phenols and substituted phenols at higher yields (over 70%) in ionic liquids. Different catalysts were evaluated possibly by facilitating the decomposition of formic acid to hydrogen and CO_2. The depolymerized products were extracted by organic solvent and used as feed for the hydrogenation study.

In the hydrodeoxygenation catalyst development, both model compounds and lignin depolymerized oligomers were used as the feedstocks. The reactor is shown in Figure 2. Three model compounds were studied first: phenol, anisole and a substituted phenol. A

Figure 2: Continuous reactor for catalyst development on oligomers hydrogenation

series of catalysts, including Pd/alumina, Ni/alumina, Ni-Mo/alumina, and some proprietary catalysts prepared in the lab, were tested for the catalytic hydrodeoxygenation activity. Phenol and substituted phenol were converted to benzene quantitatively. A mixture of benzene and phenol was produced from anisole. Two catalysts were found to be very active and contaminant-tolerant for hydrogenation of the model compounds and the oligomers for depolymerized lignin. Overall thermal efficiency of the process was estimated to be 86.9 percent, which compares favorably with the Fischer-Tropsch process.

SOUTHWEST RESEARCH INSTITUTE®

2015 IR&D Annual Report

Development of a Novel Drug-Loaded Composite Scaffold as Bone Graft Substitute Using Advanced Materials Technology, 01-R8415

Principal Investigators
Jian Ling
Joo Ong (UTSA)

Inclusive Dates: 09/01/13 – 12/31/14

Background — More than three million musculoskeletal procedures are performed annually in the United States to address damage to bone tissue due to trauma (from automobile accidents and military operations), to fix congenital deformities or bone diseases, and to heal defects created upon the removal of cancerous lesions. Currently, the use of autologous grafts is considered the "gold standard" for grafting procedures. However, this approach is associated with tissue scarcity and donor site morbidity due to the additional surgery. The objective of this project was to develop a novel biomimetic bone substitute loaded with growth factor for musculoskeletal procedures to address the growing unmet needs of the $2.5 billion per year bone graft market.

Approach — SwRI used a patented technology to fabricate biomimetic collagen-hydroxyapatite (Col-HA) scaffolds with different HA loadings through a perfusion-based method. Then the Col-HA scaffolds with different degrees of HA loadings and stiffness were evaluated by human mesenchymal stem cells (hMSCs) cultured on these scaffolds in osteogenic media. Based on the osteogenic response of hMSCs, an optimized mineralization level was identified. At UTSA, microparticles encapsulation with growth factor TGF-β were developed, which would be incorporated into the biomimetic scaffolds to form a drug-loaded composite grafting material for bone repair.

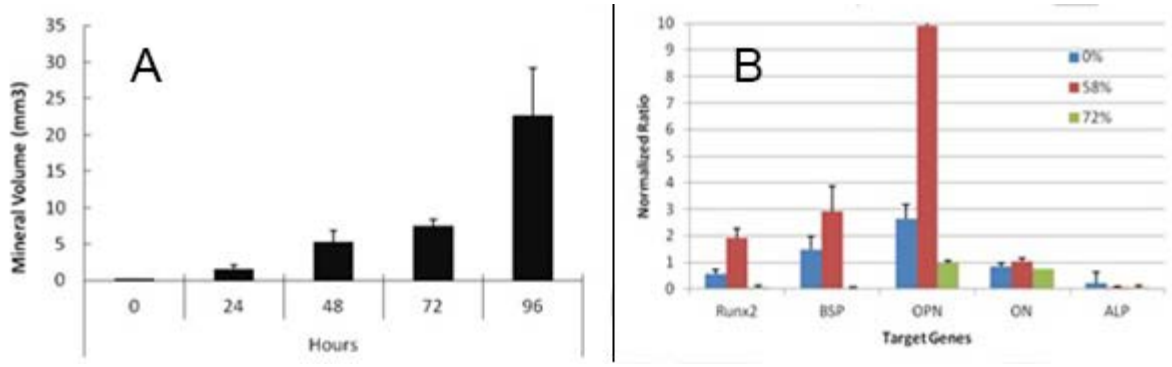

Figure 1: (A) MicroCT shows the mineral volume of the composite scaffolds with different mineralization time. (B) The comparison of osteogenic gene expression after the hMSCs were cultured on the scaffolds with different mineralization levels (0%, 58%, and 72%).

Accomplishments — Highly porous collagen scaffolds were fabricated. The scaffolds were exposed to mineralization solutions using a perfusion flow bioreactor system to form Col-HA composite scaffolds. Col-HA composites of different mineral loadings were fabricated by varying the mineralization time (Figure 1A). The osteogenic gene expression illustrated in Figure 1B suggests that scaffolds with a medium mineralization level around 58 percent had the highest osteogenic response from hMSCs.

SOUTHWEST RESEARCH INSTITUTE®

2015 IR&D Annual Report

Evaluation of Anti-Bacterial Effects of Novel Formulations that Target an Essential Metabolic Pathway of the Agent of Lyme Disease, 01-R8487

Principal Investigators
Gloria E Gutierrez, SwRI
Janakiram Seshu, UTSA

Inclusive Dates: 09/01/14 – 08/31/15

Background — Resistance to antibacterial drugs is a growing global threat to human and animal health with many bacterial species developing resistance against commonly used antibiotics resulting in extensive morbidity, health care costs, and mortality. Among the novel strategies to develop the next generation of antibacterial drugs is the use of genomic and proteomic approaches to identify inhibitors of essential metabolic pathways in drug-resistant bacteria. Lyme disease is the most prevalent arthropod-borne infectious disease in the United States, with 300,000 cases occurring annually, and there are no vaccines available against *B. burgdorferi*, a vector-borne pathogen intimately dependent on its host for survival. The mevalonate (Mev) pathway is essential for survival of this pathogen, and blocking this metabolic pathway offers a powerful tool to reduce or eliminate this bacteria in the tick vector, infected reservoir hosts, or humans.

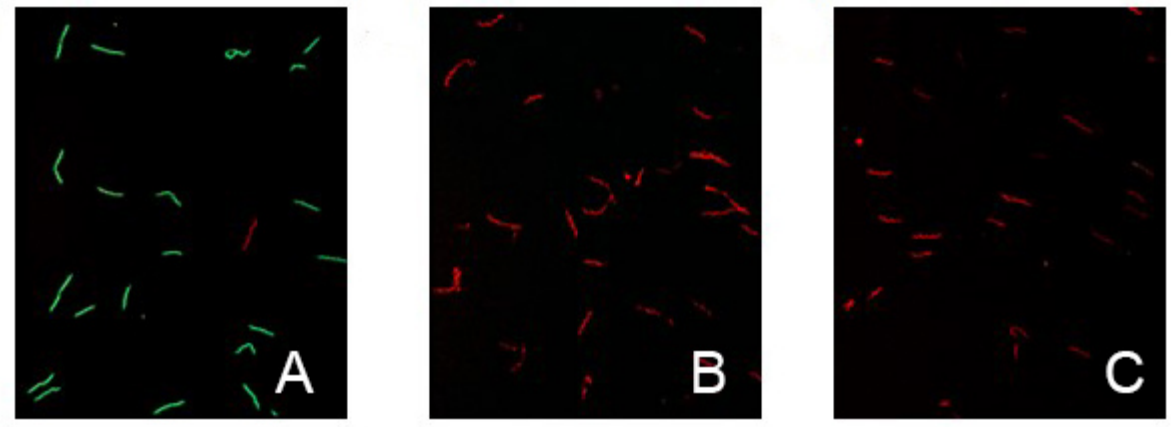

Figure 1: Sensitivity of B. burgdorferi to statins. (A-C) Confocal microscopy of BacLight™ Live/Dead stained B. burgdorferi Treated with DMSO (A) are green, indicating live cells while those treated with 160 µg/ml of Simvastatin (B) or Lovastatin (C) are red, indicating cell death.

Approach — The objective was to find alternate uses of clinically approved compounds to interfere with the survival of *B. burgdorferi*. Based on the hypothesis that inhibiting the Mev pathway might help reduce the incidence and persistent clinical manifestations of Lyme disease, we developed different formulations of statins, known inhibitors of the enzyme HMG-CoA reductase. We determined the efficacy of these formulations on *in vitro* growth kinetics of *B. burgdorferi*.

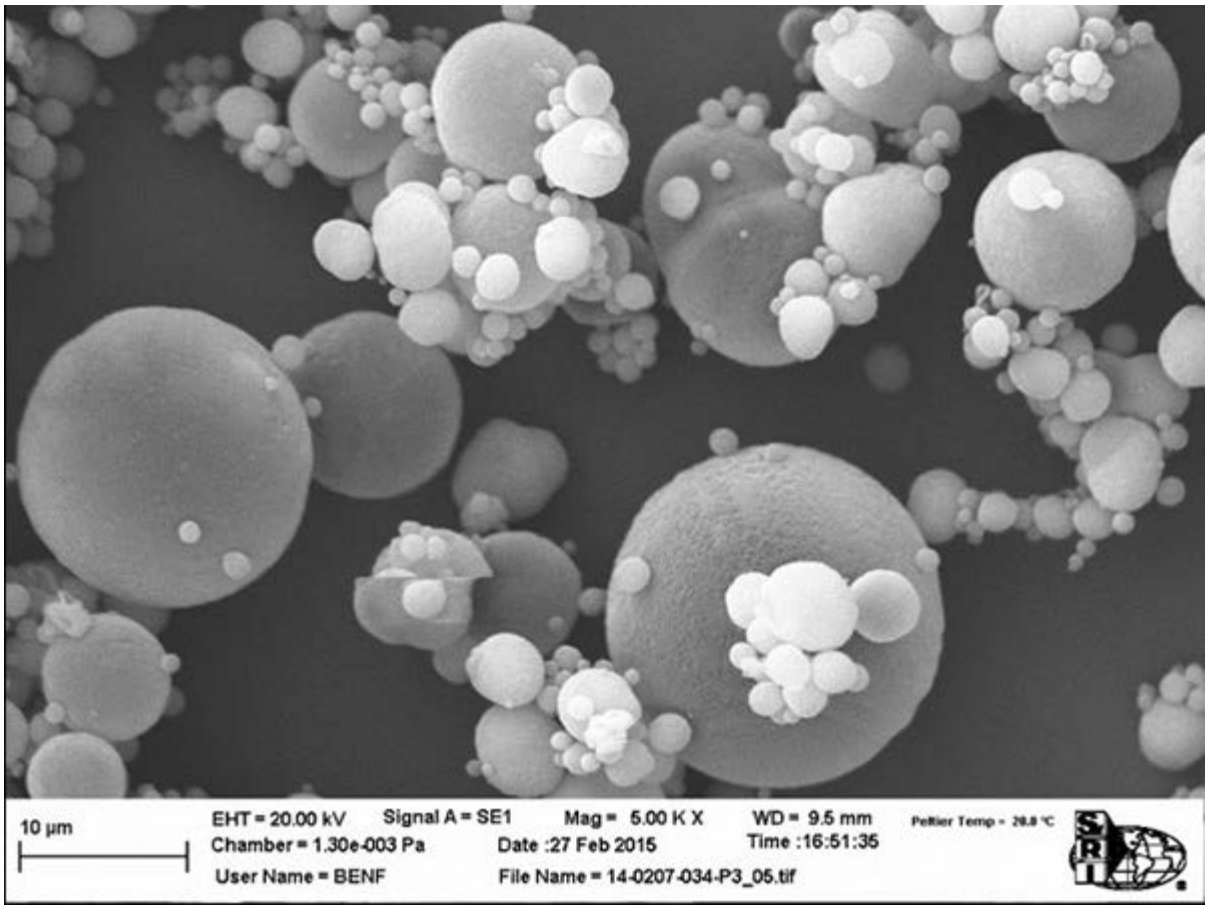

Figure 2: SEM picture of spray dried PLGA-pitavastatin microsphere sample.

Accomplishments — We completed the synthesis and characterization of four formulations of statins (simvastatin and pitavastatin) by two different routes, intramuscular and oral. There was significant growth reduction *in vitro* in the Bb- B31-A3 strain with both statins, with PLGA compared to no drug or PLGA by itself under *in vitro* growth conditions. This work has significant translational implications such as formulation of inhibitors of the mevalonate pathway as therapeutic agents against Lyme disease in humans. A complemented strain-restoring AckA was generated in the mutant strain lacking the first enzyme of the mevalonate pathway. Experiments to test the effect of these formulations on *B. burgdorferi* survival and virulence in animal models of Lyme disease are still underway.
